LOAD DEFORMATION BEHAVIOUR OF STONE COLUMN IN EXPANSIVE SOIL REINFORCED WITH GEOSYNTHETICS

A Thesis Submitted
in Partial Fulfilment of the Requirements
For the Degree Of

DOCTOR OF PHILOSOPHY

by

ISTUTI SINGH
(2K16/PhD/CE/14)

Under the supervision of

PROF. A. K. SAHU
DELHI TECHNOLOGICAL UNIVERSITY

DEPARTMENT OF CIVIL ENGINEERING

DELHI TECHNOLOGICAL UNIVERSITY
(Formerly Delhi College of Engineering)
Shahbad Daulatpur, Main Bawana Road, Delhi-110042, India

DECEMBER, 2025

LOAD DEFORMATION BEHAVIOUR OF STONE COLUMN IN EXPANSIVE SOIL REINFORCED WITH GEOSYNTHETICS

A Thesis Submitted
in Partial Fulfilment of the Requirements
For the Degree Of

DOCTOR OF PHILOSOPHY

by

ISTUTI SINGH
(2K16/PhD/CE/14)

Under the supervision of

PROF. A. K. SAHU
DELHI TECHNOLOGICAL UNIVERSITY

DEPARTMENT OF CIVIL ENGINEERING

DELHI TECHNOLOGICAL UNIVERSITY
(Formerly Delhi College of Engineering)
Shahbad Daulatpur, Main Bawana Road, Delhi-110042, India

DECEMBER, 2025

ACKNOWLEDGEMENTS

I wish to convey my profound gratitude and heartfelt appreciation to the individuals who have been instrumental in supporting and assisting me in the successful completion of this thesis. It is with deep gratitude that I express my appreciation for their contributions, and I would like to dedicate the following words to acknowledge their invaluable assistance.

First and foremost, I extend my deepest gratitude, special thanks, and heartfelt appreciation to my supervisor, **Prof. A. K. Sahu**. His unwavering support throughout my PhD journey has been nothing short of remarkable. There were moments when I felt lost and demotivated, but his guidance and presence were my guiding lights. Professor Sahu's exceptional ability to motivate, lead, and pursue new frontiers in academia are qualities I deeply admire. Words cannot adequately express the depth of my gratitude for his support and cooperation.

I am equally appreciative of the support I received from the department head, Prof Awadhesh Kumar and DRC chairman, Prof. Raju Sarkar, during my doctoral journey. I hold him in high regard and will always be respectful of his contributions. I extend my sincere thanks to the heads and faculty members for providing me sensible guidance, faultless planning, helpful advice, and kind cooperation at various stages of my PhD journey.

Special gratitude goes to the members of the SRC, Prof. B. D. Manna from the Department of Civil Engineering at IIT, Delhi for their insightful and constructive feedback.

I am immensely grateful to the staff at the Geotechnical Engineering Laboratory and Computer-Aided Design Laboratory within the Department of Civil Engineering. I extend my sincere thanks to lab technician Mr. Shashikant and lab assistants, Mr. Atul, for their unwavering support during the experimental and simulation phases of my research.

My sincere appreciation extends to my colleagues and juniors, Mrs Shivangi

Bhardwaj, Dr Inderjeet Singh, Dr. Dinesh K. Reddy, and Dr. Sushant Kumar for their valuable suggestions and assistance whenever I sought their guidance.

I also want to express my gratitude to Mr. Siddharth Rawat, Mr. Anurag Tripathi and Mr. Rahul Kumar, Dr. Kamakshi Rawat their unwavering support during my PhD journey will forever remain etched in my memory. Your presence was akin to that of supportive friends, and I am immensely grateful for that.

I also want to express my gratitude to Dr. Shobha Ram and Mr. Vikas Kumar whose consistent support from my PhD days through to my thesis submission was instrumental in my success. Their priceless review comments, suggestions, and discussions were crucial pillars in the successful submission of my thesis.

I extend my deepest gratitude to the pillars of my life, whose unwavering support has been my constant motivation throughout this doctoral journey. First and foremost, I express my heartfelt appreciation to my parents, Mr. Ganga Ram and Mrs. Pushpa Devi whose boundless love, sacrifices, and encouragement have shaped my academic path and instilled in me the values that drive my pursuit of knowledge. To my dear younger brother, Mr. Nikhil Singh and younger sister Miss Nivedita Singh, whose camaraderie and guidance have been a source of strength and who have stood rock solid behind me through this journey. To my beloved Husband, Mr. Pradip Kumar, your unwavering belief in me, patience, and sacrifices have been the cornerstones of my success. Your constant support and understanding have made this journey not only possible but immensely meaningful. Last but certainly not least, my sincerest gratitude goes to my daughter, Prati. Your boundless enthusiasm, curiosity, and the joy you bring into our lives have been a daily reminder of the significance of the work I do and the legacy I hope to leave behind. Together, you have been my rock, my motivation, and my greatest cheerleaders. This achievement is as much yours as it is mine. Thank you for being the foundation upon which my academic dreams have flourished. I am sincerely thankful and deeply grateful to all those who have supported and contributed to this significant milestone in my life.

(ISTUTI)

DELHI TECHNOLOGICAL UNIVERSITY

(Formerly Delhi College of Engineering)
Shahbad Daulatpur, Main Bawana Road, Delhi-42

CANDIDATE'S DECLARATION

I Istuti Singh hereby certify that the work which is being presented in the thesis entitled **"LOAD DEFORMATION BEHAVIOUR OF STONE COLUMN IN EXPANSIVE SOIL REINFORCED WITH GEOSYNTHETICS"** in partial fulfilment of the requirements for the award of the Degree of Doctor of Philosophy, submitted in the Department of Civil Engineering, Delhi Technological University is an authentic record of my own work carried out during the period from 2016 to 2025 under the supervision of Prof. A. K. Sahu, Professor, Department of Civil Engineering, Delhi Technological University, Delhi, India.

The matter presented in this thesis has not been submitted by me for the award of any other degree or in any other Institution.

Candidate's Signature

This is to certify that the student has incorporated all the corrections suggested by the examiners in the thesis and the statement made by the candidate is correct to the best of our knowledge.

Signature of Supervisor **Signature of External Examiner**

DELHI TECHNOLOGICAL UNIVERSITY

(Formerly Delhi College of Engineering)
Shahbad Daulatpur, Main Bawana Road, Delhi-42

CERTIFICATE BY THE SUPERVISOR

Certified that Istuti Singh (2K16/PhD/CE/14) has carried out their search work presented in this thesis entitled **"LOAD DEFORMATION BEHAVIOUR OF STONE COLUMN IN EXPANSIVE SOIL REINFORCED WITH GEOSYNTHETICS"** for the award of **Doctor of Philosophy** from department of Civil Engineering**,** Delhi Technological University, Delhi under my supervision. The thesis embodies results of original work, and studies are carried out by the student herself and the contents of the thesis do not form the basis for the award of any other degree to the candidate or to anybody else from this or any other University/Institution.

Signature

Prof. A. K. Sahu

Professor

Department of Civil Engineering

Delhi Technological University, Delhi

Date:

ABSTRACT

The present study investigates the improvement of weak soils using granular columns, with emphasis on the role of geosynthetic encasement and iron dust inclusion in enhancing load-bearing capacity and reducing settlement. Soft soils often exhibit excessive compressibility and inadequate strength, making them unsuitable for direct foundation support. To address these challenges, granular columns are widely employed; however, their efficiency depends on factors such as column arrangement, diameter, and confinement. This research systematically explores the behavior of both single and group columns under different conditions to identify optimum configurations for practical applications.

The primary objectives of the study were to evaluate the load–deformation behaviour of ordinary and geosynthetic-encased stone columns in expansive soil, to investigate the influence of column configuration, encasement material, and iron dust stabilization on bearing capacity and settlement characteristics, and to identify the most efficient ground improvement system for expansive soils.

The study employed both experimental and numerical methods. Laboratory model tests were conducted on single columns of diameters 50 mm and 70 mm, as well as group columns arranged in triangular, square, and hexagonal patterns with varying spacing-to-diameter (s/d) ratios. Both ordinary and encased stone columns were examined, using geotextile and geogrid as encasement materials. The stone column mix was prepared using stone dust, fly ash, cement, and iron dust to enhance column strength. Tests were performed under monotonic vertical loading, and settlements were measured up to 50 mm. The experimental results were further validated using numerical modeling in PLAXIS 3D.

The findings revealed that untreated clay beds had very low load capacity (5.9 kN at 50 mm settlement). Single ordinary stone columns improved the load resistance, with 70 mm end-bearing columns carrying 7.2 kN and floating columns 6.5 kN. Encased single columns showed further gains, with geotextile-encased end-bearing

columns sustaining up to 8.15 kN, about 38% higher than untreated clay. In group configurations, the triangular pattern consistently gave the best performance, followed by square and then hexagonal arrangements. Geosynthetic encasement enhanced group behavior significantly, with geotextile generally outperforming geogrid due to better fines retention and hoop stress mobilization. The inclusion of iron dust in the column mix further reduced settlement and improved strength, particularly in group columns.

Overall, the study concludes that the triangular arrangement of group stone columns, encased with geotextile or geogrid and stabilized with iron dust, provides the most efficient configuration. This system achieves the highest load-bearing capacity and the least settlement, demonstrating its practical applicability for soft soil improvement. The research

contributes valuable insights into the design and optimization of granular column foundations and establishes the benefits of combining geosynthetic encasement with stabilizing additives.

Additionally, the experimental program was conducted using single columns of diameters 20 mm, 30 mm, and 50 mm, along with group columns arranged as double columns along the mould diameter and triangular columns with a spacing-to-diameter ratio of 1. Tests were performed with and without encasement using geotextile and geogrid to assess their relative performance. Additionally, iron dust was introduced as a stabilizing additive to study its effect on settlement and strength. Load–settlement responses were recorded and analyzed to evaluate the comparative performance of each configuration.

The results revealed that single columns performed best when encased with geotextile, with the 30 mm diameter column providing maximum load capacity. Group column behavior was influenced more by arrangement, with triangular patterns offering superior settlement resistance compared to double columns. Among the encasement materials, geogrid provided better confinement in group columns, whereas geotextile was more effective for single columns. The inclusion

of iron dust consistently enhanced overall performance, lowering settlements and increasing load capacity, particularly in group column arrangements.

It is concluded that the most efficient configuration for ground improvement in weak soils is the triangular group arrangement of granular columns encased with geogrid and stabilized with iron dust. This combination delivers the highest load-bearing efficiency and the least settlement, offering a practical and effective solution for foundation support in soft soils. The findings provide valuable insights into the design and application of granular columns, contributing to the advancement of ground improvement techniques in geotechnical engineering.

List of publications

(a) Papers in SCI/SCIE Journal (Published/Accepted)

S. No	Title of the paper	Name of the Authors	Name of the Journals	Indexing Status of Journal with Indexing Agency
1.	Multi-blended granular columns encased with geosynthetics	**Istuti Singh** & Anil Kumar Sahu	Z. Dt. Ges. Geowiss. (J. Appl. Reg. Geol.) Published online February 2024, DOI:10.1127/zdgg/2024/0412	Science Citation Indexed
2.	Load Deformation of Multi-Blended Granular Columns using Geosynthetic Encasement	**Istuti Singh** & Anil Kumar Sahu	Z. Dt. Ges. Geowiss. (J. Appl. Reg. Geol.), Published online on October, 2024.	Science Citation Indexed

(b) Papers presentation in the International Conference

S. No	Title of the paper	Name of the Authors	Name of the Journals
1.	A Review on Stone ColumnsUsed for Ground Improvement of Soft Soil	**Istuti Singh** & Anil Kumar Sahu	4th World Congress on Civil, Structural and Environmental Engineering April 07-09, 2019, Rome, Italy. 4th International Conference on Geotechnical Research and Engineering (ICGRE'19)
2.	Load Carrying Capacity of Grouted Stone Columns	**Istuti Singh** & Anil Kumar Sahu	Second ASCE India Conference on Challenges of Resilient and Sustainable Infrastructure Development in Emerging Economies (CRSIDE-2020) organized during March 02-04, 2020 at Kolkata.

TABLE OF CONTENTS

PLAGIARISM REPORT
CURRICULUM VITAE

LIST OF TABLES

LIST OF FIGURES

LIST OF SYMBOLS

A_r	area replacement ratio
c	cohesion
C_c	coefficient of curvature
C_s	swelling index
C_c	compressibility index
C_u	undrained shear strength
Cu	coefficient of uniformity
d	average diameter of the aggregate
D	diameter of the stone column
EA	axial stiffness
E_s	soil's elastic modulus
E_c	column elastic modulus
E_{50}	secant modulus at 50% strength
E_0	tangent modulus
E_{ur}	unload-reload modulus
GA	in-plane shear stiffness
h	thickness of the soil layer
I_f	settlement improvement factor
K_0	earth pressure at rest
K_{ps}	coefficient of passive earth pressure of the stone column.
l_e	target element dimension
L	length of the column
Lr	length of the reinforcement
m_v	soil’s volumetric compressibility coefficient
N	standard penetration test value
n	stress concentration ratio
N_c	terzgahi bearing capacity factor

q_{ult}	ultimate bearing capacity
R	settlement reduction ratio
r_e	relative element size factor
S	spacing between the columns
S_{cl}	settlement of the columns
S_{sl}	settlement of the soil
S_u	untreated settlement in the foundation
u_o	initial excess pore-pressure
γ	bulk unit weight
γ_{sat}	saturated unit weight
$\Delta\sigma_z$	pressure due to surcharge
μ	poisson's ratio
ϕ'	frictional angle of stone column aggregates
ψ	dilatancy angle
σ_c	stress over the column
$\sigma'_{h,0}$	initial horizontal effective stress
σ_{rL}	limiting radial stress
$\sigma_{ro'}$	initial radial effective stress around the column
σ_s	stress over the soil
σ_{vo}	average initial effective vertical stress
$\sigma'_{v,0}$	initial vertical effective stress

ABBREVIATIONS

BCR	bearing capacity ratio
BEM	boundary element method
COV	coefficient of variation
DEM	discrete element method
ESCR	effective vertical stress on the surrounding soft clay
ESSC	encased steel slag column
FDM	finite difference method
FEM	finite element method
LDCOL	lateral deformation of column
LL	liquid limit
LR	load ratio
MC	mohr-coulomb
OSC	ordinary stone columns
OSSC	ordinary steel slag column
PL	plastic limit
PTA	paraxylene terephthalic acid
PWP_{excess}	excess pore water pressure
RSM	response surface methodology
SCR	stress concentration ratio
SEM	Scanning electron microscope
SG	specific gravity
SIF	settlement improvement factor
SL	shrinkage limit
SPSS	statistical package for the social sciences
SPT	standard penetration test
SS	soft soil
SRR	settlement reduction ratio

VESC	vertically enclosed stone columns
XRD	X ray diffraction

CHAPTER 1

INTRODUCTION

1.1 GENERAL

The nation's economy, urbanization, and population growth are all contributing to the enormous expansion of its civil infrastructure. The number of appropriate sites for construction is gradually declining. This necessitates improving and honing marginal sites that would not have been considered fit for building otherwise. Soft clay, loose sand, silt, expanding soil, frozen soil, collapsible soil, organic soil, loess, and other types of soil are considered poor and challenging for construction purposes. Shear strength, compressibility, volume change, creep deformation, and permeability are the main issues with these soils (Han, 2015).

The process used to improve the properties of soil, namely its behavior in terms of strength, compressibility, and permeability, is known as ground augmentation. Many ground improvement techniques have been widely used and shown to be effective in raising the caliber of soft deposits. The stone column is a commonly used technique for increasing the stability of loose sandy soils, such as silty or clayey sands, as well as soils with poor undrained shear strength. In this process, boreholes are made in the malleable soil at predetermined spots. Granular particles of various sizes fill the area. For construction projects such as liquid storage tanks and embankments, the composite earth provides a semi-rigid and flexible base. The use of stone columns results in improved stiffness, increased bearing capacity, and decreased settlement. Consolidation proceeds more quickly as a result of improved soil drainage.

Around 1830, the use of stone columns was first implemented in France, a European nation. They have been extensively used in Europe for site improvement since the late 1950s (Barksdale and Bachus, 1983). Basarkar et al. (2009) reported that the vibro-flot technique was first applied to the

construction of stone columns in India in 1961 in Ennore, Madras. Since then, the strategy has been widely used in numerous locations around the nation.

The stone column transmits the upcoming load to the nearby earth by acting as an interconnected framework. Each stone column has a tributary area of soil encircling it that forms a regular hexagon. A comparable circular region with the same total area as the hexagon can be used to roughly represent this hexagon. Both the tributary soil and one stone column are included in the similar circle, which has a diameter that practically includes both. This is often referred to as a unit cell. The application of the unit cell notion is especially helpful when analyzing how the column group functions.

The building of the stone column can be completed using either the replacement approach or the displacement method. With the displacement method, the surrounding dirt is moved and a hole is made in the ground using a closed casing pipe. The hole that the casing produced is then filled with stones. In the replacement procedure, a hole or cavity of the desired depth is dug out of the ground and filled with stones. The displacement method works well for both unsaturated cohesive and cohesionless soils, while the replacement strategy works well for cohesive soils (Han, 2015).

The case studies of Indian foundations that use stone columns have been reported by Datye and Madhav (1988). The effectiveness of foundations for a range of uses, such as pipe pedestals, small and large groups of isolated footings, bridge abutments, and stone columns for area treatment, was examined. These cases cover a wide range of projects, including the footings for pipe rack work at IFFCO, Kandla in 1972, the treatment of foundations for the Belapur and Kasheli Bridge abutments in 1975, the improvement of soil for lagoon embankment and foundations for a sewage treatment plant near Bhandup, Bombay in 1982, the ground treatment for a pipeline at Sion-Koliwada, Bombay, and the hazardous storage liquid tanks at Manglore Chemical and Fertilizers, Manglore, as well as at IFFCO,

Kandla.

Barksdale and Bachus (1983) state that the typical design loads for stone columns fall between 20 and 50 tons. In contrast to the nearby soft soils, a composite structure with greater shear strength and less compressibility was formed inside the soft ground after a stone column was constructed. The column material is contained by the malleable earth. Stress concentration occurs in the column as a result of the superstructure's tension causing the column and the surrounding earth to slide downward simultaneously. The stress concentration is brought on by the column material's stiffness. Because of the difference in modulus between the column material and the nearby soil, the column is under more stress than the surrounding soil. The ratio of the stress on the adjacent soil to the stress across the column is known as the stress concentration ratio, or SCR. It is frequently employed to demonstrate the load transfer between soft soils and columns. IS 15284 (Part I) provides a stress concentration ratio of 2.5–5, but Barksdale and Bachus (1983) suggest a ratio of 1–5.

The length of a single stone column has a significant impact on how it fails when subjected to loads over its region. Generally speaking, if the length of the stone column is more than four times its diameter—also known as the critical length—it will collapse in the bulging state. Conversely, the column may experience punching shear failure or general shear failure if its length is smaller than the critical length (IS15284 Part 1).

Two elements contribute to the strength of traditional stone columns: the limitation provided by the surrounding loose soil and the friction between the granular components that comprise the column. The properties of higher bearing capacity and less settling are observed in the loaded ground in comparison to the original native soil. Nevertheless, the following reasons might cause its performance to still fall short of expectations (Murugesan and Rajagopal, 2009):

The stone columns' frictional properties may be reduced if the nearby loose dirt were to seep inside.

The stones may not make as much of an effect as they would have in their original, undisturbed form since they can move laterally into the soft nearby soil.

A different strategy has been investigated to solve this problem, which involves reinforcing rammed stone columns with a geogrid-encased tube. It has been discovered that this technique improves the stone columns' compressibility and strength. Numerous experiments have been carried out in a small number of projects to apply the positioning of a geogrid casing, followed by the charging of stones into it (Deshpande and Vyas, 1996; Richard and Yogesh, 2005; Raithel et al., 2006). The resultant columns have a constant diameter throughout, despite the departure from the traditional vibro-technique, and the addition of a geogrid offers the necessary lateral confinement. Laboratory model stone columns with encasement have been the subject of several studies (Sivakumar et al., 2004; Bauer and Nabil, 1996). These studies, which primarily use sand in combination with stone particles, have shown an increase in bearing capacity, which helps to explain the scaled-down effect. By adding an encasement, a stone column's stiffness and structural integrity are improved. It also helps to lessen the lateral compression that stones experience during installation, especially in low-bearing soils. This enables quicker installation procedures without compromising the drainage capacity of the column or the frictional qualities of the stones employed. Even with all of the benefits that enclosed stone columns offer, this method is not as often used as stone columns. The main cause of this is a lack of knowledge about how applied loads affect encased stone columns. Therefore, it is thought that a thorough study of encased type stone columns is necessary to clarify the process by which the encasement increases the column's strength and pinpoint the factors influencing its behavior.

Comparing encased and unencased stone columns is important to ascertain how encasement impacts the strength of a bed supported by stone columns. To make it easier to quantify the previously described impact, this investigation should be carried out under similar testing settings. As a result, the goals and scope of the study have been established.

1.2 INSPIRATION

The rapid pace of urbanization and industrial development has led to a decline in the availability of construction sites with suitable soil properties. As a result, field engineers often face constraints when selecting locations that contain weak soil layers with complex behaviours, mainly due to the presence of problematic soils with varying geotechnical characteristics. Many of these underutilized or abandoned sites are comprised of soft clay with high compressibility, low shear strength, and significant settlement potential, or loose, cohesionless soils lacking sufficient load-bearing capacity. Such conditions make these sites vulnerable to issues like landslides, liquefaction, or instability due to the presence of uncontrolled fill materials. Therefore, thorough site preparation is essential to ensure the safety and viability of construction projects. When exploring different ground improvement or modification techniques, it is crucial to select and apply a method that meets both the economic constraints and the structural design requirements.

In recent years, a widely adopted ground improvement technique involves inserting granular aggregates into weak soil layers in the form of cylindrical columns. This method is typically executed through either vibration or dynamic compaction. The use of stone columns—where columns of granular material are introduced into loose sands, alluvial silty clays, sandy silts, and soft cohesive soils—has proven to be an effective reinforcement strategy (Ketkar and Telang, 1994; Kumar et al., 2002). Since its introduction in the 1970s, stone column technology has been employed to enhance, stabilize, and rehabilitate soil foundations for a broad range of

structures, including high-rise buildings, industrial facilities, towers, and oil storage tanks.

JBF Petrochemical Industries Ltd proposed the development of a new paraxylene terephthalic acid (PTA) plant in Mangalore, India, with an anticipated annual output of 1.25 million metric tonnes. The facility was designed to include storage tanks, processing units, substations, and various support structures. Keller was commissioned to design and execute ground improvement solutions for three paraxylene tanks and two fire water tanks, measuring 64 meters and 35 meters in diameter, respectively. Alongside these tanks, construction of the corresponding tank pads was also required. Subsurface investigations revealed varying layers of sand with differing consistencies—from soft to dense—underlain by tightly packed silty sand or weathered rock. The project's primary goal was to increase the load-bearing capacity of the tank pad foundations while limiting both total and differential settlement. To achieve this, Keller implemented a ground improvement strategy using bottom feed vibro stone columns, which effectively enhanced the bearing strength of the soil and reduced settlement issues. The tank pad construction involved several critical elements, including a stone blanket, HDPE membrane, sand pad, stone ring beam, and bituminous surfacing.

Similarly, Cochin International Airport Ltd. (CIAL) proposed an expansion project to upgrade apron areas adjacent to the existing facilities, including associated airfield infrastructure. Keller was engaged by the main contractor to execute ground improvement using vibro stone columns to support the construction of new aircraft parking bays. The site posed several geotechnical challenges, notably the presence of highly compressible plastic clay and loosely filled soil layers over an area of approximately 41,000 m^2. Additionally, a subsurface nallah posed a risk of uneven settlement. Given the complexities of working in an operational airport environment, careful coordination and planning of rig movements were essential.

To address these challenges, Keller implemented an optimized foundation solution using vibro stone columns. This method effectively improved the soil's bearing capacity and settlement characteristics, while also enhancing drainage for rapid consolidation. The solution not only reduced project costs for the client but also resulted in significant time savings. The treatment zone was extended beyond the apron's footprint to provide lateral confinement and ensure a smooth transition between treated and untreated soils. The project was successfully completed within the scheduled timeframe using four rigs.

Beyond this, geotechnical experts have successfully applied the stone column technique in various notable projects. In Rohtak, Haryana, a temple foundation was constructed using granular piles with a 12-meter diameter and 500 mm rammed stone columns. Likewise, the restoration of approximately 1,000 pillars at the Kalyana Mandapa in Hanuma Konda, Warangal, involved 400 mm diameter rammed stone columns and 7-meter-long granular piles. The construction of a picture tube manufacturing facility in Karzan, Vadodara, incorporated gravel piles between 300 and 400 mm in diameter. Additionally, the fire water tank at the Indian Oil Corporation Ltd.'s LPG Bottling Plant in Madanpur Khadar was supported by a foundation consisting of a group of gravel columns measuring 3 × 22 meters.

Most recently, the foundation committee for the Ram Temple in Ayodhya has proposed the use of vibro stone columns to support the raft foundation. These examples demonstrate the widespread adoption of stone column techniques across a variety of soil conditions and structural applications, proving it to be a reliable and cost-effective solution for improving the stability of weak ground.

1.3 SIGNIFICANCE OF THE RESEARCH

Soft clay formations, which are geologically young deposits, are commonly found in various parts of the world, including several regions in India.

Notable examples include the Thane Creek area in Mumbai, where thick layers of highly deformable clay—ranging from 15 to 20 metres— are prevalent. Similarly, Cochin is underlain by a significant marine clay deposit exceeding 20 metres in thickness, posing challenges even for constructing relatively light structures such as two-storey buildings. This soft clay is typically found beneath surface fills of about 2 to 3 metres. In Vishakapatnam, particularly near the port, there exists an offshore clay deposit with a depth of approximately 100 metres, characterized by high compressibility. Likewise, the coastal region of Chennai features a soft clay layer varying in thickness from a few metres up to more than 20 metres, located beneath a crustal layer of 2 to 3 metres, which presents substantial difficulties in ensuring foundation stability.

These deposits are predominantly composed of fine-grained soils, with moderate to high clay content. The clay fractions typically display high plasticity, low shear strength, and significant compressibility. In many cases, the natural moisture content is close to or even exceeds the liquid limit, further reducing the soil's load-bearing capacity. These characteristics often lead to foundation failures, particularly when surface loads from embankments or shallow foundations are applied—resulting in large settlements that must be considered during design and may require ongoing structural maintenance.

Due to these challenges, ground improvement becomes essential for ensuring the safe and stable performance of civil engineering structures on such weak soils. A common scenario encountered by field engineers involves loose, soft soil overlying a more competent layer, such as dense sand or stiff clay. Given the prevalence of research and practical applications involving the use of stone columns for reinforcing cohesive soils, there is a strong need for further investigation into the effectiveness of this technique in enhancing the performance of soft clay foundations.

1.4 SCOPE AND OBJECTIVES OF THIS STUDY

In order to study the possibility of increasing the load carrying capacity of soft soil through the use of ordinary stone columns (OSC) and vertically enclosed stone columns (VESC), the primary purpose of this thesis is to investigate the possibility of doing so. Additionally, the present study aims for the purpose of investigating the influence of various parameters by conducting laboratory tests on scaled models. In addition, numerical analyses were performed in order to verify the findings of the experiment.

Hence, the primary aims of this study are as follows:

- To evaluate the effectiveness of ordinary and geosynthetic-encased stone columns in improving the load-bearing capacity and settlement behaviour of expansive soils.
- To investigate the influence of column arrangement, encasement type, and stabilizing additives on performance
- To identify the optimum configuration for ground improvement applications.

1.5 METHODOLOGY

To achieve the research objectives, a dedicated laboratory setup was designed and fabricated for this study. In this arrangement, a single stone column—constructed with or without geosynthetic encasement—was installed within a soft clay bed and tested under load using a rigid circular plate serving as a model footing. The experimental program explored the influence of several key factors, including column diameter, encasement length, encasement material stiffness, stone column group configurations, and the spacing-to-diameter (S/D) ratio. The aim was to evaluate how these parameters affect the load-bearing performance of encased stone columns in comparison to conventional, unencased columns. Similar investigations were carried out for stone columns arranged in group patterns.

Numerical simulations of the model tests were performed in PLAXIS using

the finite element method, and the numerical results were validated against the laboratory findings. The Mohr–Coulomb model was adopted to represent the behaviour of the clay, while the modified cam clay model was applied for the stone column material. For encased stone columns, the encasement was modelled using the Geogrid element in PLAXIS to capture its tensile stiffness alongside the models used for the soil and stone column. This combined experimental and numerical approach provided a comprehensive assessment of the effects of the selected parameters on the performance of stone columns.

To examine the particles of the soil and stone column mix XRD and SEM was also done.

In addition to the primary experimental and numerical investigations, an additional experimental study was carried out to further examine the influence of iron dust and different geosynthetic encasement materials on the performance of granular columns in expansive soil. This additional work was included to validate and extend the observations obtained from the main study under modified test configurations and material combinations. Since the findings provided supplementary insights beyond the primary objectives of the thesis, they have been presented separately in Chapter 6 under "Additional Work." The inclusion of this chapter helps to broaden the understanding of granular column behaviour and highlights the potential scope for further application of alternative stabilizing materials and encasement systems.

1.6 STRUCTURE OF THE THESIS

The thesis is structured into six distinct chapters, with each chapter being briefly summarised in the following sections.

Chapter 1 a concise explanation is provided on the importance of ground improvement, the specific constraints associated with the use of stone column approach, and the requirement for encasing the conventional stone column.

Additionally, the motivation, need and objectives of the present study are also presented.

Chapter 2 provides a detailed overview of previous research details pertaining to the behaviour and functioning of ordinary stone columns and geosynthetics encased stone columns, comprising analytical, experimental, and numerical investigations.

Chapter 3 provides a comprehensive account of the experimental inquiries conducted on stone columns and enclosed stone columns. The fundamental characteristics of the materials employed in the experiments are provided, alongside the facilities that have been constructed for the purpose of conducting model testing. The details regarding the PLAXIS 3D used for simulating experimental investigations has also been explained in current chapter. The crystalline structure of the materials and column mix is shown by using SEM and XRD tests.

Chapter 4 the findings of the experimental tests that were conducted on conventional stone columns, vertically encased stone columns (VESC) are presented. Another aspect of the stone columns that was investigated was their failure mechanism. The investigation was carried out on a single stone column as well as stone columns that were grouped together.

The experimental results were validated by numerical modeling using PLAXIS 3D for all the variation of experimental tests whose results has been presented in this chapter. In addition to that, a comparison between the numerical results and the experimental ones has been provided. The SEM and XRD results also shown.

Chapter 5 this chapter presents an overview of the findings that were gained from the inquiry. Various behaviours such as settlement, stress concentration ratio, excess pore water pressure, and lateral deformation of columns were studied.

Chapter 6 presents supplementary experimental investigations conducted as

an extension of the main research work to further evaluate the effect of iron dust inclusion and alternative encasement arrangements on granular column performance.

CHAPTER 2

LITERATURE REVIEW

2.1 GENERAL

This chapter provides foundational knowledge on soft soils and various ground improvement methods. As outlined in the previous chapter, stone columns represent a practical, rapid, and cost-effective technique for enhancing ground conditions. This method is commonly applied in the construction of embankments, liquid storage tanks, and offshore infrastructure, and it helps mitigate the risk of soil liquefaction. To illustrate the effectiveness of this technique, several brief case studies showcasing successful applications are included. However, in cases involving extremely soft soils, the settlement of the improved ground may still pose challenges even after the installation of standard stone columns. To address this, research has indicated that wrapping the granular material with geosynthetics can enhance the performance of the columns. Consequently, this chapter includes a literature review focusing on the design, construction, and performance of both conventional and geosynthetic-encased stone columns.

2.2 SOFT SOILS

Soft soils are characterized by low shear strength and high compressibility, which can lead to structural issues both during construction and after a project is completed. These soils are often geologically young and fine-grained, including normally consolidated, under-consolidated, or lightly over-consolidated materials. They may also include weathered surface clays and quick clays—soils that appear stable but have not experienced significant delayed or secondary consolidation since their formation. Common examples of soft soils include loose sands, soft clays, and silty materials, typically found in areas with recurring wetting and drying cycles, such as near rivers, lakes, and coastal zones. These environments are where such soils naturally develop. In India, soft soils are prevalent in marine and river delta regions, including the Gulf of Kutch, Gulf of Cambay, and along the Eastern and Western coastal belts. The soil classifications generally associated with soft

soils—excluding SP (poorly graded sand)—are MI, MH, CI, CH, MI-MH, CI-CH, MI-CI, and MH-CH.

The German Geotechnical Society has introduced a set of standards aimed at defining and evaluating soft soils for use in construction. These guidelines are intended to help classify such soils based on their physical and mechanical properties, ensuring their suitability for building purposes.

a. Consistency that is very soft to soft, having a consistency index (I_c) < 0.75
b. Nearly or at full saturation
c. The undrained shear strength, Cu ≤40 kN/m²
d. Low to medium plastic property
e. Inclined to flow
f. Thixotropic property
g. Very sensitive to vibrations

2.2.1 Soft soil properties

Soft soils possess certain key characteristics that contribute to their high compressibility and low shear strength:

a. Over 50% of their particles pass through a 75μm sieve.
b. They are typically found among organic and inorganic clays and silts, displaying low to moderate plasticity.
c. Their shear strength is generally less than 25 kPa, as supported by several studies (Madhav and Miura, 1994; Priebe, 1995; Muir-Wood et al., 2000; Alexiew et al., 2005; Wehr, 2006; Gniel and Bouazza, 2009; Mohanty and Samanta, 2015; Fattah et al., 2014; Dutta et al., 2016; Mehrannia, 2018).
d. According to Ranjan and Rao (2000), these soils typically exhibit low Standard Penetration Test (SPT) "N" values—less than 8 for cohesive soils ranging from medium to very soft, and less than 10 for cohesionless types.
e. The activity index is commonly used to assess the compressibility

and swell-shrink potential of clayey soils; values over 1.25 indicate active clays.

f. They often contain a high amount of organic material, which further increases their compressibility.

2.2.2 Problems Associated with Soft Soils

a. Bearing Capacity Failure: Soft soils are typically weak and may undergo bearing failure when the applied pressure from structures exceeds their ultimate bearing capacity. This failure is more pronounced when the applied loads are inclined or eccentric, leading to instability or tilting of foundations.
b. Excessive Settlement (Total and Differential): Due to their high compressibility, soft soils can experience significant settlement under loading. This includes both:
    a. Total settlement, which affects the entire structure, and
    b. Differential settlement, which affects parts of the structure unevenly and can lead to structural damage such as cracking in beams, slabs, or walls.
c. Shrinkage and Swelling (Volume Change): Soft soils rich in expansive clay minerals like montmorillonite can absorb large amounts of water, leading to swelling or ground heave during wet conditions. Conversely, during dry conditions, these soils may shrink, causing shrinkage fissures. These volumetric changes can lead to long-term structural instability.

2.2.3 Remediation of soft soil

The problem of soft soil can be resolved using the following strategies (Hausmann, 1990):

a. Permanently alter the construction site.
b. Likewise, superstructure planning.
c. Remove any damaged soils and use sturdy materials in their stead.
d. Using the proper techniques to develop the properties of the soil and the surrounding landscape.

Various ground improvement techniques are:

1. Replacement
2. Drainage and consolidation
3. Chemical stabilisation
4. Thermal and biological treatment
5. Reinforcement

Below, we briefly review each of the previously listed techniques:

1. Replacement

Both shallow and deep replacement techniques are used to address soft soil issues. For shallow depths (up to 3 meters) above the groundwater table, problematic soil is replaced with stronger, more compact materials, improving the ground's stability. Deep replacement methods involve the use of stone columns, sand compaction columns, rammed aggregate columns, vibroconcrete columns, and geosynthetic encased columns. These methods replace loose, soft soil with hard, stiff materials, typically at depths of 5 to 10 meters. Sand columns can reach depths of 5 to 15 meters, while stone columns can go as deep as 30 meters (Han, 2015). Deep replacement helps reduce the likelihood of settlement and liquefaction, while also enhancing bearing capacity, stability, and speeding up consolidation.

2. Drainage and consolidation

Drainage – To improve the load-bearing capacity and accelerate consolidation settlement on soft soils, a top layer of permeable materials, nonwoven geotextile, or geomaterials may be applied.

Consolidation – Soft soils, particularly those with saturated inorganic clays and silts, can be temporarily subjected to vacuum pressure or surcharge techniques to strengthen the soil and reduce settlement.

3. Chemical Stabilization

Soft soil deposits, whether shallow or deep, can undergo chemical stabilization. At shallow depths (up to 0.3 meters), unsaturated clays and silts can be mixed with materials such as lime, cement, or fly ash. For deeper stabilization, techniques like

grouting and deep mixing are used, where cement-based fluids are injected into the soil under high pressure. The treatment depths for grouting and deep mixing are typically 30 meters and 70 meters, respectively.

4. Thermal and Biological Treatment

The temperature of the earth can be lowered to below freezing, reducing the amount of heat escaping from beneath the surface, which causes the soil to solidify. This leads to less soil movement and reduced water flow, making it effective for temporary soil improvement, especially in saturated clay and sand during activities like soil excavation. Biological treatment involves using plants and their roots, or modifying soil properties through bio-mediated geochemical processes such as mineral formation, gas generation, biofilm construction, and biopolymer production. This method can be applied to both cohesive and non-cohesive soils, though it is still not widely established.

5. Reinforcement

This treatment consists of two main components: fill reinforcement and in-situ reinforcement. The primary goal of reinforcement is to enhance the stability of the ground. For both temporary and permanent slopes in soil and rock, steel bars combined with grout have been used, while in- situ reinforcement methods include ground anchors, soil nails, and micropiles. High-strength geosynthetics are also placed in slopes, embankments, earth walls, foundations, and roadways for tensile resistance and other applications. This treatment helps reduce settlement and improves both stability and bearing capacity.

Geotechnical experts are well-versed in these corrective measures, but they often come with limitations and may not always be practical for field applications. Stone columns play an essential role in various geotechnical tasks, such as drainage, reinforcement, and densification. This technique is particularly innovative for improving a variety of problematic soils, including waste fills, ash ponds, soft clays, and loose sands.

2.3 STONE COLUMNS

Stone columns are compressed hard rock fragments placed vertically into the soil layers beneath the surface. These columns are created in situ using ground improvement techniques such as replacement, displacement, or other methods. They function as a sub-structural component that transfers the load from the superstructure to the surrounding soil through compression, shear, or rotation, interacting with the geo-material above, below, and around them.

The use of vibro methods dates back to the 1800s when French military engineers first employed them, though they were initially forgotten. However, these methods were revived in the 1930s in Germany to construct a racetrack (McKelvey and Sivakumar, 2000). Since then, vibro stone columns have become one of the most important deep compaction techniques used worldwide (Serridge, 2005; McCabe et al., 2009). This method has become a cost-effective alternative to traditional piling techniques for construction projects that are less prone to settlement (Weber et al., 2006). The following section explores the factors that influence the strength of stone columns.

1. Stress Variation Around the Boundaries of the Stone Column

The installation of stone columns causes compression and radial displacement in the surrounding soil. To quantify the stresses around the stone column, the earth pressure at rest (K_0) is commonly used as a reference. Following the installation of stone columns, the surrounding soil undergoes horizontal displacement and compression, leading to an increase in the K_0 value. In the case of clay, radial displacement occurs around the stone column's periphery, aiding in vibrocompaction until the material fully expands horizontally to the column's radius. Changes in stress values can be measured by calculating the ratio of effective horizontal stresses to vertical stresses (Chobbasti, 2011; Rao, 1992). Results from 3D modeling tests indicate significant variations in stress concentration at the interface between the earth and the stone column.

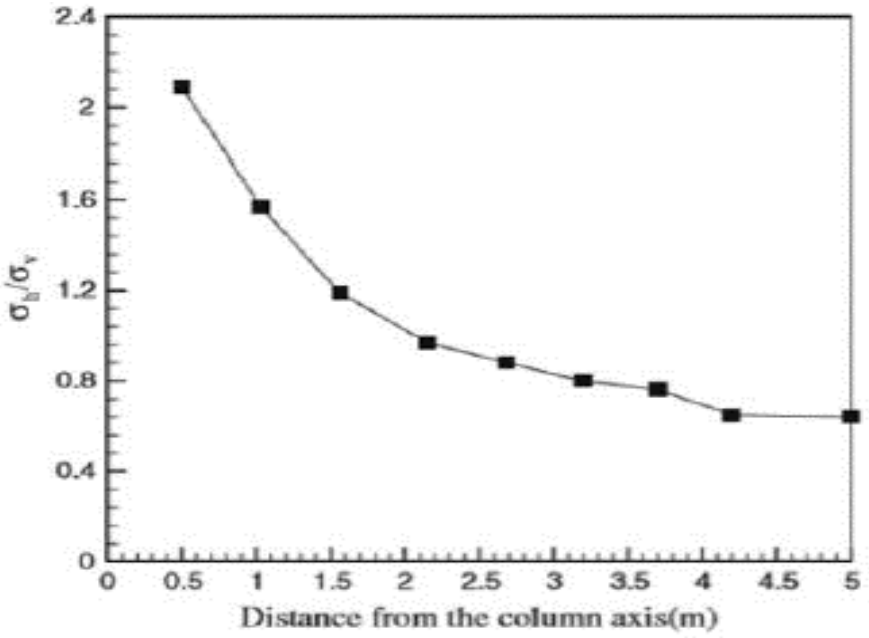

Figure 2.1. Stress variation in soft clay as a function of distance from the column (Choobasti, 2011)

In the Perm, Russia region, the effectiveness of stone column technology has been analyzed for improving foundation stability and reducing subgrade deformation. To prevent financial losses, the ideal pile depth is always chosen within the calculated foundation depth. Since the soil near the borehole compresses during stone column installation, any deformation in this area must be accounted for before the column shell is installed (Shenkman and Ponomaryov, 2016).

As the load on the structure increases, the column material begins to expand laterally. However, the geosynthetic encasement and lateral soil pressure prevent the fill material from moving horizontally. Studies that plot the effective vertical stress over time for both Geosynthetic Encased Stone Columns (GESC) and Ordinary Stone Columns (OSC) have shown that the effective stress for the GESC is 1.25 times higher than that of the OSC. This difference in effective stress is attributed to the additional lateral confinement provided by the geogrid encasement (Rajesh, 2017).

2. Confining Pressure

The magnitude of confining pressure plays a crucial role in the ability of stone columns to bear applied loads. By increasing the confining pressure, the load-

bearing capacity of stone columns is enhanced, especially when they are encased in geosynthetic materials. Extensive triaxial and uniaxial tests on Ordinary Stone Columns (OSC) and Geosynthetic Encased Stone Columns (GESC) show that the confining pressure for regular stone columns is limited to around 200 kPa, while the residual strength of geotextile-encased columns can reach approximately 800 kPa. Due to this higher confining pressure, GESCs are able to withstand substantial loads even after experiencing failure or deformation (Chen et al., 2009).

A relationship exists between the increase in axial stress for encased columns and that of conventional stone columns, which helps determine the enhancement in strength of the encased columns. The improvement is more pronounced at lower confining pressures, with the effect being more noticeable at these lower levels compared to the higher range (Miranda and Costa, 2016). Additionally, the effect of encasing the stone columns is demonstrated by the fact that the strain rate for encased stone columns is lower than for uncased columns, where the strain rate tends to be higher.

3. Settlement / Consolidation Behavior

One of the primary benefits of stone columns is the reduction of settlement and the enhancement of consolidation rates, making settlement a crucial factor when working with soil reinforced by stone columns. Research indicates that as the depth of stone columns increases within the soil strata, settlement decreases. Black et al. (2011) found a correlation between the area replacement ratio and settlement characteristics of stone column group configurations. As the area replacement ratio increases, settlement improvement also increases, but this effect is most noticeable when the area replacement is between 30-40%. Similar results were observed in a study by Shahu and Reddy (2011). The consolidation behavior of conventional stone columns is influenced by factors like the area replacement ratio (A_r), relative density, column length, and the water content of the stone material. A higher A_r leads to a higher failure stress, which in turn results in a decrease in settlement for a given vertical load.

The Response Spectra Methodology shows that settlement of stone columns depends

on their diameter and depth. During the first stage of construction, there is an improvement in soil behavior, which acts as preloading for the second stage and improves soil stiffness and shear strength (Elsawy, 2013).

To analyze the performance of floating stone columns under uniform loading, the settlement improvement factor is used. This factor is the ratio of ultimate settlement with and without columns, and β, the ratio of column length to the thickness of soft soil, is also important (Ng and Tan, 2014). The study by Priebe (1995) is a widely used semi-empirical method for this analysis. As the value of β decreases, pore pressure dissipation reduces, and pore water flows radially from the surrounding soil to the column.

The efficiency of stone columns is heavily influenced by the permeability of soft clays (Rajesh and Jain, 2015). In a study by Yoo and Kim (2009), the construction of a 6-meter-high embankment in three increments revealed that the final settlement of untreated soft clay was nearly three times greater than that of soil treated with stone columns. The ultimate settlement of Ordinary Stone Columns (OSC) and Geosynthetic Encased Stone Columns (GESC) was reduced by 43% and 61%, respectively, compared to untreated soft clay. (Figure 2.2).

When considering cyclic loading from transportation loads, elastic deformations in the column and soil occur immediately after load application due to embankment, leading to undrained settlements (Basack et al., 2016). The embankment on soft soil gradually bends due to the stiffness of the column-soil interaction (Indraratna et al., 2013). The amount of deformation is influenced by the surcharge load applied before, during, and after consolidation. For regular soil, OSC, and GESC, the dissipation of pore pressure takes 7000, 52, and 30 days on average, respectively. Rajesh (2017) found that the maximum immediate settlement of GESC was 21% less than OSC and 42% less than untreated clay.

The shear deformation of stone columns often results in complex localized bands that challenge traditional analytical models. Singh et al. (2019) found that, even with coupled formulations, refining the mesh reduced the shear band thickness inside the

stone column, with no significant effect on the overall settlement profile. The load carried by undisturbed soil is higher than that carried by disturbed soil when compressibility varies along the smear zone. According to Deb and Behera (2017), the smear zone experiences the least consolidation. If the diameter ratio increases from two to five times or the smear zone radius increases from one to three times, the time for 90% consolidation can increase two to three times.

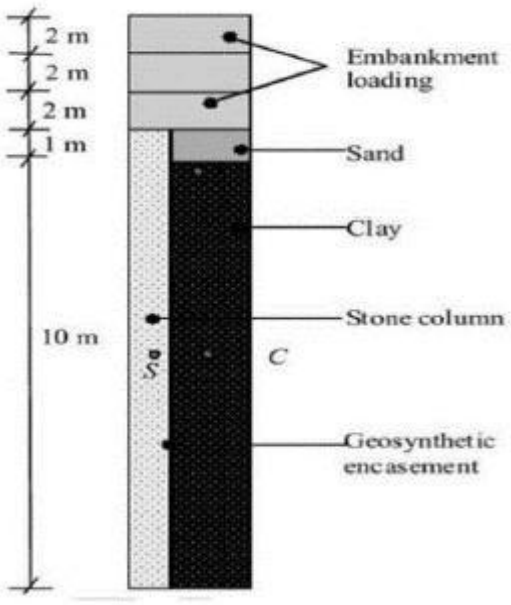

Figure 2.2. Schematic Illustration of GESC Modelling Specifications. (Rajesh, 2014)

Research using the Fast Lagrangian Finite-Difference method (Basack et al., 2017) has shown that the settlement of the stone column-soil system increases hyperbolically with applied vertical stress. Similarly, the Discrete Element Finite Difference (DEM-FEM) model by Indraratna et al. (2015) showed that applied vertical stress causes a hyperbolic increase in the settlement of the soil-column system.

The influence of stone column length and diameter on settlement was analyzed using Response Surface Methodology (RSM) software (Madun et al., 2018). The RSM provided optimal relationships between the column's diameter and settlement. Singh et al. (2018) proposed a regularized solution for shear localization in geomaterials analysis, noting that mesh refinement affects stress-strain response and shear band thickness. After refining the mesh, total settlement increased by 0.02 m.

Finally, the type of material used for stone columns affects the speed of settlement and consolidation in the surrounding soil. Laboratory studies on pebble gravel, crushed pebble gravel, and quarry stones showed that pebble gravel took the longest to consolidate, while quarry stones had the quickest consolidation time and the least settlement (Stacho and Sulovska, 2017). Quarry stones are thus considered the ideal choice for stone material.

4. The Surrounding Soil's Bearing Capacity

Enhancing the soil's bearing capacity is a critical step in using stone columns to strengthen soft soils for engineering purposes. Stone columns significantly improve the soil's load-bearing capacity by creating a composite soil-column system that acts as a support layer for the structure above (Jadid, 2013).

The bearing capacity ratio (BCR) is used to compare the bearing capacities of reinforced versus unreinforced soil. One of the key factors influencing the bearing capacity of stone columns is the size of the footing (Choobbasti, 2011; Nazaruddin, 2013). While the roughness of the footing has a minor effect on the stability and deformation of stone columns, the difference in bearing capacity between smooth and rough footings is negligible and can be disregarded in most designs.

The bearing capacity of stone columns is notably enhanced when encased with geogrid. Research indicates that the end-bearing soil has minimal influence on the strength of ordinary stone columns, as failure in these columns typically occurs through lateral bulging, which is mainly influenced by the surrounding soil. In contrast, failure in encased stone columns is due to punching, which is primarily influenced by the end-bearing soil (Fattah and Majeed, 2012).

Fattah and Majeed (2012) used the Statistical Package for the Social Sciences (SPSS) to develop a regression equation based on experimental data, which links bearing capacity to factors such as cu (undrained shear strength of the soil), Ar (area replacement ratio), L/D ratio, Ns (number of stone columns), and the formula is as follows:

$$q_u = 15.34 \times cu^{0.401} \times As^{0.266} \times Ns^{0.084} \times (L/D)^{0.526} \quad (2.1)$$

Additionally, Bowels (1996) and Bouassida et al. (1995) proposed various other formulas for calculating the bearing capacity of stone columns.

To further assess the relationship between bearing capacity and influencing parameters, Design Expert software and Response Surface Methodology (RSM) were applied. The RSM response plots provided an optimal relationship between the stone column's length, diameter, and load- bearing capacity. According to the ANOVA results, the highest bearing capacity of 3260.7 N was achieved with a diameter of 44 mm and a length of 10 cm, yielding a desirability of 77% (Madun et al., 2018).

5. Area Replacement Ratio (A_r)

The Area Replacement Ratio (A_r) refers to the ratio of the stone column area to the surrounding soil area. One way to increase this ratio is by increasing the diameter of the stone columns.

Cimentada et al. (2011) compared two different stone column diameters: 8.47 cm and 6.35 cm. The calculated A_r values were 11.11% and 6.25%, respectively. The Stress Concentration Ratio (SCR) for these diameters ranged from 0.68 to 0.75. This variation resulted from a decrease in the stiffness ratio between the surrounding soil and the stone column as the pressure increased. The bearing capacity improvement starts even at low Length/Diameter (L/D) ratios when A_r increases. This suggests that A_r has a more significant influence on enhancing the bearing capacity of stone columns than the column's length (Fattah and Majeed, 2012).

Shahu and Reddy (2011) found that as A_r increases, the stiffness of floating columns improves in comparison to end-bearing columns. Other factors, such as the angle of internal friction, loading intensity, and post-installation pressure, also affect the consolidation rate. However, A_r has the most significant impact. Ng and Tan (2014) presented a design equation that shows how A_r, the internal friction angle, loading intensity, and post-construction pressure influence the settlement of

stone columns.

6. Depth of Penetration or L/D Ratio

The stiffness of a stone column improves as its Length to Diameter (L/D) ratio increases. Furthermore, increasing the column's burial depth enhances the soil's overall bearing capacity, while enlarging the diameter helps reduce the risk of the stone column bulging (Shahu and Reddy, 2011).

According to Black et al. (2011), a rise in the L/D ratio leads to a better settlement profile for the stone column. The optimal L/D ratio for a typical column range from 7 to 8. However, beyond an L/D ratio of 8, there is no significant change in the q treated/q untreated ratio. In contrast, for Geosynthetic Encased Stone Columns (GESCs), this ratio continues to increase even when L/D = 8, indicating that there is no limiting value for the L/D ratio in the case of reinforced stone columns (Fattah and Majeed, 2012).

Madun (2018) conducted a separate analysis using Design Expert software to assess the effects of the stone column's height and diameter on bearing capacity and settlement. The maximum bearing capacity, which was 3260.7 N, was achieved at a 44 mm diameter and 10 cm length, with 77% desirability.

7. Stress Concentration Ratio

A crucial factor when designing stone columns is the Stress Concentration Ratio (SCR), which is the ratio of the stress carried by the surrounding soil to that carried by the stone column itself. The primary objective of introducing stone columns into soft soil is to reduce the load on the surrounding soil, as the stone column will bear a greater portion of the load. Thus, a higher SCR leads to improved efficiency of the stone column.

Elsawy (2013) found that the SCR in Geosynthetic Encased Stone Columns (GESCs) increases with load, while it remains nearly unchanged in Ordinary Stone Columns (OSC). The SCR for GESCs increases steadily throughout the consolidation period, while for OSCs, the effective stress concentration ratio

increases during the initial loading phase, then gradually decreases after reaching the saturation limits, stabilizing at a constant value (Rajesh, 2017). GESCs experience an effective stress that is 1.25 times higher than that of OSCs. Early in the loading process, stress concentration is lower, but as the load increases, the stress in the columns rises, stabilizing after reaching a certain point. Stress concentration is notably higher at low stress levels during the initial phase of loading.

Rajesh and Jain (2015) studied the effect of permeability on the strength and performance of stone columns, discovering that the Effective Stress Concentration Ratio (ESCR) for GESCs rises as consolidation progresses. Soil permeability plays a significant role in the treated ground's behavior and the post-construction settlement of soft clays.

2.4 STONE COLUMN CONSTRUCTION METHODS

There are two primary techniques for creating a stone column: the displacement method and the non-displacement method, also known as the replacement method. The replacement method involves backfilling the borehole with granular material, while the displacement method involves laterally displacing the surrounding soil and backfilling it with the new material. These techniques are detailed in IS 15284 (Part -1): 2003. Other commonly used construction methods include the rammed stone column (Datye and Nagaraju, 1981), the simple boring method (Ranjan and Rao, 1983), and the vibro-compaction method.

2.4.1 Displacement Method of Construction

In the displacement method of stone column construction, the process begins by lowering a vibrator into the soft soil. This action creates a void in the ground, which is then filled with stone aggregates. The aggregates are compacted by vibrating them into a dense state as the vibrator is reinserted. This technique reduces the compressibility and settlement of the ground, while simultaneously improving its stiffness, shear strength, and bearing capacity (Charles and Watts, 1983). The most effective results are typically achieved when a bearing stratum is present (Barksdale

and Bachus, 1983).

2.4.2 Replacement Method of Construction

As illustrated in Figure 2.3, the replacement method, involves the creation of a cavity using strong air or hydraulic pressure, which removes the soft soil. This soil is then replaced with stone aggregates. The remaining steps are similar to the displacement method: stone aggregates are backfilled gradually and compacted using a vibrator to ensure uniform density.

A simple technique developed by Rao (1982) and Ranjan and Rao (1983) is particularly beneficial for use in developing countries. In this method, a borehole is made using a spiral auger and manual labor. Once the borehole reaches the required depth, it is thoroughly cleaned. Layers of powdered material are placed in the borehole, with each layer measuring 300–500 mm and separated by 50–100 mm layers of sand. To provide the necessary compaction, a power winch operates a 125 kg cast-iron hammer with a diameter smaller than the borehole. This hammer applies compactive force to the granular material, while s/and fills the gaps left during the compaction process, causing the surrounding soil to become fully compacted.

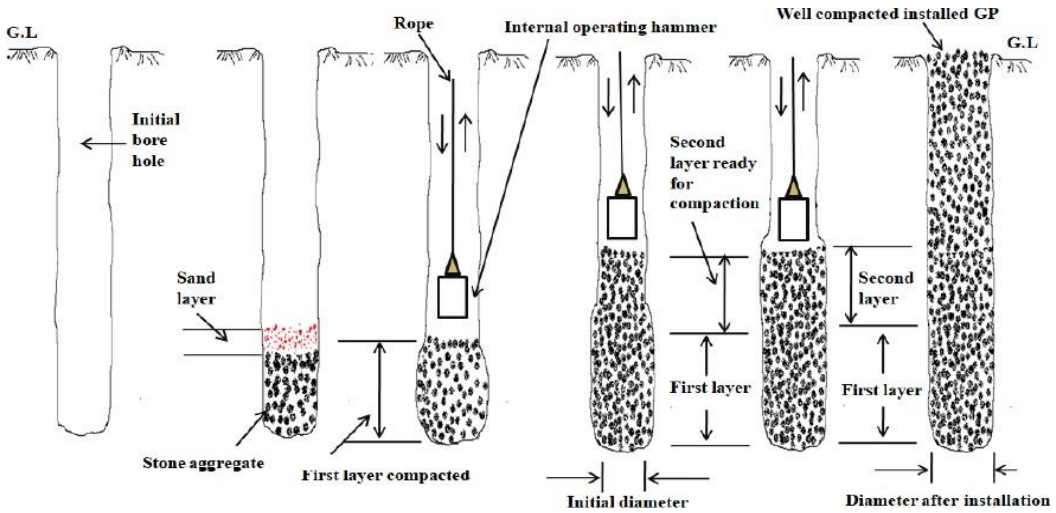

Figure 2.3. Granular pile construction using an easy auger boring technique (Rao, 1982)

2.5 FAILURE MECHANISM OF STONE COLUMNS

2.5.1 Mechanism of Load Transfer of Stone Columns

In geotechnical analysis, two key loading and displacement conditions are considered optimal: equal strain and equal stress. These conditions are commonly encountered in both flexible and rigid loading scenarios. Flexible loading, such as tire pressure, and rigid loading, such as a rigid footing, are examples of these conditions.

Stress concentration ratio (n), which is frequently used to characterise the transfer of load between columns and soft soils, is known as the ratio of the stress over the column (σ_c) to that over the soil (σ_s). In contrast, under an equal stress condition, the soil and columns have different settlements (i.e., $S_{sl} > S_{cl}$) but bear the equal stress (i.e., n = 1). The consequence is a difference in settlement between the soil and the columns. (Figure 2.4)

In practical terms, the stone columns undergo more stress than the surrounding soil because they are stiffer and more resistant to deformation. This causes a greater share of the applied load to be transferred to the columns rather than the surrounding soil, thereby enhancing the overall load- bearing capacity and reducing the settlement of the foundation.

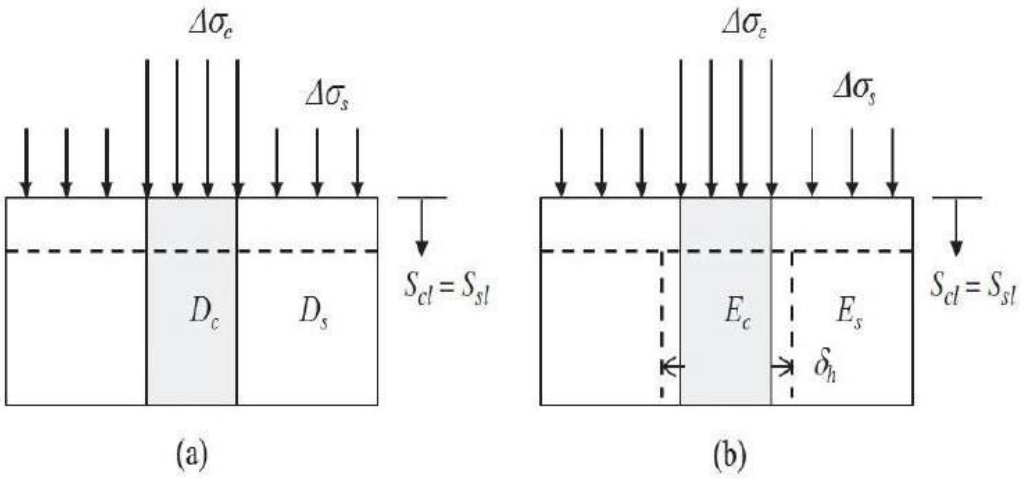

Figure 2.4. (a) Unit cells that are not deformed laterally (b) Unit cells that are deformed laterally (Han, 2015)

2.5.2 Failure Modes of Stone Columns

Generally, two different sorts of columns that are built, depending on their length and the resistance forces that are created within them (Barksdale and Bachus, 1983):

- End-bearing, or reaching the entire depth of a hard, sustaining stratum and
- Floating (partial depth), resisting pressures by side friction

Figure 2.5, shows that the slenderness ratio, which is the ratio of the column's diameter to its length, determines whether the columns are long or short (McKelvey et al., 2004). Failures of the following kind might occur:

a. Bulging failure: the column has been limited from the top to the lower solid layer. The column's lateral length increases as a result of its resistance to the approaching load. Equilibrium has been achieved as the surrounding material is now under stress rather than the bulged area.

b. Short columns ($L/D<6$) situated above a bearing stratum may experience local shear failure. L and D stand for the column's length and diameter, respectively, in these columns (McKelvey et al., 2004).

Short columns in weak strata may fail in end bearing or punching before the bulging occurs inside the critical length, and both floating and end-bearing columns may fail in bulging (Hughes and Withers, 1974). It is crucial to consider the potential for local bearing capacity failure before bulging when constructing a short end bearing column, especially if the column is supported by weak strata. Punching shear failure may occur if the columns are not lowered to an appropriate depth (Barksdale and Bachus, 1983).

An ordinary column may help a stone column in many ways if it is encased in the proper geosynthetic material. According to Murugesan and Rajagopal (2009), it can, for instance, provide more lateral confinement, function as a semirigid element to facilitate load transfer to deeper depths, minimize stone loss by preventing stones from being squeezed into nearby soft clays, allow for a higher degree of compaction than with traditional stone columns, promote vertical drainage by acting as an efficient filter, maintain the aggregates' frictional qualities, and increase the

shear resistance of the stone column.

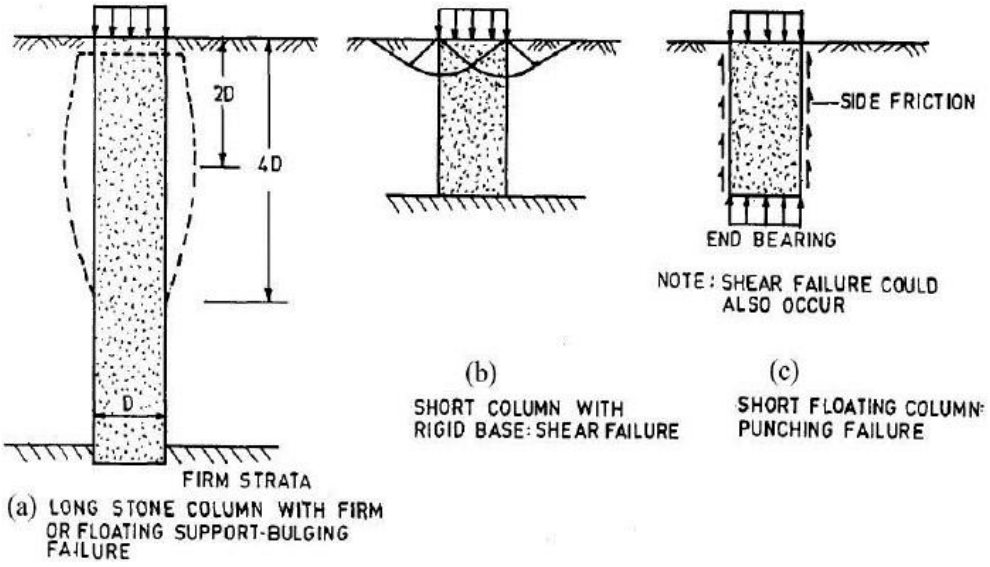

Figure 2.5. Failure mechanisms for a stone column in cohesive soil that is not homogeneous (IS 15284)

2.6 DESIGN OF STONE COLUMNS

Conventional (unencased) and geosynthetic-encased stone columns are the two main varieties of stone columns. Bearing capacity and settling studies ought to be divided into the two groups described above.

2.6.1 Ordinary Stone Columns

2.6.1.1 Enhanced Bearing Capacity in Stone Columns: A Review

Many researchers have explored how stone columns can improve the load-bearing performance of foundations. Their studies indicate a clear correlation between the frictional characteristics of the column material and the degree of lateral support provided by the surrounding soil. In an experimental study, Hughes and Withers (1974) examined the deformation behavior around a stone column embedded in kaolin clay. They observed that the column tends to bulge within a zone extending up to four times its diameter from the top of the column. Moreover, both the stone column and the adjacent soil contribute jointly to resisting the vertical load. These insights laid the groundwork for future developments in the design and analysis of

stone columns.

Hughes et al. (1975) proposed a failure mechanism involving both the surrounding soil and the stone column itself, characterized by a triaxial stress condition within the column. This theory was based on the earlier laboratory model tests conducted by Hughes and Withers (1974). In their framework, the confining stress (σ_{rL}) refers to the maximum radial pressure that the surrounding soil can exert to laterally support the column. The ultimate vertical stress the column can sustain (σ_v) is then determined by multiplying this confining stress by the passive earth pressure coefficient (K_{ps}) specific to the granular material of the column. The load-settlement curve that was acquired for their investigation is presented in the Figure 2.6 and the setup in Figure 2.7.

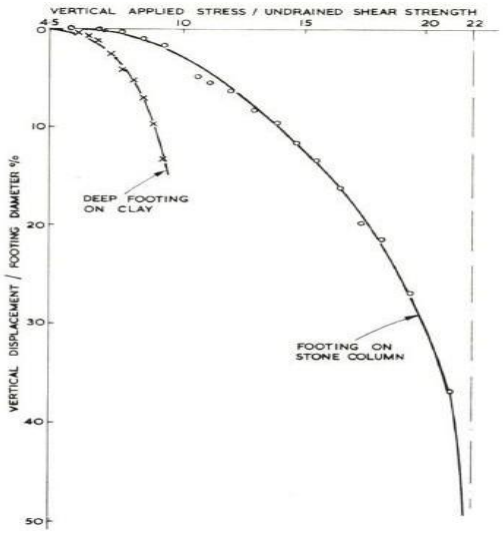

Figure 2.6. Load-Settlement curve (Hughes and Withers, 1974)

$$\sigma_v = \sigma_{rL} \frac{(1- sin\phi')}{(1+ sin\phi')} \quad (2.2)$$

$$K_{ps} = \frac{(1- sin\phi')}{(1+ sin\phi')} \quad (2.3)$$

where, σ_{rL} = Limiting radial stress,

ϕ' = Frictional angle of stone column aggregates,

K*ps* = Coefficient of passive earth pressure of the soil.

$$\sigma_{rL} = 4c_u + \sigma_{ro}, + u_o \quad (2.4)$$

where, σ_{ro}, = Initial radial effective stress around the column,

σ_{rL} = Total limiting radial stress of the column,

u_o = Initial excess pore-pressure,

c_u = Undrained shear strength of soil.

For the analysis of a solitary stone column present in a saturated soft clay stratum under the undrained conditions, Brauns (1978) suggested a convenient method to calculate the confining stress of the neighbouring soil.

$$\sigma_r = (\Delta\sigma_s + \frac{\Delta c_u}{sin2\Psi})(1+ \frac{tan\Psi_p}{tan\Psi}) \quad (2.5)$$

where, σ_r = Lateral confinement from the neighbouring soil,

Ψp = Column passive failure plane angle,

Ψ = Angle of surrounding soil failure plane,

c_u = The surrounding soil's undrained shear strength.

According to Equation (2.5), the confining stress varies with the soil failure plane's angle. Finally, the confining stress can be determined by taking the derivative of the previous equation with respect to the failure plane angle and setting it equal to zero. The granular column's coefficient of passive earth pressure (K_p) multiplied by the confining stress gives the ultimate vertical stress that the column is capable of withstanding (σ_c).

$$\sigma_c = K_p \times \sigma_r \quad (2.6)$$

where, σ_c = Ultimate vertical stress,

K_p = Coefficient of passive earth pressure of the stone column

Barksdale (1987) suggested that both the stone column and the surrounding soil reach their strength under the same level of strain, a condition known as the equal strain approach. Based on this assumption, he expressed the ultimate bearing capacity of the composite foundation (q_{ult}) with the following equation:

$$q_{ult} = q_{ult,c} \times A_s + q_{ult,s} \times (1 - A_s) \quad (2.7)$$

Here, As represents the area replacement ratio, $q_{ult,c}$ is the column's ultimate bearing capacity, and $q_{ult,s}$ is the ultimate bearing capacity of the surrounding soil. Barksdale further proposed approximating qult,s as $5c_u$, where cu is the undrained

shear strength of the surrounding clay. Substituting this into Equation (2.7) simplifies it to:

$$q_{ult} = 5c_u \times (3A_s + 1) \quad (2.8)$$

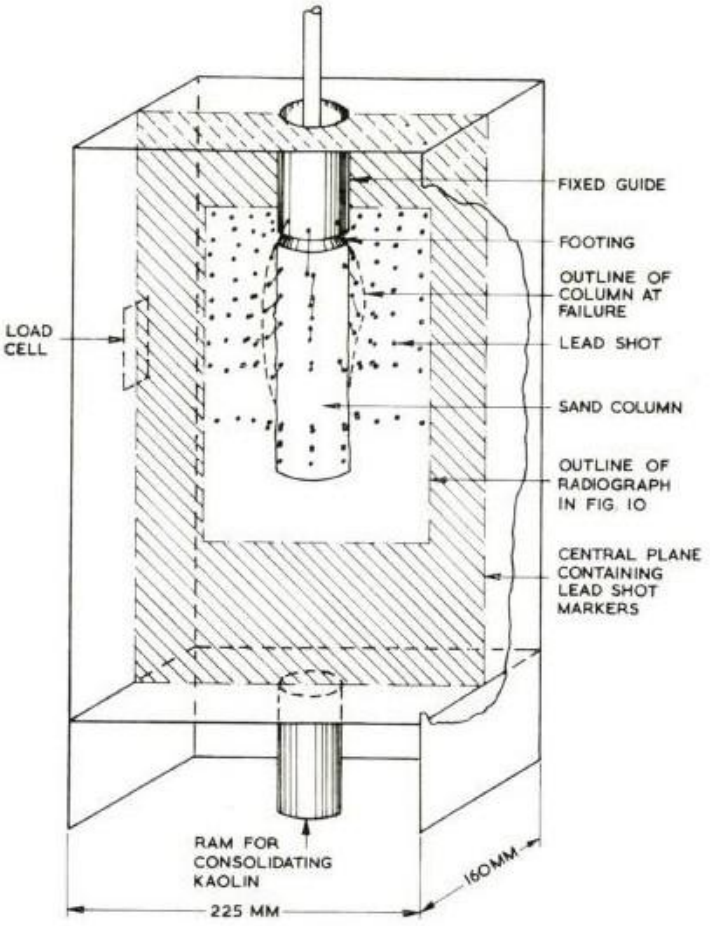

Figure 2.7. Consolidometer test on single stone column (Hughes and Withers, 1974)

IS Code Method (IS 15284 Part 1: 2003)

(1) Capacity Determined by Column Bulging

$$\sigma_v = \sigma_{rl} \,.\, K_{pcol} \quad (2.9)$$

where, σ_v = Limiting axial stress generated in the column when it gets closer to shear failure because of bulging,

σ_{rl} = Limiting radial stress

$$\sigma_{rl} = \sigma_{ro} + 4c_u \quad (2.10)$$

K_{pcol} = Column's passive earth pressure coefficient

$$\sigma_v = (\sigma_{ro} + 4c_u)\, K_{pcol} \quad (2.11)$$

σ_{ro} = Initial effective radial stress

c_u = Undisturbed undrained shear strength of the clay around the column.

$$\sigma_{ro} = K_o\ \sigma_{vo} \quad (2.12)$$

K_o = For clay soils, the mean lateral earth pressure coefficient has a value of 0.6, or alternatively, it can be calculated using the formula K_o = 1-sinϕ_s, where ϕ_s is the effective angle of soil's internal friction.

σ_{vo} is the average initial effective vertical stress, calculated by taking the column's diameter (γ2D) twice as the average bulging depth.

γ = The soil's effective unit weight in the influence zone,

D = Diameter of the column.

$$K_o = 1\text{-}\sin\phi \quad (2.13)$$

$$K_{pcol} = \tan^2 (45° + \phi_c/2) \quad (2.14)$$

Safe load on column alone,

$$Q_1 = (\sigma_v . \frac{\pi}{4} D^2) /2 \quad (2.15)$$

where, 2 is the factor of safety.

(2) Surcharge Effect

$$\Delta \sigma_{ro} = q_{safe} (1 + 2\ K_o) / 3 \quad (2.16)$$

q_{safe} = Soil safe bearing pressure with a 2.5 safety factor $q_{safe} = C_u\ N_c / 2.5$

C_u = Undrained shear strength,

N_c = Terzgahi bearing capacity factor.

For a safety factor value of 2, increase in the safe load due to surcharge,

$$Q_2 = Kp_{col} . \Delta \sigma_{ro} . A_s / 2 \quad (2.17)$$

(3) Intervening soil support

For a column, area of the intervening soil,

$$A_g = 0.866\ S^2 - \pi/4\ D^2 \quad (2.18)$$

Safe load supported by the intervening soil,

$$Q_3 = A_g . Q_{safe} \quad (2.19)$$

(4) Total safe load on every column and the surrounding soil

$$Q = Q_1 + Q_2 + Q_3 \quad (2.20)$$

Ambily and Gandhi (2007) conducted an in-depth study on the behavior of both single and group end-bearing stone columns under various influencing factors, such as column spacing, the undrained shear strength of soft clay, and different loading conditions. Two types of loading scenarios were tested: (i) loading confined to the stone column area (to assess its load-bearing capacity), and (ii) loading applied across the full unit cell area (to evaluate improved ground stiffness).

Stone columns used in the study had dimensions of 100 mm in diameter and 450 mm in height. Model tests were conducted using tanks ranging from 210 mm to 420 mm in diameter for single columns, and a large tank of 835 mm diameter for a group of seven columns, maintaining required spacing. Soft clay with undrained shear strengths of 7, 14, and 30 kPa was used as the foundation material. Stone aggregates (2–10 mm size) were installed using a light compaction method to minimize bulging during construction.

Axial stresses between 100 and 150 kPa were applied until settlements exceeded 10 mm. Bulging was observed at a depth of 0.5 times the column diameter when only the column was loaded, but not when the full area was loaded—indicating the effectiveness of confinement from surrounding soil in group scenarios.

Finite Element Method (FEM) analysis using PLAXIS (with 15-noded triangular elements) was performed to validate experimental results. The stress-settlement relationship was found to be consistent across different shear strengths for single column loading at a constant spacing-to- diameter (s/d) ratio. It was noted that as the s/d ratio increased to 3, the limiting axial stress decreased significantly, beyond which the change became negligible.

The study introduced a stiffness improvement factor, defined as the ratio of treated to untreated ground stiffness. This factor was influenced by the s/d ratio but

remained unaffected by the clay's shear strength. For s/d ratios greater than 3, no substantial stiffness improvement was observed. Behavior of column groups was found to closely align with that of single columns for s/d ratios up to 3, validating the use of the unit cell concept in modeling.

FEM analysis also helped in evaluating the stress concentration ratio across both single and group column setups. Results showed consistent stress concentration in both cases, further supporting the reliability of the unit cell approach. Additionally, stress concentration on the stone column was observed to increase as the surrounding soil's shear strength decreased.

2.6.1.2 Studies on the reduction of settlement in ordinary stone columns

Over the last three decades, numerous methods have been developed to predict the settlement behavior of weak soil layers reinforced with stone columns. One of the foundational approaches was introduced by Priebe (1976), who considered the stone column as a rigid-plastic, incompressible, and end-bearing element. He demonstrated that, under these assumptions, the stress concentration ratio ($n = q_p/q_s$), which is the ratio of stress carried by the column to that carried by the surrounding soil, decreases proportionally with $1/\alpha$, where α represents the earthquake design reduction factor.

Using the unit cell concept, Priebe formulated a fundamental improvement factor method illustrated in Figure 2.8, This method accounted for the following key parameters:

- Poisson's ratio (μ) of the surrounding soil
- Friction angle (φ) of the column material
- Area replacement ratio (Ar), which is the ratio of the column area to the area of the unit cell

The elastic soil in the unit cell was assumed to undergo oedometric (one-dimensional) settlement, leading to the derivation of a simplified expression for the settlement reduction or improvement factor, which estimates how much the

settlement of the ground is reduced due to the inclusion of stone columns. Following the previous figure's improvement factor (I_f) computation, the decreased settlement can be computed using the formula below:

$$S' = \frac{S_u}{I_f} \tag{2.21}$$

$$I_f = 1 + A_r \left[\frac{0.5 + f(\mu, A_r)}{(K_a)_s \, f(\mu, A_r)}\right] \tag{2.22}$$

$$f(\mu, A_r) = \left[\frac{1-\mu^2}{1-\mu-2\mu^2}\right] \left[\frac{(1-2\mu)+(1-A_r)}{1-2\mu+A_r}\right] \tag{2.23}$$

$$K_a = \tan^2(45 - \phi/2) \tag{2.24}$$

where, S′ = The introduction of granular columns results in lesser settlement,

S_u = Untreated settlement in the foundation

Under the influence of larger loading area, S_u can be obtained as:

$$S_u = m_v . \Delta\sigma_z . h \tag{2.25}$$

where, m_v = Soil's volumetric compressibility coefficient,

h = Thickness of the soil layer,

$\Delta\sigma_z$ = Pressure due to surcharge.

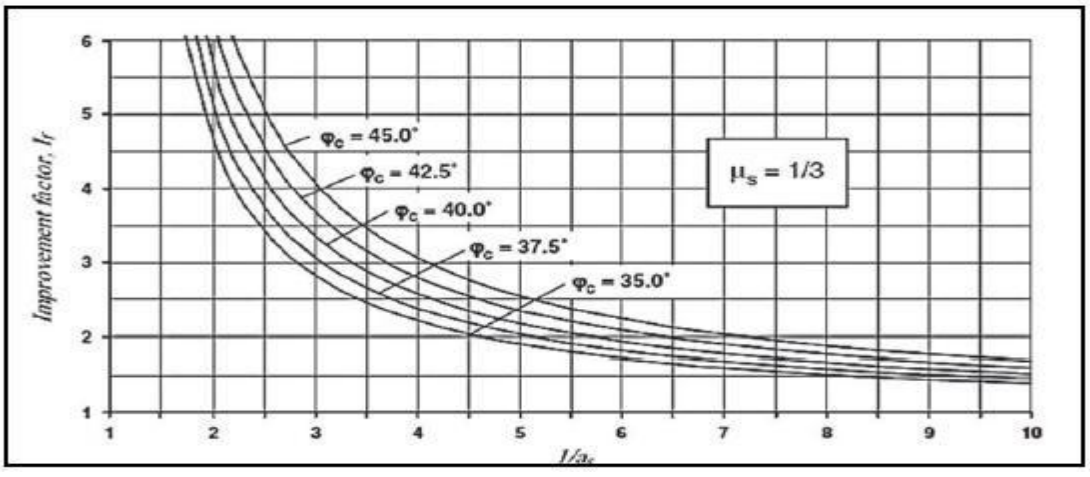

Figure 2.8. Chart for Improvement Factor (Priebe, 1976)

Building on the unit-cell concept, Aboshi et al. (1979) analyzed a scenario where the vertical displacement in both the stone column and the surrounding soil is assumed to be equal, implying a condition of equal settlement. They also considered that the

total vertical load applied at the surface is shared between the column and the soil, maintaining equilibrium. A key assumption in their analysis was that the vertical stress remains uniform along the entire length of the stone column. This simplification allowed for easier calculation of load distribution between the column and the surrounding soft soil while adhering to the equal strain principle.

The replacement factor (A_r) and stress concentration ratio (n) have been linked to the settlement reduction ratio (R). The total settlement (S_t) is determined as:

$$S_t = m_v (\mu_c.\sigma) H \quad (2.26)$$

where, m_v = Soil's volumetric compressibility coefficient,

σ = Unit normal stress,

H = the height of stone column.

The settlement reduction ratio, R was given by

$$R = \mu_c = \frac{1}{1+(n-1)A_r} \quad (2.27)$$

IS Code Method (IS 15284 Part1:2003)

Consolidation settlement of the treated composite soil S_t, is given as:

$$S_c = m_v \sigma_z h \quad (2.28)$$

$$\sigma_z = \sigma / \{1 (n - 1) a_s\} \quad (2.29)$$

where, m_v = Coefficient of volume compressibility,

σ_z = Vertical stress in the neighbouring ground,

h = Thickness of the treated soil,

σ = Applied stress,

n = Stress concentration factor / ratio,

a_s = Area replacement ratio.

In their research, Han and Ye (2001, 2002) developed a theoretical method to estimate the consolidation rate of foundations reinforced with granular (stone) columns. Their method notably incorporates two critical factors often overlooked in simpler models:

1. Smear Zone – This refers to the disturbed zone of soil around the stone column, formed due to the intrusion of column material into the surrounding

soft soil during installation. This disturbed zone has lower permeability, affecting the rate at which pore water dissipates during consolidation.

2. Well Resistance – This accounts for the reduction in permeability within the stone column itself, caused by clay particles migrating into the column material, which can restrict water flow and delay consolidation.

In their 2002 work, Han and Ye expanded on their earlier simplified model (2001) by introducing a more comprehensive unit cell model which includes these real-world effects to more accurately simulate the drainage and consolidation behavior of the improved ground. (Figure 2.9)

Han and Ye (2002) developed a theoretical method to evaluate the consolidation rate of foundations reinforced with granular columns, taking into account key real-world factors like the smear zone and well resistance. Their model includes various unit cell components such as the equivalent diameter (d_e), elastic moduli of the soil (E_s) and column (E_c), and permeabilities in both the radial and vertical directions (k_r and k_v), along with those of the stone column (k_c) and the smear zone (k_s). Geometric parameters include the radius of the stone column (r_c), the equivalent radius of the unit cell (r_e), the radius of the smear zone (d_s), and the thickness of the soil layer undergoing consolidation (H), with pore pressure depth denoted by z.

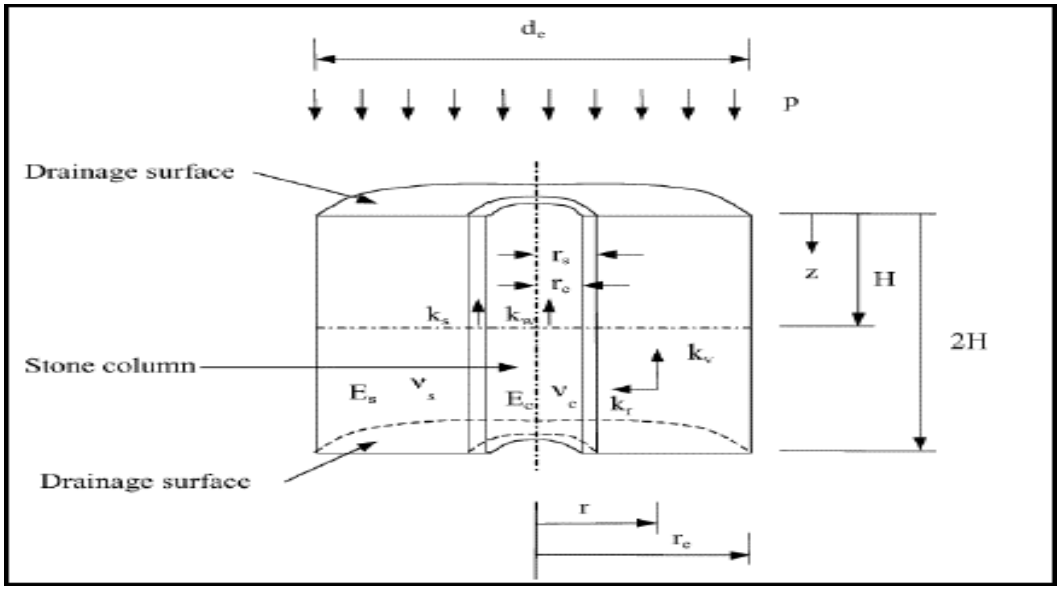

Figure 2.9. Unit cell model (Han and Ye, 2002)

A parametric analysis was carried out to assess six variables affecting the consolidation rate. First, an increase in column diameter reduces the diameter ratio ($N = d_e/d_c$), thereby shortening the drainage path and accelerating consolidation. Second, the permeability of the stone column (k_c) may decrease due to clogging by fine soil particles during installation, which raises the k_r/k_c ratio and slows the consolidation process. Third, the stress concentration ratio ($n_s = \sigma_c/\sigma_s$) increases as more load is taken by the column, promoting faster radial consolidation. Fourth, a larger smear zone ($S = d_s/d_c$) reduces the surrounding soil's permeability, which delays the consolidation rate. Fifth, the smear zone's permeability (k_s) often drops due to structural changes and damage to horizontal drainage paths during installation, leading to a significant slowdown in pore pressure dissipation. Lastly, an increase in the thickness of the soil layer (H) elongates the drainage path, thereby decreasing the average rate of consolidation. These findings highlight the importance of optimizing column design, installation technique, and soil improvement strategies to enhance the overall consolidation performance.

Kolekar and Dasaka (2014) introduced an innovative gravity loading method using lever arm technology to generate large, uniformly consolidated clay bed samples without the need for placing heavy dead weights directly on the clay surface (as shown in Figure 2.10. In their approach, clay beds were first prepared in a slurry state and then subjected to consolidation through a controlled gravity loading system. Two separate test series, labeled Series A and B**,** were conducted, each comprising seven individual tests**.** The clay beds in both series were consolidated under applied pressures of 18 kPa, 36 kPa, and 72 kPa**,** respectively. The results showed that the coefficients of variation (COV) for both the measured shear strength and recorded water content of the consolidated clay beds remained below 10%**,** indicating a high level of consistency and uniformity in the sample preparation process, which is considered acceptable for geotechnical testing.

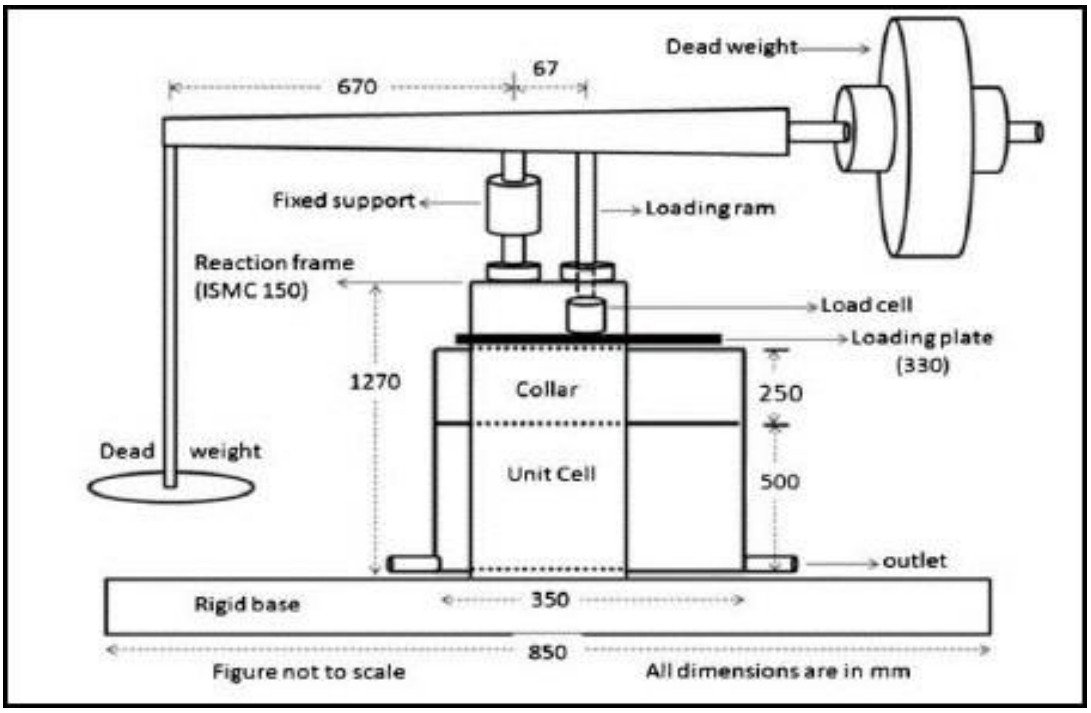

Figure 2.10. The response frame's schematic diagram (Kolekar and Dasaka, 2014)

Deb and Shiyamalaa (2015) proposed a mathematical model that accounts for the particle migration-induced blockage when estimating the consolidation rate of soil improved by stone columns. The model considers that fine particles and impurities in the soil, along with fluid in the pores, can be displaced during consolidation. These fluid-containing particles move out of the soil and into the surrounding stone column, leading to clogging in the column material. The extent of clogging is determined by the concentration of particles in the seepage water**,** which in turn reduces the permeability of the stone column**.** This reduction in permeability slows down the consolidation rate of the ground improved by stone columns. The study focuses on a single stone column and its area of influence, represented as a unit cell. The unit cell is cylindrical, with a circular ring of soil surrounding the stone column as seen in Figure 2.11. The unit cell is divided into four distinct zones: the soil zone, the smear zone**,** the clogged zone**,** and the unclogged zone**.** These zones represent the areas affected by the stone column, with particular attention given to the impact of clogging on consolidation behavior.

As seen in Figure 2.12, the results of the study by Deb and Shiyamalaa (2015) are

compared with various existing models that estimate the consolidation rate for stone column-improved ground, both with and without the effects of clogging. The study also investigates how several parameters influence the consolidation rate in the model. Notably, it was observed that as clogging increases, both the diameter ratio and stress concentration ratio also increase, indicating that higher clogging leads to changes in the stone column's geometry and the load distribution, which affects the consolidation process.

In a related study, Rangeard et al. (2016) conducted an experimental investigation on the settlement of clay reinforced with sandy columns under continuous pressure. This research focused on the impact of the construction method and compaction force during the installation of sand columns on the hydromechanical behavior of the soil-column system. The sand used for the columns had particles ranging from 1 to 1.25 mm, while the kaolin soil (CH), which is a type of clayey soil, was selected as the foundation material. To prepare the soil bed, the wet kaolin bed was subjected to continuous pressure for a specified period, simulating the conditions under which soft soils typically undergo consolidation and improvement through stone or sand columns.

The study investigated how different methods of installing sand columns affect the behavior of kaolin clay. These methods varied depending on whether the clay was displaced and whether the sand was compacted. The approaches included NR-NC (no clay displacement and no sand compaction), NR-WC (no displacement but with sand compaction), and WR-WC (with displacement and compaction). Across all cases, the area replacement ratio was kept between 1% and 6%.

One of the key findings was that the clay surrounding the sand columns experienced localized densification. This densified zone extended about one column radius from the column itself. As a result, the permeability of the clay in this area decreased, and its coefficient of consolidation increased. However, this localized change did not significantly influence the rapid drainage that occurred during the sand column installation process.

To assess how the reinforcement affected settlement, the study used a parameter called the settlement reduction rate (T_r), calculated using the formula $T_r = [(\Delta h_{ur} - \Delta h_r) / \Delta h_r] \times 100$, where Δh_{ur} is the settlement without reinforcement and Δh_r is the settlement with reinforcement. It was observed that T_r increased as the column diameter increased, regardless of the construction method. However, the effectiveness of settlement reduction also depended on the installation approach. The WR-WC method, which involved both displacing the clay and compact the sand, was found to be the most effective. The NR-WC method also showed improved performance over NR-NC, highlighting the importance of sand compaction even when the clay is not displaced.

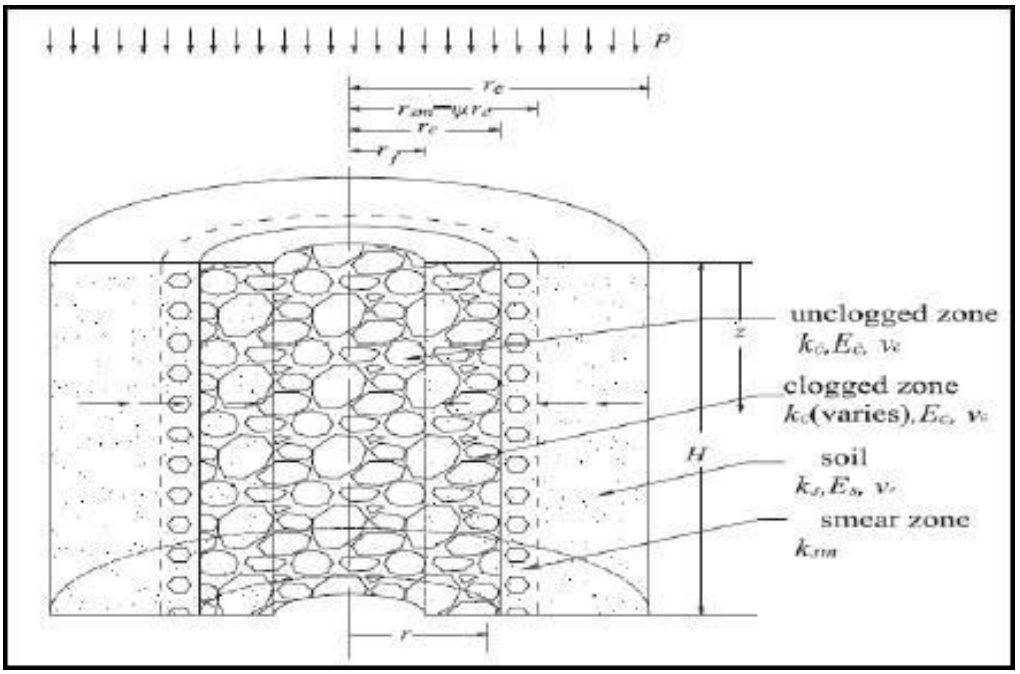

Figure 2.11 Unit cell cross section (Deb and Shiyamalaa, 2015)

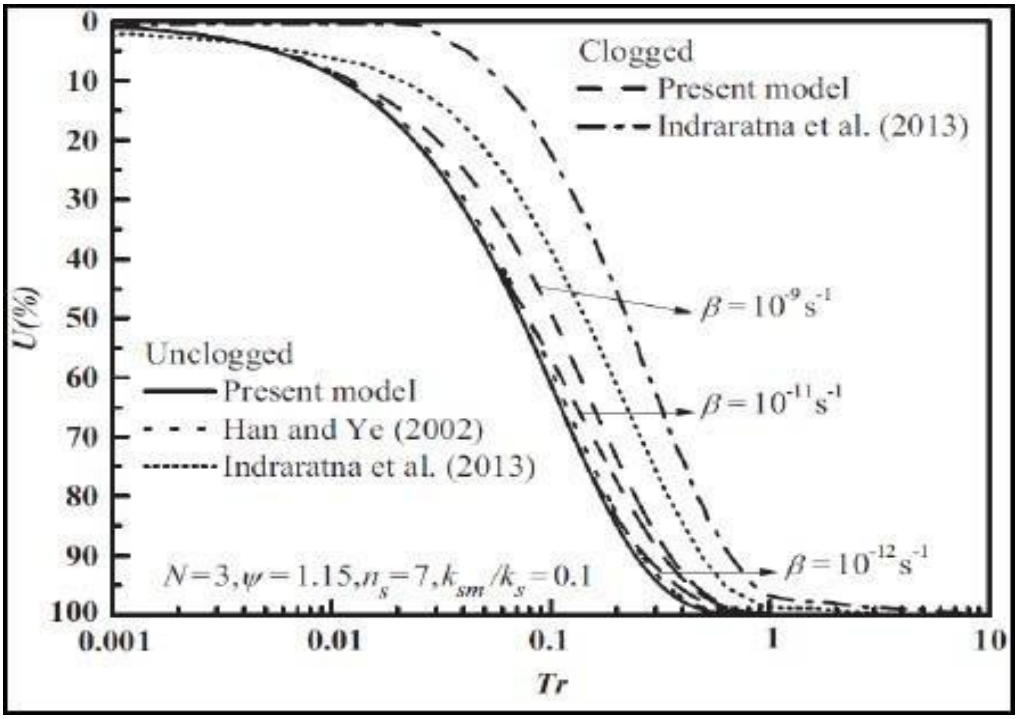

Figure 2.12 Calculated rate of consolidation compared with various methods (Deb and Shiyamalaa, 2015)

Finally, it was noted that the time required for settlement to begin was nearly the same for all methods and column sizes, indicating that the initiation of settlement is not significantly influenced by the installation technique.

Chardrawanshi (2018) examined the settlement behavior of extremely soft soils, characterized by an undrained shear strength ranging from 2.5 to 7.5 kPa, under sustained loading conditions of 100, 150, and 200 kPa for a minimum duration of thirty hours. Notably, IS 15284 (Part 1): 2003 does not provide guidance for evaluating the settlement of such soft soils with undrained shear strength below 7 kPa. To address this, Chardrawanshi developed design charts (Figure 2.13) based on specific area replacement ratios observed in the field, which can be used to determine the expected settlement reduction ratio (SRR). Stone columns, used in this context, enhance the consolidation of the composite foundation by offering shorter radial drainage paths in addition to the vertical ones, thanks to the high permeability of the column material. Furthermore, due to their significantly higher stiffness compared to the surrounding soil, stone columns are able to absorb

a greater share of the vertical load. This reduces the load on the surrounding weaker soil and accelerates the overall consolidation process.

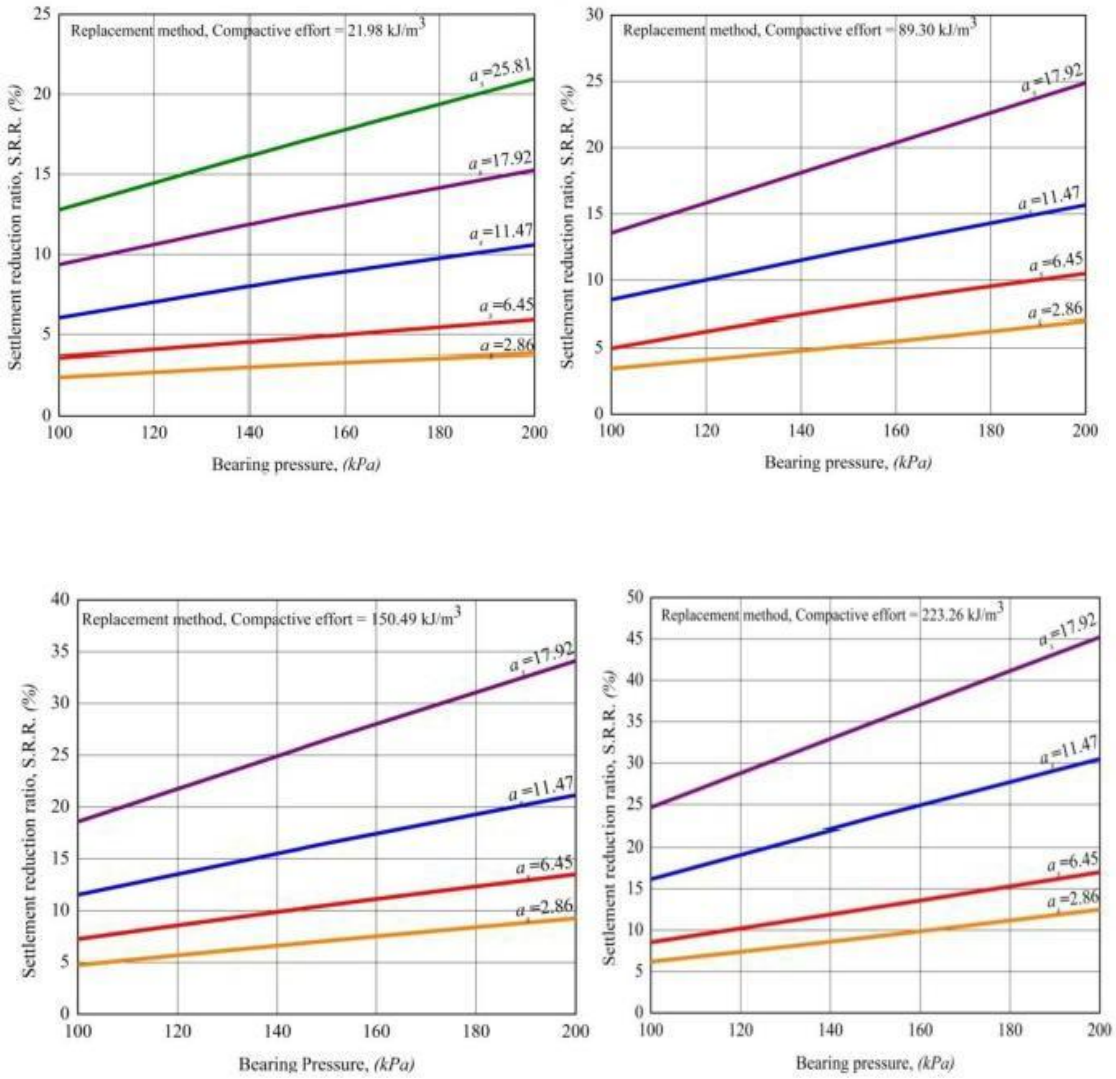

Figure 2.13. S.R.R. vs. Bearing pressure for various compactive effort (Chardrawanshi, 2018)

2.6.1.3 Limitations of Ordinary Stone Columns

The application of stone columns, while beneficial in many ground improvement scenarios, is subject to certain limitations under specific soil conditions. One such limitation arises in soils with high organic content—particularly those containing peat layers that exceed the diameter of the stone column. As noted by Waltham (2009), these soils can hold moisture up to ten times their weight, which may

lead to significant long-term settlements due to the gradual dissipation of excess pore water pressure. Furthermore, Priebe (2005) emphasized that stone columns should not be used in soils with an undrained shear strength (cu) of less than 15 kPa, as these soils may lack the necessary strength to support the installation process. Lastly, McCabe et al. (2009) warned that long-term settlements must be carefully considered in the design phase to avoid unexpected failures. Soils such as loose fills and soft clay fills are particularly prone to ongoing settlement, which can undermine the effectiveness of the improvement technique over time.

2.6.2 Geosynthetic Encased Stone Column

Stone columns serve multiple functions in ground improvement, including densification of the soil, enhancement of drainage, reinforcement, and material replacement. While most soils and geomaterials possess good strength in compression and shear, they tend to be weak in tension. To address this, geosynthetics—such as geotextiles and geogrids—are often used to provide tensile resistance. These materials also act as separators between incompatible materials, preventing mixing and thereby preserving the integrity of both layers. This separation reduces the "smear zone" between the column and the surrounding soft soil, effectively enhancing the performance of the stone column (Han and Ye, 2002).

The use of geosynthetic encasement significantly improves the load-bearing capacity of stone columns, especially in very soft soils. The typical tensile stiffness of these encasements ranges from 1500 to 6000 kN/m, while their ultimate hoop tensile strength varies between 100 and 400 kN/m. Geosynthetic-encased stone columns are particularly suitable for soils with undrained shear strengths between 5 and 15 kPa, whereas conventional (non-encased) stone columns are more effective in soils with shear strengths above 15 kPa (Han, 2015). These encased columns are generally installed to depths ranging from 5 to 10 meters.

Moreover, geosynthetic-encased stone columns demonstrate high stress concentration ratios, with values reaching up to 8.5, according to Castro et al. (2013). However, one potential failure mode for these systems is the rupture of the

geosynthetic encasement under excessive stress. For design purposes, Alexiew and Thomson (2013) recommend an area replacement ratio between 0.1 and 0.2 for encased stone columns.

2.6.2.1 Bearing Capacity Enhancement of Geosynthetic-Encased Stone Columns

Malarvizhi and Ilamparuthi (2004) conducted an experimental study to examine the load-settlement behavior of stone columns both with and without geogrid encasement. The investigation considered various influencing factors, including the length-to-diameter (l/d) ratio and the type of geogrid material used. Granite stone chips were selected as the column material, while marine clay was used to simulate a soft soil foundation. The study employed three different geogrid types, each with distinct aperture sizes and tensile strengths, to assess their effect on column performance.

The results revealed that the load-carrying capacity of stone columns improved significantly with the increase in the length of the geogrid encasement, regardless of whether the column was end- bearing or floating. The stiffer the encasing material, the higher the ultimate load capacity achieved. In soft clay beds, the ultimate load capacity of geosynthetic-encased stone columns was observed to be approximately three times greater than that of the untreated ground, whereas conventional stone columns achieved about a twofold increase. Furthermore, encased stone columns were found to be more effective in minimizing settlement compared to their non-encased counterparts.

Murugesan and Rajagopal (2006) conducted a comprehensive parametric study using finite element analysis to assess the improvements in the load-bearing capacity of stone columns when encased with geosynthetics. Their study provided both qualitative and quantitative insights, highlighting that encased stone columns significantly outperform conventional stone columns in terms of load capacity. The encased columns exhibited reduced vertical compression and less lateral bulging under load, which was attributed to the increased lateral confining pressure provided by the encasement. The analysis showed that encasing just the upper

portion of the column—up to a height of twice its diameter—is sufficient to substantially enhance its performance. Furthermore, the results indicated that the load-bearing capacity of the encased column improves progressively with the stiffness of the encasing material, underscoring the importance of selecting appropriate geosynthetics for optimal reinforcement.

Murugesan and Rajagopal (2010) extended their previous work by conducting a detailed parametric study using finite element analysis to further explore the enhancement in load-bearing capacity of stone columns due to geosynthetic encasement. Their findings reaffirmed that encased stone columns outperform conventional stone columns by demonstrating significantly higher load capacities, reduced vertical deformation, and minimized lateral bulging. This improvement is attributed to the greater lateral confining pressure generated by the geosynthetic encasement.

Their study also emphasized that the improvement in load-carrying capacity is positively correlated with the stiffness of the encasing material—the stiffer the geosynthetic, the more substantial the performance gain. To model the enhanced bearing capacity, they proposed a method that incorporates the additional confinement provided by the geosynthetic encasement. For the purposes of calculation, they assumed a bulging length equivalent to four times the diameter of the stone column. This assumption helped in developing a more realistic and practical estimation of bearing capacity, tailored to account for the mechanical interaction between the column and the encasement.

$$q_{ult,c} = (\sigma_{ro} + 4c_u + \sigma_{r,g})K_p \qquad (2.30)$$

where, σ_{r0} = The initial radial stress of the surrounding soil;

K_p = The coefficient of passive earth pressure of the granular material.

The extra confinement that the geosynthetic ($\sigma_{r,g}$) provides is directly proportional to the encasement's hoop tensile strength (T_g), which may be computed as follows:

$$\sigma_{r,g} = 2T_g/d_c \quad (2.31)$$

The hoop strain (ε_g) and stiffness modulus (J) of the geosynthetic can be used to compute the geosynthetic hoop tensile strength as follows:

$$T_g = J.\varepsilon_g \quad (2.32)$$

$$\varepsilon_g = \frac{1-\sqrt{1-\varepsilon_a}}{\sqrt{1-\varepsilon_a}} \quad (2.33)$$

where, ε_a = the compressive strain of the column vertically (vertical compression divided by the bulging length).

Kumar and Jain (2013) explored the load-settlement behavior of soft expansive black cotton soil, characterized by an unconfined compressive strength (UCS) of 50 kPa, using the granular pile technique. Sand was used as the column material, and end-bearing piles with diameters of 50 mm, 65 mm, and 80 mm were constructed through the replacement method. These piles were installed in cylindrical test tanks with corresponding spacing-to-diameter (s/d) ratios of 3.3, 3.2, and 3.5. The researchers assessed performance by placing a footing on test beds containing both regular granular piles and granular piles encased in geogrid.

Test results revealed significant improvements in load-bearing capacity: regular granular piles supported approximately 300% more load than the untreated clay base, while geogrid-encased granular piles supported up to 470% more. Furthermore, when comparing the two types of piles, encased granular piles were able to support 25% to 50% more load than their non-encased counterparts, highlighting the added benefit of geosynthetic encasement in enhancing the performance of granular piles in soft expansive soils.

In a laboratory experiment conducted by Hasan and Samadhiya (2016), a short-term load-settlement study was performed using a floating granular pile placed in a clay substrate with an undrained shear strength of 5 kPa (Figure 2.14). The experiment was carried out in a model tank with a diameter of 200 mm and a height of 525 mm, with the granular pile measuring 375 mm in length and 75 mm in diameter. The pile was installed using the replacement method. The study investigated the effect of

different reinforcement directions, including vertical reinforcement with geotextile, horizontal reinforcement using circular geogrid strips, and a combination of both vertical and horizontal reinforcement. Additionally, the spacing of the horizontal reinforcement strips was varied as a study parameter.

The results were compared to untreated soft soil beds and conventional granular pile beds. The applied load was distributed by a plate matching the diameter of the granular pile. The findings revealed that the maximum load intensity for the treated clay bed, relative to the untreated clay bed, increased by 195% for conventional granular piles, 440% for vertically encased piles, and 396% for horizontally reinforced piles (with a 50 mm spacing between strips, center-to-center). When combining vertical and horizontal reinforcement, the ultimate load intensity for the floating granular pile increased by 485%, 432%, and 428% for horizontal reinforcement spacings of 25 mm, 50 mm, and 75 mm, respectively. These results indicate that both vertical and horizontal reinforcement significantly enhance the load-carrying capacity of the granular piles, but the effect of horizontal reinforcement spacing on the combined vertically encased and horizontally reinforced piles is minimal.

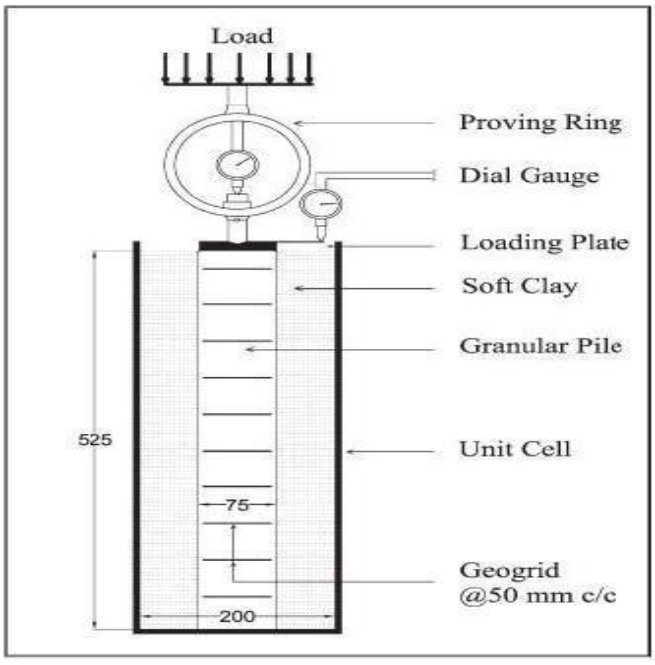

Figure 2 . 1 4 Model test set up **(**Hasan and Samadhiya, 2016)

2.6.2.2 Geogrid Encased Stone Column Settlement Reduction Studies

Raithel and Kempfert's (2000) approach for calculating the settlement of a granular column-reinforced foundation enclosed in geosynthetic encasement is based on a set of key assumptions:

1. Loading Size and Soil Thickness: The applied load is large enough that the added stress from the load does not diminish with depth, implying that the effects of loading are considered uniform across the depth of the soft soil.
2. Equal Settlement: It is assumed that both the soft soil and the top of the column will settle equally under the applied load, meaning there is no relative displacement between them.
3. No Settlement below the Column's Toe: The settlement is assumed to occur only above the column's toe, with no settlement expected beneath the column.
4. Active Earth Pressure: The column experiences active earth pressure, which affects the interaction between the soil and the column material.
5. Initial Soil Condition: The soil is assumed to be in an at-rest state prior to loading. The coefficient of earth pressure for the soil in an excavation installation method is given by $K_{o,s}= 1- \sin\phi_s$ where ϕ_s is the soil's friction angle. For displacement installation methods, a higher ground pressure coefficient, $K_{o,s}$ should be used.
6. Linear Elastic Behavior of Geosynthetic: The geosynthetic encasement is assumed to behave in a linearly elastic manner under stress.
7. Constant Volume of Granular Columns: The granular columns are assumed to have constant volumes, as they are considered incompressible.
8. Drained Condition Design: The design assumes a drained condition, meaning that the pore water pressure dissipates quickly enough to prevent significant undrained behavior during loading.

The approach is modeled using the unit cell concept (Figure 2.15), which forms the basis for calculating the settlement of a granular column-reinforced foundation with geosynthetic encasement.

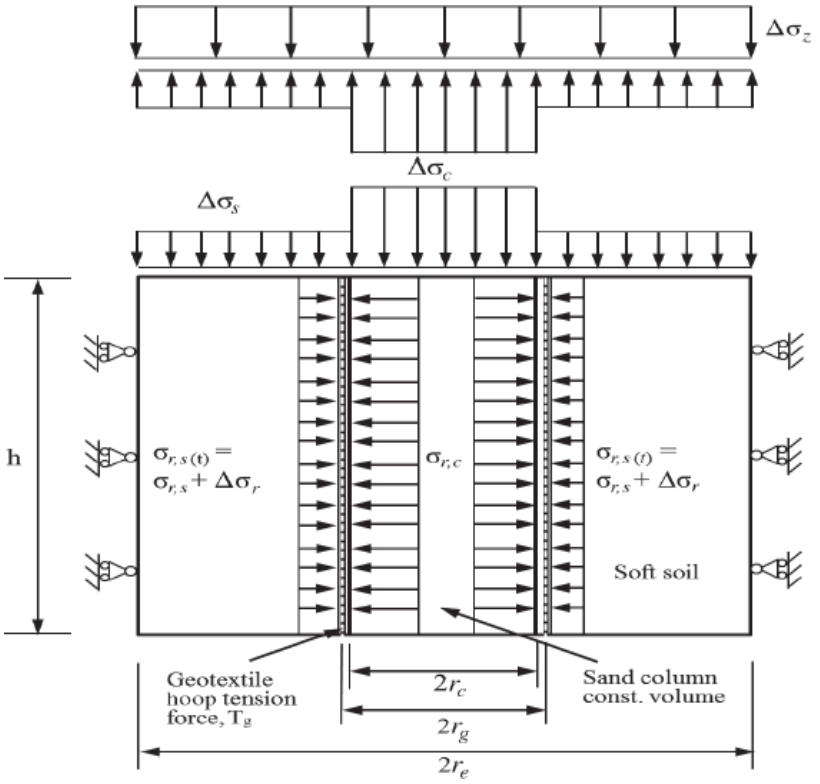

Figure 2.15. Geosynthetic encased column – Unit cell model (Raithel and Kempfert, 2000)

The overburden stresses on the soil and column as well as the additional stresses on them as follows contributes to the radial stresses in the soil and column:

$$\sigma_{r,c} = \Delta\sigma_c \,.\, K_{a,c} + \sigma_{z0,c} \,.\, K_{a,c} \quad (2.34)$$

$$= (1/a_s \,\Delta\sigma_z - (1 - a_s) / a_s \,\Delta\sigma_s)\, K_{a,c} + \sigma_{z0,c}\, K_{a,c} \quad (2.35)$$

$$\sigma_{r,s} = \Delta\sigma_s \, K_{0,s} + \sigma_{z0,s} \, K_{o,s} \quad (2.36)$$

where, $\sigma_{z0,c}$= Overburden stress of the column,

$\sigma_{z0,s}$= Overburden stress of the soil,

$\Delta\sigma_c$= Additional vertical stress in the column,

$\Delta\sigma_s$= Additional vertical stress in the soil,

$K_{a,c}$= Active earth pressure coefficient in the column,

$K_{0,s}$= At-rest earth pressure coefficient in the soil, ($K_{0,s}$, should be used if a displacement installation method is used).

Malarvizhi and Ilamparuthi (2007) conducted a finite element analysis using the PLAXIS program to study the behavior of a stone column encased in geogrid

within a soft soil bed. Their parametric study provided the following key findings:

1. Activation of Hoop Force: The hoop force within the geogrid encasement is activated at the top 1D depth of the column. As pressure is applied, the hoop force progressively activates along the entire length of the column, with the highest value of hoop stress occurring at the 1D depth of the column.
2. Stress Concentration and Load Distribution: The geosynthetic encasement increases the stress concentration on the stone column, which in turn reduces the load transferred to the surrounding clay. This effect slows the settlement of the composite soil, enhancing the column's performance.
3. Effect of Encapsulation Stiffness: The stress concentration factor increases, and settlement decreases as the stiffness of the geogrid encasement increases. However, the contribution to the settlement reduction ratio (SRR) becomes negligible when the stiffness exceeds 2000 kN/m, indicating that there is a point of diminishing returns beyond which further increases in stiffness do not provide substantial improvements.
4. Impact of Column Material Shearing Resistance: The shearing resistance of the material inside the column plays a critical role in the settlement reduction ratio (SRR). The efficiency of the stone column improves when the column material is compacted, enhancing its ability to resist shearing and contributing to better performance in terms of settlement reduction.

These findings highlight the importance of both the mechanical properties of the geosynthetic encasement and the material within the column in determining the effectiveness of stone columns in soft soil improvement.

Gniel and Bouazza (2009) conducted a series of small-scale model tests to investigate the behavior of encased stone columns. Their study highlighted the advantages of using geogrid over geotextile as the preferred geosynthetic material for column encasement. The geogrid was found to be more resilient and rigid, offering the necessary compression to achieve the required density in the column material. The research focused on the settlement reduction of both solitary and group columns, comparing encased columns (with both partial and full geogrid

encasement) to non-encased columns and untreated soft soil beds.

The soft soil used for the tests had the following properties: clay with a liquid limit (LL) of 62, plasticity index (PI) of 32, specific gravity (G) of 2.64, saturated unit weight (γ_{sat}) of 16.2 kN/m³, moisture content of 63%, compression index of 0.80, and an undrained shear strength (C_u) of 5 kPa. These soil properties were consolidated to create homogeneous soil conditions representative of natural deposits. The replacement method, known for its ease of application in soft soils, was used to install the stone columns. The column material was sand, with particle sizes ranging from 11 to 4 mm, specific gravity (G) of 2.80, and compacted saturated unit weight of 20.2 kN/m³.

The study observed the impact of different percentages of column encasement (25%, 50%, and 75% of the column length). The results showed that the vertical strain was reduced by 30%, 40%, and 50%, respectively, as the encasement percentage increased. In fully-encased columns, there was an approximately 80% reduction in vertical strain. Additionally, the stress concentration ratio for non-encased columns was 2, while for fully encased columns it was significantly higher at 10. This increase in stress concentration was attributed to the geogrid's confinement effect, which enhances the stiffness of the column and controls its radial strain. The study also noted that failure of isolated columns occurred due to radial expansion beneath the level of the encasement. The vertical strain of both solitary and group columns decreased progressively as the length of encasement increased. The column capacity for isolated columns improved with increasing encasement length, while the strain at failure remained relatively constant. Fully-encased columns exhibited a marked improvement in capacity. However, pronounced radial bulging was observed immediately beneath the base of the encasement. For group columns, this bulging extended through the non-encased portion, while for isolated columns with partial encasement, the bulging was limited to approximately two column diameters.

These findings emphasize the significant role of geogrid encasement in improving the performance of stone columns, especially in terms of reducing vertical strain

and enhancing load-bearing capacity, with the full encasement providing the most substantial improvements.

Deb et al. (2011) investigated the effect of geogrid reinforcement placed beneath a footing on stone columns in improved soft clay. The study explored how variables like the thickness of the sand cushion, the thickness of the geogrid sand bed, and the diameter of the geogrid layer influenced the load-settlement behavior of the improved clay bed. In their experiments, the stone columns were made using pebbles ranging in size from 2 to 6 mm, and the soft clay used was classified as CL with an unconfined compressive strength (UCS) of 19 kPa. The biaxial geogrid used for reinforcement was 1 mm thick, with its diameter adjusted between 200 mm and 500 mm.

The researchers performed a short-term load test to determine the optimal thickness for both unreinforced and geogrid-reinforced sand beds. Their findings showed that the ideal thickness for an unreinforced sand bed was 0.5 times the footing diameter, while for a geogrid-reinforced sand bed, the optimal thickness was 0.3 times the footing diameter. Additionally, the optimal diameter of the geogrid reinforcement was found to be three times the diameter of the footing when the sand bed was reinforced with geogrid.

This study provides important insights into the effectiveness of geogrid reinforcement in enhancing the performance of stone columns beneath a footing, particularly in improving load- bearing capacity and settlement control in soft clay conditions.

Castro et al. (2013) conducted a comprehensive experimental and numerical study on the consolidation and deformation behavior of stone columns. They performed small-scale laboratory experiments with a scale factor of 1:10 and compared the results to those obtainedthrough numerical analysis using the finite element method (FEM). The experimental parameters were carefully selected to align with the numerical model to ensure consistency in the comparison.

The study found that the stress concentration factor of the stone columns was

significantly affected by the friction angle and dilatancy angle of the surrounding soil. These factors played a key role in the soil-column interaction, influencing how stress was transmitted through the soil and affecting the column's settlement. The findings indicated that the settlement of the columns increased with a higher rate of consolidation, which in turn influenced the effectiveness of the stone column in reducing settlement.

One of the key insights from the study was that the stiffness ratio (the ratio between the stiffness of the stone column and the surrounding soil) had little impact on the reduction of settlement. This suggests that factors like stress concentration and consolidation rate were more critical in determining the column's performance. Furthermore, the study emphasized the importance of excess pore water pressure dissipation in the consolidation process. The stress concentration factor's variation over time was shown to significantly influence the rate at which excess pore pressure dissipates, which is essential for understanding the long-term behavior and effectiveness of stone columns in soft soil improvement.

These findings contribute valuable knowledge to the design and analysis of stone columns, highlighting the roles of soil mechanics parameters such as friction and dilatancy, as well as the complex interactions between stress concentration and consolidation during the settlement process.

Hanna et al. (2013) investigated the behavior of both single and group stone columns during failure by developing a numerical model and conducting a parametric analysis. Their parametric studies revealed that the load ratio increased hyperbolically as the D/B ratio (the ratio of the column diameter to the foundation width) increased. This increase was particularly notable when D/B was less than 0.6, but it became nearly constant when D/B reached 1, which corresponds to the case where the total diameter of all the stone columns in the group is equal to the foundation width.

The study also showed that for a given D/B ratio, the load ratio increased when the Poisson's ratio of the sand and clay decreased. This indicates that the soil's elasticity

and compressibility have a significant impact on the stone column's performance. Furthermore, the modulus ratio (the ratio of the modulus of elasticity of the column material to the surrounding soil) and the shear resistance angle of the stone material were found to increase the load-carrying capacity of the columns.

One of the key findings was related to the type of failure the columns experienced. The study concluded that shear failure occurred when stone columns replaced 10–35% of the area beneath the foundation, whereas bulging failure occurred when the area replacement ratio was less than 10%. This highlights the importance of column design in preventing bulging failure and ensuring optimal load-bearing capacity.

These findings contribute to the understanding of how stone columns behave under various loading conditions and the influence of material properties and geometry on their performance, especially when considering different failure modes and their impact on the overall foundation performance.

According to Najjar et al. (2013), the failure of stone columns occurred when they were loaded from the top, with bulging taking place between 0.5 and 3 times the column's diameter. When subjected to distributed loads, the load-carrying ability of the columns increased, accompanied by a significant reduction in bulging. The failure modes of the columns varied, including shearing, bending, or bulging. Shorter columns tended to punch and penetrate into the soft soil, while longer columns experienced deformation primarily in the upper portion of the column. For encased columns, the bulging was significantly reduced, and the bulging was shifted from the top to the lower portion of the column's length.

It was also found that the bulging of columns was more pronounced in soft clays than in stiffer clays, which affected the columns' behavior under load. As the area replacement ratio increased, the stiffness and strength of the composite system improved. Furthermore, for a given area replacement ratio, increasing the length-to-diameter ratio (L/D) resulted in higher ultimate stress and stiffness of the columns. The study revealed that columns with a L/D ratio between 5 and 8 times their diameter facilitated efficient load transfer.

The stress concentration factor was also found to increase up to a certain loading level, after which it declined. Covering the columns with geotextiles or geogrids helped reduce pore pressure, while simultaneously increasing the stiffness and load-bearing capacity of the composite ground. Moreover, columns with smaller diameters exhibited a greater improvement in efficiency than those with larger diameters.

The study highlighted that loosely packed specimens gained strength more effectively than those in a densely packed state. Additionally, the lateral earth pressures around the columns were significantly influenced by the column spacing. For group loading, the matrix soil was found to be more critical than factors like the installation technique, type of column, and composition.

These findings offer important insights into optimizing the performance of stone columns, including the effects of column dimensions, encasement, soil conditions, and column spacing. The study underscores the importance of these factors in improving the stability and load- carrying capacity of stone columns, especially in softer soils.

Castro et al. (2014) conducted a study to explore the reduction in composite ground settlement after installing stone columns, using numerical calculations. Their findings revealed that when modest loads were applied and columns were spaced widely apart, poor column installation could actually lead to increased ground settlement, especially in overconsolidated clay. The study highlighted the impact of soil anisotropy, where the soil fabric rotates from cross anisotropy to vertical and back to horizontal as the embankment is loaded. This shift increases the radial stresses, which in turn reduces settlement as the stiffness of the composite ground increases with higher radial stresses. Additionally, the study noted that excess pore water pressure reduces effective stress, contributing to increased settlement. Moreover, the settlement was found to increase as soil plastic stresses rose, particularly with a decrease in the over consolidation ratio.

In another investigation, Kumar et al. (2014) examined the effects of vacuum

application through enclosed stone columns and its impact on the strength of soft clay. The model experiments showed that the level of vacuum pressure applied influenced the undrained shear strength of the clay soil. The application of vacuum pressure was found to significantly enhance the columns' stiffness and their ability to support loads. Furthermore, stone columns subjected to vacuum pre-loading exhibited greater load-bearing capacity compared to those with surcharge loading. The results confirmed that pre-loaded columns had much higher load-carrying capacity than non-pre- loaded columns, especially when vacuum consolidation was employed. The study validated that the use of enclosed columns offers an effective method for applying vacuum pressure, further improving the performance of the stone columns in soft clay environments.

Ng and Tan (2014) utilized the unit cell concept in two-dimensional finite element analyses to investigate the consolidation and settlement behavior of floating stone columns under spread loading. They observed that as the depth ratio decreased, the consolidation properties of the improved ground also decreased, leading to increased settlement. They also found that, at a certain depth ratio, floating columns exhibited similar settling behavior to end-bearing columns, which led to satisfactory consolidation for long-term ground settlement. Moreover, the study indicated that factors such as the area replacement ratio, the ground pressure after installation, loading intensity, and the friction angle of the stone column aggregates had a significant effect on settlement. The study also determined that the modular ratio, influenced by the passive resistance of surrounding soil, had a negligible impact on the behavior of the floating columns.

Hasan and Samadhiya (2016) performed a comparative study on granular piles reinforced with geosynthetics, using laboratory testing and numerical analysis. The study considered short-term loading scenarios and the unit cell approach. The results showed that the construction of granular columns—whether reinforced or unreinforced—increased the ground's weight-bearing capacity. Reinforced floating columns outperformed unreinforced ones, especially in terms of reduced bulging. For both unreinforced and vertically encased columns, bulging occurred at

depths ranging from approximately 1.0 to 1.6 times the column diameter. However, horizontally reinforced and combined reinforced columns showed similar bulging behavior. The study also found that longer columns and clay beds with higher undrained shear strength contributed to improved column performance. The ultimate load-bearing capacity of unreinforced columns remained constant, while that of reinforced columns decreased as the column diameter increased. Additionally, floating columns demonstrated a higher load-bearing capacity with decreased geogrid strip spacing.

Basack et al. (2017) used numerical methods to assess the behavior of soft soil reinforced with stone columns, emphasizing lateral deformation. Their study found that the time before column bulging occurred and the zone of bulging were close to the surface of the ground. The restraint coefficients had a significant impact on column deformation, with lateral stress on the columns varying linearly with depth. Vertical stress increased with column depth, reaching a maximum value. When the radial distance from the column increased, so did the vertical stress on the surrounding soft soil. Bulging decreased in magnitude but grew in depth as the initial undrained cohesiveness strength of the soft soil increased. The magnitude of bulging also increased as column diameter decreased. Furthermore, when column spacing grew, both the ultimate load- carrying capacity and the magnitude of bulging increased. Columns' bulging depth decreased as the stress concentration ratio rose.

Debnath and Dey (2017) carried out studies on reinforced and unreinforced sand beds on vertical stone columns. Their findings revealed that the installation of stone columns significantly increased the weight-bearing capability of the ground, with the increase being particularly pronounced for encased columns. The geogrid-reinforced sand bed on encased columns reduced the maximum bulging depth and significantly decreased the amount of bulging. The study determined that the best length for encased columns with a geogrid-reinforced sand substrate was six times the column diameter, with three times the column diameter being the ideal encasement length.

Miranda et al. (2017) conducted small-scale laboratory experiments to examine the impact of geotextile encasement on soft clay reinforced with geotextile-encased stone columns. Their results showed that encased columns could withstand a vertical load approximately 1.7 times greater than regular columns. The stress concentration factor for the reinforced ground was nearly two to four times greater than that for regular columns. The study also found a decrease in settlement when the ground was reinforced with both regular and encased stone columns compared to untreated ground.

Rajesh (2017) carried out a numerical analysis to study the behavior of fully and partially penetrated geosynthetic encased stone columns (GESC) under time-dependent stress conditions. The study demonstrated that geosynthetic encasement reduced the time required for excess pore water dissipation and decreased lateral distortion or bulging of the columns, thus reducing settlement. The effective stress concentration ratio (ESCR) for encased columns increased significantly compared to regular stone columns, with the ESCR rising consistently during the consolidation period. However, after significant consolidation, the ESCR for regular stone columns increased initially and then declined. The study also revealed a considerable increase in load transfer from the column to the surrounding soft soil as the stiffness of the geosynthetics increased.

Das and Deb (2018) investigated the time-dependent behavior of improved ground under embankment stress conditions using model experiments and numerical analysis. The study showed that with increased spacing to diameter ratio, embankment height, and modular ratio, the stress concentration ratio increased, eventually stabilizing over time. However, due to arching effects, the stress concentration ratio decreased after reaching a peak value. The study also found that the maximum stress concentration ratio did not significantly affect the relative densities of the soft soil thickness and embankment material. The results indicated negligible differential settlement when the embankment height was twice the column spacing. Over time, lateral distortion of the columns increased, with the greatest deformation observed at depths approximately 2.5 times the column

diameter. Pore water pressure around the stone columns and surrounding soil was similar under steady-state conditions, but a larger pore water pressure occurred in the unimproved ground due to water buildup.

These studies provide comprehensive insights into the behavior of stone columns, their interaction with surrounding soils, and the impact of geosynthetic reinforcement on their performance.

Das and Dey (2020) investigated the use of a soil–cement bed placed over stone columns to improve the bearing capacity and reduce settlement in soft clayey soil. A series of laboratory plate load tests were conducted on single and group stone columns with and without the soil–cement bed. The study examined the effects of soil–cement bed thickness, stone column length, and spacing between columns on load-carrying capacity and settlement behaviour. The results showed that the inclusion of a soil–cement bed significantly reduced lateral bulging of the stone columns and enhanced bearing capacity. The load-carrying capacity of soft soil improved by about 5.5 times for a single stone column and 8.5 times for group stone columns with the soil–cement bed. The optimum thickness of the soil–cement bed was found to be 0.75 times the footing diameter, while the optimum stone column spacing and length were 2.5 times the column diameter and 2 times the footing diameter, respectively. The study also reported considerable reduction in bulging and settlement due to the stiff soil–cement layer, demonstrating its effectiveness as an economical alternative to geosynthetic reinforcement systems in soft ground improvement.

Pandey et al. (2022) presented a comprehensive review on the behaviour of ordinary and geosynthetic-encased stone columns used for soft ground improvement. The study reviewed previous experimental investigations, analytical approaches, field studies, and numerical modelling techniques to evaluate settlement reduction, stress concentration ratio, bulging behaviour, and bearing capacity improvement of stone columns. The review highlighted that ordinary stone columns are less effective in very soft soils due to inadequate lateral confinement, whereas geosynthetic encasement significantly improves stiffness and load-carrying

capacity by restricting radial deformation. The authors also discussed the influence of encasement stiffness, area replacement ratio, column spacing, and loading conditions on the overall performance of stone columns. Numerical modelling studies using PLAXIS were found to provide satisfactory prediction of stone column behaviour and were recommended for future parametric investigations and design optimization.

Srijan and Gupta (2023) experimentally investigated the performance of horizontally layered and vertically encased geosynthetic-reinforced stone columns installed in soft clay soil. Large-scale laboratory model tests were conducted to study the influence of different reinforcement configurations on settlement reduction, bearing capacity improvement, and bulging behaviour. The study compared ordinary stone columns with vertically encased columns and stone columns reinforced with horizontal geosynthetic layers. The results showed that geosynthetic reinforcement significantly improved lateral confinement and reduced radial deformation of the columns. Combined reinforcement arrangements exhibited maximum improvement in bearing capacity and minimum settlement compared to ordinary stone columns. The study concluded that geosynthetic reinforcement effectively enhances the load transfer mechanism and overall performance of stone columns in weak soils.

Mohamed et al. (2023) carried out a three-dimensional numerical investigation using PLAXIS 3D to evaluate the behaviour of ordinary and geosynthetic-encased stone columns in soft clay. The study examined the effects of encasement stiffness, encasement length, and column spacing on settlement reduction, radial deformation, and load-carrying capacity. The numerical results showed that ordinary stone columns experienced significant bulging near the top portion of the column, whereas geosynthetic encasement effectively restricted lateral deformation and improved confinement. Increasing encasement stiffness and encasement length considerably reduced settlement and enhanced bearing capacity. The study concluded that PLAXIS 3D successfully simulated the behaviour of geosynthetic-

encased stone columns and can be effectively used for design optimization and parametric studies.

Liu et al. (2023) investigated the static and dynamic load transfer behaviour of geosynthetic-encased stone columns through laboratory experiments and numerical simulations. The study evaluated the response of encased stone columns under monotonic and cyclic loading conditions. The results demonstrated that geosynthetic encasement improved stiffness, reduced settlement, and enhanced stress transfer efficiency under both static and repeated loading. Numerical analyses further indicated that encased stone columns maintained greater stability and lower deformation compared to ordinary stone columns under cyclic loading. The study concluded that geosynthetic-encased stone columns are highly effective for improving soft ground foundations subjected to traffic and seismic loading conditions.

Wang et al. (2023) conducted field tests and numerical analyses on composite foundations reinforced with geosynthetic-encased stone columns. Numerical modelling was performed using PLAXIS to evaluate settlement behaviour, stress distribution, and bearing capacity improvement under field loading conditions. The results showed that geosynthetic-encased stone columns significantly reduced foundation settlement and improved stress transfer efficiency compared to ordinary stone columns. The encased columns also exhibited reduced radial expansion and more uniform load distribution within the composite ground system. The study concluded that geosynthetic encasement effectively enhances the stability and deformation behaviour of soft clay foundations under practical field conditions.

Kumar et al. (2023) numerically investigated the performance of dual-layer geosynthetic-encased stone columns installed in soft soil using finite element analysis. The study examined the influence of multiple encasement layers on settlement behaviour, bulging control, and load-carrying capacity. The results showed that dual-layer encasement provided higher stiffness and improved confinement compared to single-layer encased stone columns. The multilayer reinforcement effectively restricted radial deformation and reduced settlement of

the surrounding soil. The study concluded that dual-layer geosynthetic systems can significantly improve the performance of stone columns in very soft ground conditions.

Kang et al. (2023) studied the bearing capacity and failure mechanisms of multilayer geosynthetic-encased stone columns under static and dynamic loading conditions through numerical analysis. The study investigated the influence of multiple encasement layers on settlement reduction, deformation characteristics, and failure patterns of stone columns. The results demonstrated that multilayer encasement significantly improved lateral confinement and increased resistance against bulging failure compared to ordinary stone columns. The study further reported that multilayer reinforcement effectively reduced dynamic deformation and enhanced the long-term stability of soft ground foundations subjected to repeated loading conditions.

Abid et al. (2023) numerically investigated the behaviour of geosynthetic-encased stone columns in unsaturated soils using three-dimensional finite element analysis in PLAXIS 3D. The study focused on the influence of matric suction and unsaturated soil conditions on settlement behaviour, stress distribution, and load transfer mechanism of stone columns. The results indicated that unsaturated soil conditions improved lateral confinement and reduced settlement due to the presence of matric suction. The numerical analyses showed that consideration of unsaturated soil mechanics leads to more realistic prediction of field performance and improved design accuracy of geosynthetic-encased stone columns.

Saxena et al. (2024) experimentally examined the use of recycled construction aggregates as filler material in ordinary and geosynthetic-encased stone columns. Laboratory model tests were conducted to evaluate settlement reduction, bearing capacity improvement, and sustainability aspects of the proposed system. The results showed that recycled aggregates performed satisfactorily as alternative granular material and provided considerable improvement in bearing capacity and settlement reduction when used with geosynthetic encasement. The study also reported reduced bulging deformation and improved confinement in encased stone

columns filled with recycled aggregates. The authors concluded that recycled construction waste can be effectively utilized in sustainable ground improvement applications.

Ji et al. (2024) numerically evaluated the contribution of geosynthetic encasement to the shear strength behaviour of stone columns using finite element analysis. The study investigated the influence of encasement stiffness, column diameter, interface interaction, and soil properties on shear resistance and deformation characteristics. The results demonstrated that geosynthetic encasement significantly enhanced shear strength by providing additional confinement to the granular column material. Higher encasement stiffness and improved interface interaction reduced radial deformation and increased overall stability of the composite ground system. The study concluded that proper selection of encasement properties is essential for optimizing the performance of geosynthetic-encased stone columns in soft soils.

Mohammed et al. (2025) conducted detailed experimental and numerical investigations on geosynthetic-encased stone columns installed in saturated and unsaturated soft soils. Laboratory model tests and finite element simulations using PLAXIS 2D were carried out to study the influence of matric suction, encasement stiffness, and area replacement ratio on settlement and bearing capacity behaviour. The results showed that unsaturated soil conditions provided additional confinement due to matric suction, resulting in reduced settlement and improved load transfer efficiency. The geosynthetic encasement effectively minimized radial bulging and enhanced stiffness of the stone columns. The study concluded that consideration of unsaturated soil behaviour in numerical modelling leads to more realistic prediction of field performance compared to conventional saturated soil assumptions.

Fansuri et al. (2025) carried out a comparative numerical investigation on the seismic performance of ordinary stone columns, micro-piles, and geosynthetic-encased stone columns for liquefaction flow-slide mitigation. Three-dimensional finite element modelling using PLAXIS 3D was performed to study deformation behaviour, excess pore water pressure generation, and stability of reinforced ground

under seismic loading conditions. The results demonstrated that geosynthetic-encased stone columns exhibited significantly better deformation resistance and stability compared to ordinary stone columns and micro-piles. The study concluded that geosynthetic encasement improves stiffness and integrity of stone columns during seismic excitation and is highly effective for liquefaction mitigation in soft ground conditions.

Bahi and Houhou (2025) conducted a three-dimensional parametric analysis on embankments supported by geosynthetic-encased stone columns considering radial expansion effects using PLAXIS 3D. The study investigated the influence of encasement stiffness, column spacing, and radial deformation on settlement behaviour beneath embankments constructed on soft clay. The results showed that ordinary stone columns experienced significant radial expansion and bulging under embankment loading, whereas geosynthetic encasement effectively restricted lateral deformation and improved stress transfer efficiency. Increasing encasement stiffness considerably reduced settlement and enhanced stability of the composite foundation system.

Rahman et al. (2026) developed a simplified analytical approach for evaluating the performance of geotextile-encased stone columns in soft soils. The proposed analytical model incorporated the interaction between the stone column, surrounding soil, and geosynthetic encasement to predict settlement and stress distribution behaviour. The analytical predictions were validated using previously published experimental and numerical results obtained from PLAXIS simulations. The study showed that geotextile encasement significantly improved lateral confinement and reduced radial deformation, resulting in enhanced bearing capacity and reduced settlement. The authors concluded that the proposed analytical approach can be effectively used for preliminary design and practical assessment of geosynthetic-encased stone columns.

Lu et al. (2026) carried out a coupled DEM–FDM numerical investigation to evaluate the influence of gravel size and geogrid aperture on the performance of geosynthetic-encased stone columns. The study utilized coupled PFC–FLAC

numerical modelling to simulate particle-scale interaction and confinement behaviour of granular materials within the stone columns. The results demonstrated that proper selection of gravel size and geogrid aperture significantly improved interlocking behaviour, reduced radial deformation, and enhanced load-carrying capacity. The study emphasized the importance of particle-scale interaction in controlling the performance and confinement mechanism of geosynthetic-encased stone columns.

Hassanzadeh et al. (2026) investigated wall mesh-encased stone columns using recycled rubber concrete and asphalt aggregates as sustainable alternative column materials. Experimental testing and numerical simulations using ABAQUS were conducted to evaluate settlement behaviour, bearing capacity improvement, and deformation characteristics of the proposed system. The results showed that recycled aggregate materials combined with wall mesh encasement provided satisfactory load-carrying performance and significantly reduced settlement in soft soils. The wall mesh encasement effectively improved lateral confinement and minimized bulging deformation of the columns. The study concluded that sustainable recycled materials can successfully be utilized in eco-friendly ground improvement applications without significant compromise in engineering performance.

CHAPTER 3

METHODOLOGY

3.1 GENERAL

This chapter explores the behavior of stone columns in clayey soil through a series of laboratory model tests. The study examines both conventional stone columns and those encased with geosynthetics, placed within a soft soil environment. The investigation evaluates the performance of individual columns as well as groups comprising three, four, and six columns arranged in triangular, square, and hexagonal patterns. Key factors such as the stiffness of the geosynthetic material, and stone column parameters including diameter, length, and spacing, were considered. Two experimental series were carried out: the first focused on individual stone columns with varying reinforcement configurations, while the second examined group behavior under different conditions. Both unencased and geosynthetic-encased columns were tested in each scenario. To ensure the reliability of the findings, the experimental results were validated using numerical modeling conducted with PLAXIS 3D software.

3.2 MATERIALS USED

This study utilized three primary materials: a sample of clayey soil, a specially formulated stone column mix, and a polymeric geotextile used for encasement. The stone column mix was prepared using a combination of fly ash, stone dust, iron dust, and cement to achieve the desired properties. The characteristics of each of these materials are detailed below:

3.2.1 Clay

A comprehensive review of existing literature revealed a widespread presence of soft cohesive soils throughout the region, with weak cohesive layers extending to a certain depth below the natural ground level. Given these conditions, a detailed subsurface soil analysis is essential to determine an appropriate ground improvement strategy. Specifically, evaluating the effectiveness of stone

columns in cohesive soils, such as clay, is critical for accurately predicting their load-bearing capacity and settlement behavior. To facilitate this, soil samples were collected from various locations in Raisen District, Abdullahganj, Bhopal, Madhya Pradesh, India and transported to the laboratory for testing. The index properties of the fine-grained soil were assessed using a series of standard procedures, including the hydrometer test (IS: 2720 Part 4 – 1985), specific gravity test (IS: 2720 Part 3 – 1980), Atterberg limit test (IS: 2720 Part 5 – 1985), the light compaction test (IS: 2720 Part 7 – 1980) and tri axial test (IS: 2720 Part 11 - 1993). The results of these tests, including the determined soil parameters, are summarized in Table 3.1.

The liquid limit is more than 50% and plasticity index 33% therefore as per IS classification soil is of high plasticity or high compressibility clay. The percentage finer than 2 micron is 25% and the activity of the soil is found to be 1.32 which is more than 1.25 therefore the soil is active and consistency of mineral of expansive soil which is confirm from the XRD analyses also. The differential swell index is found to be 33% which confirms the soil is expansive in nature.

Table 3.1: Properties of Expansive Soil

Parameter	**Expansive Soil**
Differential swell index (%)	35
Liquid Limit (%)	60
Plastic Limit (%)	27
Plasticity Index (%)	33
Shrinkage Limit (%)	10
Optimum Moisture Content (%)	19.23
Maximum Dry Density (kN/m^2)	17.16
Cohesion c (kN/m^3)	32.37
Angle of internal friction (ϕ)	18.20
Specific Gravity	2.56

IS Classification System	CH

3.2.2 Fly ash, Stone Dust, Iron Dust and cement

The fly ash, stone dust, and iron dust were procured from the India mart. Fly ash, industrial waste is in grey, showed binding properties like cement. Fly ash had a specific gravity of 2.02. Stone dust is a waste material obtained from the crusher plant. Stone dust was used as a replacement for sand in concrete. The specific gravity of stone dust was 1.89. The basic properties of iron dust, fly ash and stone dust are shown in Table 3.2, Table 3.3 and Table 3.4.

Table 3.2: Properties of Iron Dust

Parameter	**Specifications**
Appearance	Amorphous, lustreless, grey powder
Iron Content	99.8% min
Arsenic	<0.001
Lead	<0.001
Mercury	<0.001
Carbon	0.04
Phosphorus	0.005
Sulphur	0.022
Copper	0.001
Sieve analysis	+400 mesh – max 5% -400 mesh – min 95%

Table 3.3: Properties of Fly Ash

Characteristics	**values**
Specific Gravity	2.02
Colour	Grey
Bulk Density	1200 kg/m^3

Particle size distribution Sand (%) Silt (%) Clay (%)	 97.47 2.53 Nil
Coefficient of uniformity (C_u)	2.06
Coefficient of Curvature (C_c)	0.432

Table 3.4: Properties of Stone Dust

Characteristics	**values**
Specific Gravity	2.72
Coefficient of uniformity (C_u)	1.12
Coefficient of Curvature (C_c)	0.11
Particle size distribution Sand (%) Silt (%) Clay (%)	 90.8 9.2 Nil

Table 3.5: Properties of Cement

Characteristics	**values**
Specific Gravity	3.15
Colour	Grey
Initial Setting Time	31 min
Final Setting Time	520 min
Fineness	320 m^2/kg
Normal Consistency	31%
Soundness	2 mm
Compressive Strength 3 Days 7 Days 28 Days	 27 MPa 38 MPa 46 MPa
Bulk Density	1440 kg/m^3

3.2.3 Geosynthetics used

In this study two types of geosynthetic encasement i.e. geogrid and geotextile

were provided in single and group of columns. The manufacturer of geosynthetics is Tech Fab India. The properties of geosynthetics were given by the manufacturer. Geogrid is comprised of polypropylene with longitudinal and transverse ribs. By limiting the vertical pressure on granular columns and avoiding additional settlement, these ribs can provide the greatest potential interplay between geogrid, multi-blended granular columns, and expansive soil. The geotextile utilised in this experiment was woven. It is also made up of polypropylene, having tensile strengths of 45 kN/m in machine direction and 34 kN/m in cross machine direction.

Table 3.6: Properties of geosynthetics used

Geosynthetics	**Properties**	**Value**	**Unit**	**Test method**
Geogrid	Polymer type	Polypropylene	-	-
	Carbon black content	2	%	ASTM D4218
	Structure	Bi-oriented geogrids	-	-
	Stiffness at 0.5% strain machine direction	550	kN/m	ISO 10319
	Cross machine direction	350	kN/m	ISO 10319
	Aperture size Machine direction Cross Machine direction	 30 30	 mm mm	 - -
	Residual resistance to chemical degradation	100	%	EN 14030

	Residual resistance to weathering	100	%	EN 12224
	Installation damage factor	1	-	ASTM D5818
	Apparent coefficient of friction soil/ Geosynthetics at 10 kPa soil/ geosynthetics at 20 kPa	1.78 1.14	-	EN 13738

Geotextile	Polymer Type	Polypropylene	-	-
	Tensile strength Machine direction Cross Machine direction	45 34	kN/m kN/m	IS 1969
	Elongation at break Machine direction Cross Machine direction	30 28	kN/m kN/m	IS 1969
	Puncture resistance	700	N	ASTM D4833
	Apparent opening size	0.075	mm	ASTM D4751
	Weight of fabric	200	g/m^2	ASTM D5261

3.3 EQUIPMENTS & APPARATUS

3.3.1 Tank

A model tank was built with dimensions of 1500 mm in length, 900 mm in

width, and 600 mm in height to replicate the behavior of a clay bed reinforced with stone columns. The design and proportions of the tank are shown in Figure 3.1. The tank walls were constructed with adequate thickness to resist any lateral deformation that could occur during the filling process. To reduce friction between the clay and the tank walls, a thin layer of grease was applied to the inner surfaces of the tank.

Fig 3.1: Model Test Tank with Loading Frame

3.3.2 Loading and Measurement System

The model tank was equipped with a sturdy loading frame and a single loading system designed to apply loads to both the soft soil and the stone column materials, as illustrated in Figure 3.1. A circular iron foundation plate with a diameter of 300 mm, a thickness of 10 mm, and a weight of 7200 grams was suggested for use with both single and multiple columns. The loading system operated under a stress-controlled mechanism, with the load applied using a hydraulic jack (Figure 3.2) capable of exerting up to 50 kN of force. During testing, a vertical monotonic load was applied to the clay reinforced with stone columns to evaluate the load-displacement behavior of the soft clay. Settlement measurements were taken using three dial gauges positioned 120^{o} apart, and the final settlement value was calculated as the average of the readings from these three gauges.

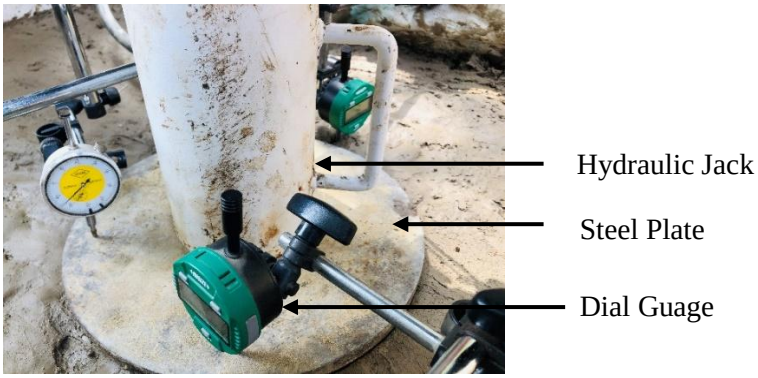

Figure 3.2. Test setup showing various components

3.3.3. Pipes for construction of Stone Column

Steel pipes with an internal diameter matching that of the stone columns were used to construct the columns using the replacement method. The pipe sizes were chosen to ensure that the area replacement ratio remained within the recommended range of 5% to 35%. These hollow pipes were utilized to form cavities within the soft soil bed for the placement of stone column material. Each pipe measured 2 mm in thickness and 600 mm in length, with one end bevelled to reduce disturbance during insertion into the soft clay bed. The pipe used in the study is depicted in Figure 3.3.

Figure 3.3. Pipes used for making stone column

3.3.4 Compaction Tools

A specially designed tamper unit, measuring 200 × 200 mm in plan, was used to compact the clay layer by dropping it from a height of 250 mm. For compacting the stone fill within the stone columns, a steel rod was utilized, weighing 1.5 kg with a diameter of 20 mm and a length of 100 mm.

3.4 MODELLING CONSIDERATIONS

While modeling the stone column and test tank dimensions (length, L, and diameter, D), factors such as boundary effects, L/D ratio, and geometric similitude ratio were taken into account. According to Wood et al. (2000), prototype stone column diameters typically range between 0.6 m and 1 m, while the minimum intact column diameter is about 13 mm (Shahu and Reddy, 2011). The L/D ratio for prototypes generally falls between 5 and 20 (Shahu and Reddy, 2011). Based on these guidelines, the present study employed column diameters of 50 mm and 70 mm, with L/D ratios maintained between 5 and 10. The corresponding similitude ratio ($D_{model}/D_{prototype}$) was found to be within 0.05 to 0.1.

A key consideration in designing the model tank was ensuring that boundary effects remained minimal, meaning the tank walls were placed far enough from the test zone to avoid stress constraints that could lead to overestimation of results. Accordingly, the overall testing box depth was set at 0.4 m for end-bearing columns and 0.25 m for floating columns. Similar cylindrical tank model setups for single and multiple reinforced stone columns were also reported by Ali et al. (2014).

3.5 CLAY BED PREPARATION

Clay beds were prepared in a model tank measuring 1500 mm × 900 mm with a height of 600 mm. A thick plastic cover was placed inside the tank to prevent friction between the wall and the tank and water loss. The remoulded expansive earth of soft consistency was piled 400 mm high in the steel tank. The soil was placed using the rainfall method. The clay pieces were extracted from the paddy field, ground cleaned of grass, soil biota, gravel, pebbles, and other unwanted objects, and then left in the daylight to dry. The required quantity of water was thoroughly incorporated into the fine clayey soil to create a soft consistency. The soil is compacted into four layers of 100 mm each with the help of a rammer of 25 kgs and left for seven days so that the moisture content was

evenly distributed throughout the soil. To ensure consistency, the bulk density of each layer was maintained at 18 kN/m³ and was regularly checked during the filling process using a mould of known volume at three different points within the layer**.** In all experiments, the top surface of the clay bed was trimmed and levelled to maintain a uniform thickness and an even surface. The same procedure was followed for preparing the clay layer in each test. Moisture content was measured by an oven distribution method at 10 cm intervals throughout the clay layers to ensure uniform water distribution across the entire model tank. In every case, the variation in moisture content within the clay bed was minimal, with deviations of less than 1.5%. The tank was covered with plastic sheets and iron sheets to reduce evaporation.

Figure 3.4: (a) Testing Tank (b) clay bed prepared

3.6 Forming of stone column mix

To find the optimum mix of stone dust, fly ash, iron dust and OPC different samples of cubes were cast and examined in a compression testing machine after 7 day curing. The area of the cube was 4900 mm^2. The 1:3 mix was prepared with 3 samples each to opt for the average strength value. Figure 3.5 The sample was mixed thoroughly by a mixer and compacted by a vibrating machine in the cube sampler. The only ratio of cement, fly ash, and iron dust mixed with three parts of stone dust and water. Water added = P/3 + 4 where P is the cement consistency (Pallavi and Sahu, 2019). The multi-blended column was

cast using the combination with the highest strength.

In this study, sample 4 was used to cast the multi blended column because this gave optimum compressive strength of the cube, and less percentage use of cement as a binder material was shown from an economic point of view. Fly ash and cement worked as binder materials. (Table 3.7)

The specific gravity of the multi blended column mix was calculated as 2.61.

Table 3.7: Column mix selection

Sample	Proportion (cement + fly ash + iron dust)	Compressive Strength (kN/mm^2)
1	45% cement + 50% fly ash + 5% iron dust	9.61
2	50% cement + 45% fly ash + 5% iron dust	9.03
3	45% cement + 45% fly ash + 10% iron dust	9.19
4	40% cement + 50% fly ash + 10% iron dust	10.2
5	50% cement + 40% fly ash + 10% iron dust	9.65
6	45% cement + 40% fly ash + 15% iron dust	9.51
7	40% cement + 45% fly ash + 15% iron dust	8.61

Figure 3.5: a) Failed sample in CTM loading b) Cubes for testing

3.7 STONE COLUMNS CONSTRUCTION FOR UNENCASED COLUMNS

In determining the stone column specifications, factors such as boundary effects and the geometric similitude ratio (L/D) were taken into account. Based on these considerations, the present study used column diameters of 50 mm and 70 mm, with L/D ratios maintained between 5 and 10. Steel pipes with internal diameters of 50 mm and 70 mm, and a wall thickness of approximately 2 mm, were used to construct the stone columns. To minimize disturbance to the surrounding soil during installation, a thin layer of oil was applied to both the inner and outer surfaces of the pipes for each sample.

3.7.1 Single Stone Column

The center of the tank was precisely marked, and a pipe of the required diameter was positioned vertically in the clay bed, with careful measures taken to maintain its alignment. The stone columns were constructed using the soil replacement method, which is suitable for small-scale modeling, unlike the force penetration and soil displacement techniques commonly used in the field. Steel casings with internal diameters of 50 mm and 70 mm, and a wall thickness of 2 mm, were used to form the stone columns and were inserted into the test soil. The top-down construction method was adopted primarily to prevent soil collapse during borehole formation. A screw auger with a diameter of 38 mm was used to remove clay from within the casing, and any remaining soil was scraped out to complete the cavity preparation. To minimize the smearing effect, the pipe had a thin coating of oil both inside and out. The floating column and end bearing were cast in the soil bed. The column's length after soil was removed from the pipe was examined by the scale of the desired length then in the column, the mixture was placed in 5 layers and compacted with the help of 20 mm diameter rod having weight of 1.5 kg and left for 24 hours to get its maximum strength. A trial-and-error approach was employed to determine the necessary drop height and the total number of blows required to achieve a target relative density of 68% (equivalent to 15.8 kN/m^3). Given the impermeable nature of the surrounding soil, this level of compaction is considered effective

for ensuring successful load transfer. Literature indicates that relative densities ranging from 50% to 80% have been used in clayey soils. In this process, aggregates were discharged into a container, compacted, and the casing was then removed in a single step. The resulting relative density of the placed aggregate showed a variation within the range of 68±2%. Figure 3.4 represents a constructed hole by a pipe for d= 70 mm.

Figure 3.6: (a) Single Stone column (b) Column mix filled column

3.7.2 Group of Stone Columns

The initial stage of the process resembled that of a single stone column without any reinforcement. A critical step involved selecting the appropriate spacing and arrangement pattern for the stone columns before forming the hollow pipe. Stone columns were constructed in both triangular, square and heaxgonal patterns using spacing-to-diameter (S/D) ratios: 2, 2, and 3. Groups of three, four, six stone columns were cast using the soil replacement method for the triangular, square and hexagonal patterns, respectively. The same auger mentioned earlier was employed to remove soil from the pipes. Figure 3.7 illustrates the triangular and hexagonal arrangements for a typical column diameter of 50 mm with an S/D ratio of 2 and 3. Similar arrangements were also prepared for other S/D ratios, as required for testing purposes.

3.8 STONE COLUMNS CONSTRUCTION FOR VERTICALLY ENCASED STONE COLUMNS

Geosynthetics was shaped into the necessary diameter tube and inserted with the casing for the encased stone columns. The casing pipe's diameter was marginally less than the stone column's formation diameter to guarantee that the ultimate diameter of the encased stone column is equal to the stone column's diameter. At first, length of geotextile reinforcement was provided throughout the length of the column (Lr=L) for which geosynthetics was wrapped for the whole length of the pipe. The pipe was completely encased by the geosynthetics and was lowered into the desired position. The column mix were put into the geotextile-wrapped tube and compacted similarly to that done during ordinary stone column case.

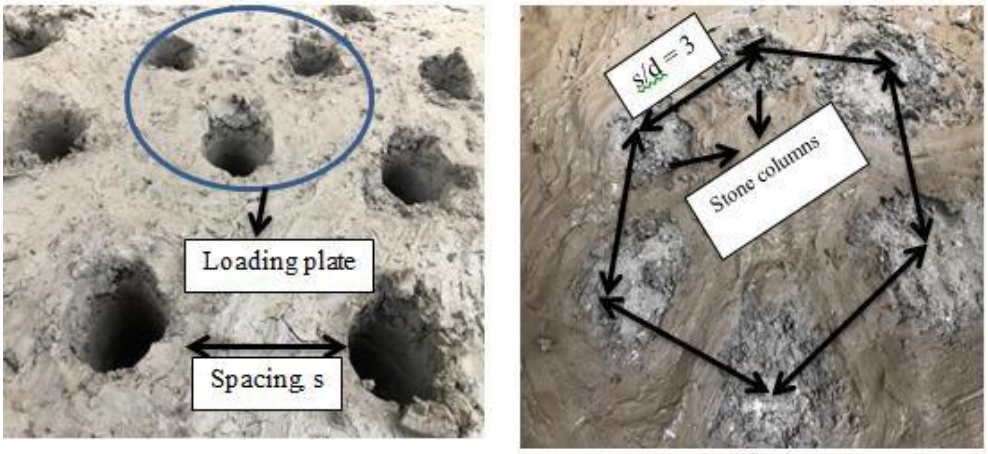

Figure 3.7: Typical arrangement of triangular and hexagonal pattern of stone column in groups for D = 50mm and S/D = 2 & 3

For stone column in groups, again triangular, square and hexagonal pattern of columns were arranged for s/d ratio of 2, 2 and 3. The required pipes as per the desired pattern were encased around it and lowered into the soil as the designated position. The pipes are subsequently filled with the amount of column mix calculated and compacted as it was done in the previous case.

3.9 TEST PROCEDURE

In stone column research and design, the area replacement ratio (A_r) is a key parameter influencing load distribution and settlement behaviour. As reported in the literature, A_r is defined as the proportion of the cross-sectional area of the stone columns relative to the total area of the foundation, with practical values

typically ranging from 5% to 35%. In the present study, individual stone column tests were conducted using a 300 mm diameter loading plate on columns of 70 mm diameters for single columns and 50 mm diameters for groups of columns, corresponding to Ar values of 7.09% and 6.25%, respectively. The loading plate thickness was determined through an iterative process of repeated trials and analysis to ensure minimal deformation under loading. A plate thickness of 10 mm was ultimately adopted, as it exhibited negligible distortion during testing. The loading system was stress-controlled, with load applied using a 50 kN capacity hydraulic jack at a regulated rate. A monotonic vertical load was applied to the treated clay through the plate positioned centrally over the column, and load application was terminated when the settlement reached 50 mm. In total, 25 stone column tests were performed. For all tests, a minimum length-to-diameter (L/D) ratio of 5 was maintained, exceeding the critical value of 4 recommended in the literature to prevent bulging failure. Table 3.8 summarises the complete details of the experimental programme.

3.10 DETAILS OF EXPERIMENTAL PROGRAM

To accomplish the required goals, the laboratory research is basically separated into various test series. The test series were divided into two portions. First series was done for single stone column for unencased and encased case. Two types of columns are designed i.e. end bearing columns and floating columns for unencased and encased case. The encasement was provided up to the length of the column. Also two types of encasement was tested i.e. geotextile and geogrid.

Second series of tests was done for group of columns for end bearing and floating columns arranged in triangle, square and hexagonal pattern for varying S/D ratio of 2, 2 and 3. Both type of encasement were used to study the encasement effect similar to that done in the analysis of a single stone column.

Table 3.8: Brief description of an experimental test

S.No.	Type of Reinforcement	Specific characteristics		No of test
		Single column	Group of columns	

1	Natural expansive soil	-	-	1
2	Expansive Soil + stone column (end bearing and floating)	l = 400mm (end bearing) l = 250 mm (floating) Dia 70 mm No of experiment = 2	l = 400 mm (end bearing) l = 250 mm (floating) Dia 50 mm, s/d = 2 (triangle & square) and 3 (hexagonal). No of experiment = 6	8
3	Expansive soil + stone column (end bearing and floating) with geosynthetic encasement	l = 400mm (end bearing) l = 250 mm (floating) Dia 70 mm No of experiment = 4	l = 400 mm (end bearing with encasement) l = 250 mm (floating with encasement) Dia 50 mm, s/d = 2 (triangle & square), 3 (hexagonal). No of experiment = 12	16

3.11 COLUMN EXHUMATION

Column exhumation is a post-construction investigative procedure carried out to assess the in-situ geometry, continuity, and material quality of ground improvement columns such as stone columns, sand columns, or cement/lime-treated columns. The process involves the careful excavation of a constructed column, typically in a trial or test section, to expose its full or partial length without significantly disturbing its structure. During excavation, measurements of diameter, depth, and shape are recorded at various levels, and any variations such as bulging, necking, or voids are noted. Representative material samples are collected for laboratory testing to determine gradation, density, and other relevant properties. This method provides direct visual and physical verification of construction quality and enables comparison between the as-built column and design specifications, making it valuable for both research studies and quality assurance in ground improvement projects.

In this study after the test done, the column mix from the column was carefully removed, and to address the column's misaligned shape, a thin plaster of Paris paste was put to the hole. By scraping away the surrounding earth, the cured

plaster of Paris was extracted for further investigation. After the test, the length of the deformed columns and the penetration of the bottom of the column were measured.

3.12 NUMERICAL MODELLING

3.12.1 General

For a geotechnical problem to have an exact solution, the conditions of compatibility, equilibrium, material efficiency, and boundary constraints for both forces and displacements must be satisfied. In recent years, it has been found that numerical analysis techniques fully meet these requirements. This discovery has driven significant progress in numerical methods, supported by the widespread use of advanced technologies and software capable of performing complex computations within a reasonable time. Commonly used numerical approaches include the discrete element method (DE), boundary element method (BE), finite element method (FE), and finite difference method (FD).

In this analysis, the finite element method (FEM) is employed. FEM studies the behaviour of an infinite system by representing it with a finite number of elements, expressed through ordinary or partial differential equations. This method allows the modelling of any shape through flexible arrangements of elements, removing the need for various analytical solutions when dealing with non-linear equations or complex geometries. FEM effectively handles continuum behaviour, composite equations, and irregular boundary conditions. Its major advantage is the ability to accommodate variations in material stiffness, even at the element level. Furthermore, it enables the application of multiple boundary conditions, making it possible to produce universally acceptable approximate solutions to physical problems.

3.12.2. Plaxis 3D

Owing to its theoretical foundation, which relies on the concept of virtual work to estimate stress and pressure distribution within a continuum, the Finite

Element Method (FEM) has proven to be a valuable tool for addressing complex engineering problems. PLAXIS 3D, a three-dimensional FEM software specifically developed for geotechnical engineering, is particularly effective in simulating the intricate behaviour of small groups of granular columns. This software was therefore employed for the finite element analysis in the present study. It incorporates advanced constitutive models—described in detail in a later chapter—to represent the properties of both soil and stone. To ensure the reliability of the numerical results, preliminary investigations such as mesh sensitivity analysis and assessment of the influence of boundary distance were conducted.

The numerical analysis involved comparing the load–settlement responses obtained from experimental investigations with those derived from the PLAXIS 3D model. The Mohr–Coulomb model was adopted to define the boundary conditions for both the soil and stone columns. A drained behaviour was assumed for the clay and column materials. Fifteen-node triangular elements were used for meshing. Boundary conditions were set to restrict medium deformation, allowing for the evaluation of the performance of the stone column within the soil matrix, typical deformation patterns, and column meshing. Aggregates, surrounding soil, and geotextiles were modelled using various constitutive options available in PLAXIS 3D.

3.12.3 Material Properties

The Mohr–Coulomb model is a widely used and straightforward approach for representing the behaviour of soils that are linearly elastic until yielding and then fully plastic. The model's elastic component is based on Hooke's law for isotropic elasticity, while its plastic component follows the Mohr–Coulomb failure criterion, formulated within a non-associated plasticity framework. A perfectly plastic constitutive model—such as Mohr–Coulomb—has a yield surface entirely defined by its parameters and unaffected by plastic straining. For stress states lying within this yield surface, the soil response is purely elastic and all strains are reversible. Once the stress state reaches the yield surface,

plastic deformation occurs without any change in the size or shape of the yield surface. Figure 3.8 illustrates the nonlinear behaviour of soil as represented by two bilinear segments.

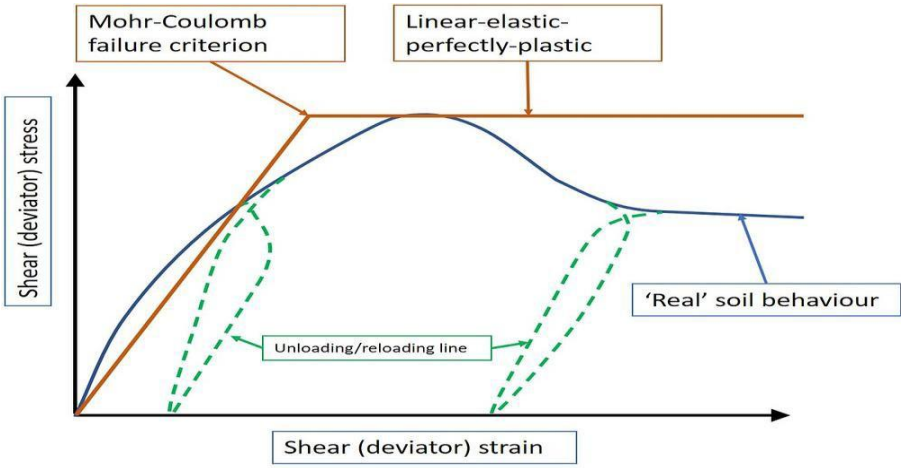

Figure 3.8. Real soil behaviour by Mohr - Coulomb model

In the present study, the Mohr–Coulomb model was adopted to represent the behaviour of the soft clay. The linear elastic, perfectly plastic Mohr–Coulomb formulation requires a total of five parameters, all of which can be obtained from basic laboratory tests on soil specimens and are generally familiar to geotechnical engineers. These parameters, along with their standard units, are listed below:

E: Young's modulus [kN/m^2]

ϕ: Friction angle [º]

ν: Poisson's ratio [-]

ψ: Dilatancy angle [º]

c: Cohesion [kN/m^2]

In PLAXIS, both the Elastic and Mohr–Coulomb models use Young's modulus as the primary measure of stiffness, although additional stiffness moduli are also provided. Since stiffness has the dimensions of stress, careful selection of parameter values is essential, as many geomaterials display nonlinear behaviour from the very onset of loading. In triaxial testing, the secant modulus corresponding to 50% of the material's peak strength is referred to as E_{50},

while the initial slope of the stress–strain curve is termed the tangent modulus, E_0. For materials with an extensive linear elastic range, E_0 can be used; however, for most soil-loading scenarios, E_{50} is preferred. In cases where unloading and reloading occur, the unload–reload modulus, E_{ur}, should be used instead of E_{50}.

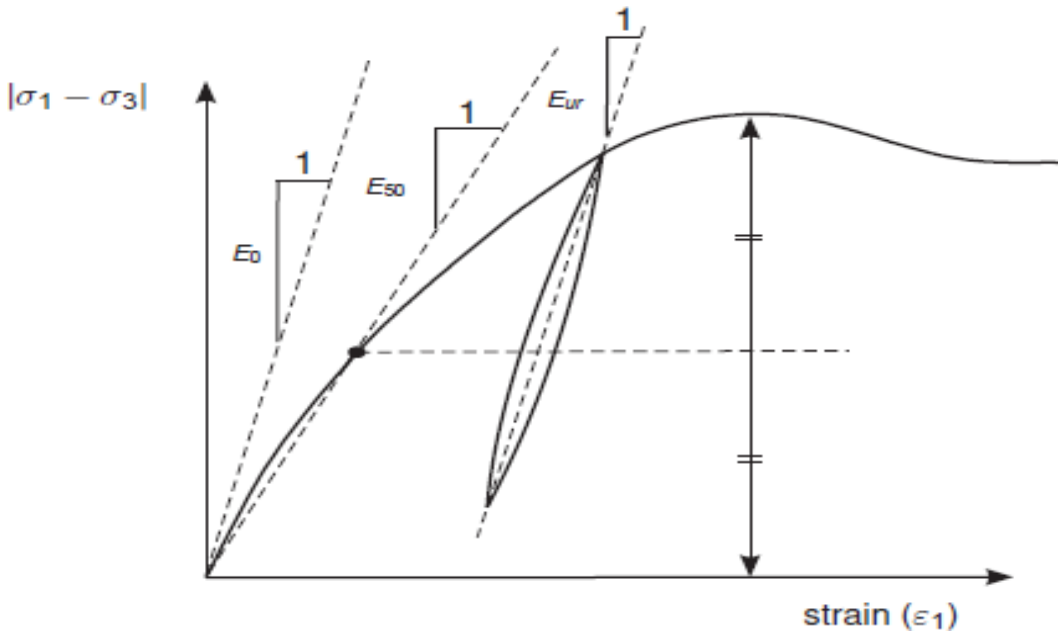

Figure 3.9. E_0, E_{50} and E_{ur} of a soil sample from triaxial test results

In the Mohr–Coulomb model, one-dimensional compression under gravity loading is used to determine realistic $K_0 = \sigma_h' / \sigma_v'$ ratios. For this loading condition, PLAXIS produces $\{\sigma_h' / \sigma_v'\} = \{\nu/(1-\nu)\}$ making it straightforward to select a Poisson's ratio that matches the desired K_0. This approach typically yields ν values between 0.3 and 0.4, which can also be applied to loading conditions beyond one-dimensional compression. Cohesion, like stiffness, has the dimensions of stress. In the Mohr–Coulomb model, the soil's effective cohesion c' is defined along with a realistic effective friction angle ϕ'. While dense sands may exhibit high friction angles, excessively large values increase computational effort in plastic analyses and may lead to unrealistic behaviour due to strain-softening—where very high friction cannot be maintained under large strains. The dilatancy angle ψ (in degrees) defines volumetric expansion during shear; for clays, except for heavily over-consolidated layers, ψ is

generally close to zero.

The Modified Cam Clay (MCC) model is a critical state soil model widely used to represent the stress–strain behaviour of normally consolidated and lightly overconsolidated clays. Based on the principles of critical state soil mechanics, the MCC model accounts for both elastic and plastic volumetric strains, with stiffness being stress-dependent rather than constant. In this model, the yield surface is elliptical in the q–p′ plane and expands or contracts according to the preconsolidation pressure. The primary input parameters include the slopes of the normal compression line (λ) and the swelling line (κ) in the void ratio–logarithmic mean effective stress space, the slope of the critical state line (M) in the deviatoric stress–mean effective stress space, Poisson's ratio (ν), and the initial preconsolidation pressure (p′c0). In Plaxis, the elastic bulk modulus and shear modulus are calculated internally from these parameters and the current stress state, with the bulk modulus expressed as

$$K = \frac{(1+\nu)\,p'}{\kappa} \tag{3.1}$$

and the shear modulus as

$$G = \frac{3(1-2\nu)\,K}{2(1+\nu)} \tag{3.2}$$

Consequently, the instantaneous Young's modulus can be obtained from

$$E = 2G(1+\nu), \tag{3.3}$$

but it varies throughout the analysis as the mean effective stress changes. The MCC model is particularly suitable for simulating embankment loading, consolidation, and undrained shear behaviour of clays, although it is less applicable to sands or heavily overconsolidated soils. In present study value of ν = 0.3 and λ = 0.05.

The main limitation of simulating column mix in PLAXIS is the inability to explicitly define column mix sizes. As presented in Table 3.6, the shear strength parameters and unit weights for both the modelled aggregates and the surrounding soil were obtained from laboratory testing.

Table 3.9. Properties of soil and aggregate

Properties	**Soil**	**Stone Column mix**	**Geogrid**	**Geotextile**
Soil	Clay	-	-	-
Cohesion (c)	32.37 kN/m^2	1 kN/m^2	-	-
Friction Angle (ϕ)	18.2º	40º	-	-
Bulk Unit Weight (γ_{unsat})	17.16 kN/m^3	15.8 kN/m^3	-	-
Saturated Unit Weight (γ_{sat})	18.75 kN/m^3	17.1 kN/m^3	-	-
Modulus of Elasticity	20,000 kN/m^2	80000 kN/m^2	100000 kN/m^2	120000 kN/m^2
Poisson Ratio	0.33	0.34	-	-
Compressibility Index (Cc)	0.50	-	-	-
Swelling Index (Cs)	0.10	-	-	-
Material Model	Mohr Coulomb	Cam Clay	Elastic	Elastic

Geogrids are elastic, flexible sheet-like elements that resemble a grid or fabric and are incapable of carrying compressive forces. In PLAXIS 3D, each geogrid dataset corresponds to a specific material type and can be assigned to the relevant geogrid element or group within the geometry model. For elastoplastic behaviour, geogrid properties are defined in terms of stiffness and strength.

For elastic behaviour, the axial stiffness EA must be specified. PLAXIS supports orthotropic and anisotropic material properties, defined as:

EA1 - The normal elastic stiffness in 1-direction (in-plane).
EA2 - The normal elastic stiffness in 2-direction.
GA - In-plane shear stiffness (anisotropic behaviour).

Axial stiffness, typically provided by the manufacturer, can be obtained from force elongation diagrams. It is calculated as:

$$EA = \frac{F}{\Delta l / l} \qquad (3.4)$$

Where F is the axial force per unit width, Δl is the elongation, and l is the

original length. For isotropic behaviour, only $EA_1$is required, $EA_2 = EA_1$ and $GA = EA_{1/2}$.

For elastoplastic modelling, two strength parameters are needed:

Np,1 - The maximum force in 1-direction.
Np,2 - The maximum force in 2-direction.

Here, Np is the maximum axial tension per unit width. Exceeding Np causes stress redistribution according to plasticity theory, resulting in irreversible deformations. Since output axial forces are calculated at element nodes, extrapolation from stress points may lead to nodal values slightly exceeding Np. In isotropic mode, only Np1 is required, with Np,2 = Np,1

3.12.4 Model Generation/ Geometry Modelling Process

The various model setups created for the experimental analysis of single stone columns and stone columns in groups were replicated in the numerical modelling. Figure 3.10 represents modelling a clay bed inside the tank of the same dimension used for the experimental analysis. A 70 mm column diameter for single column and 50 mm column diameter for group of columns was taken to show the generated model of an ordinary stone column, vertically encased stone columns for end bearing and floating columns. The model setup has been represented for both single and group of stone columns arranged in triangular, square and hexagonal patterns for varying S/D ratios. Figure 3.11 represents the model setup of a single ordinary type stone column. Figure 3.12 represents model of encased stone column. The images gave in 3.11 and 3.12 are the reference images of end bearing column. Similar modeling is done for the floating columns.

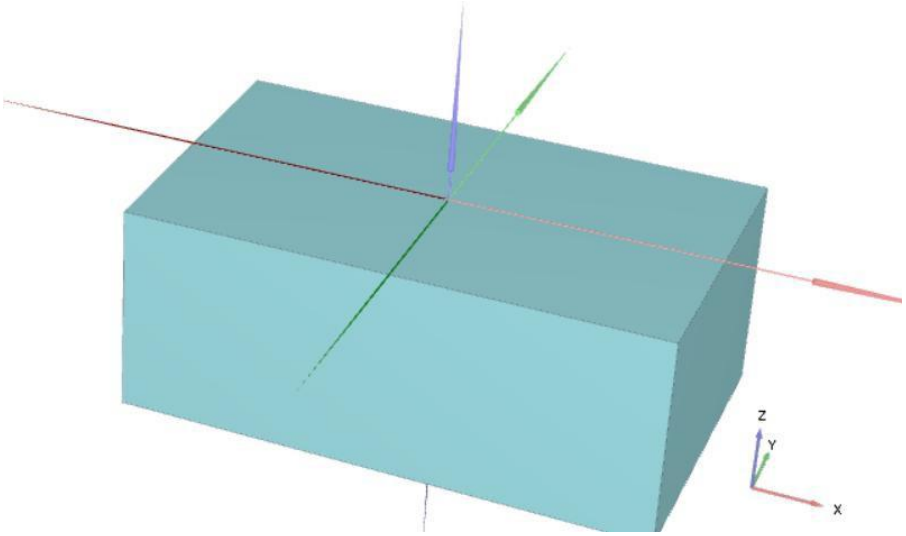

Figure 3.10. Model setup of soft clay

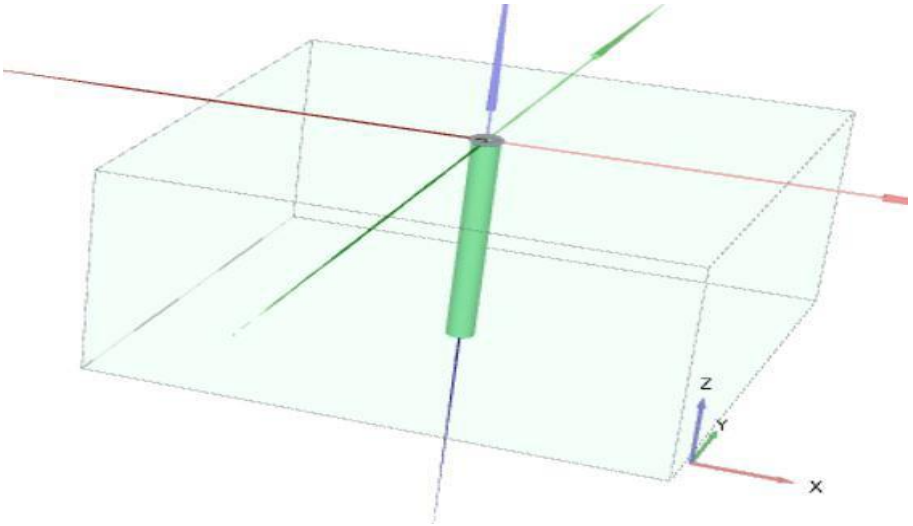

Figure 3.11. Model setup of an ordinary stone column for diameter of 70 mm

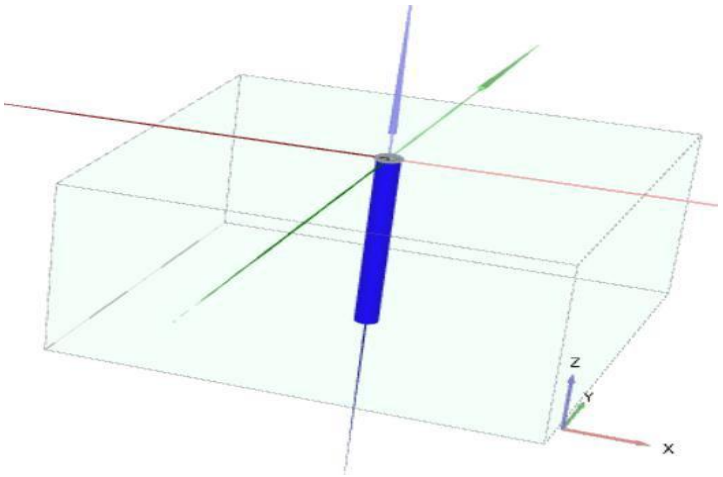

Figure 3.12. Model setup of encased stone column

For group analysis, Figure 3.13, represents ordinary stone column arranged in triangular pattern with S/D = 2, respectively. Figure 3.14, represents ordinary stone column arranged in square pattern with S/D = 2 respectively. Figure 3.15 represents encasement for end bearing column arranged in triangular pattern with S/D = 2 respectively. Figure 3.16 represents encasement for end bearing column arranged in square pattern with S/D = 2 respectively. The images gave in 3.13, 3.14, 3.15 and 3.16 are the reference images of end bearing column. Similar modeling is done for the floating columns and for hexagonal pattern too.

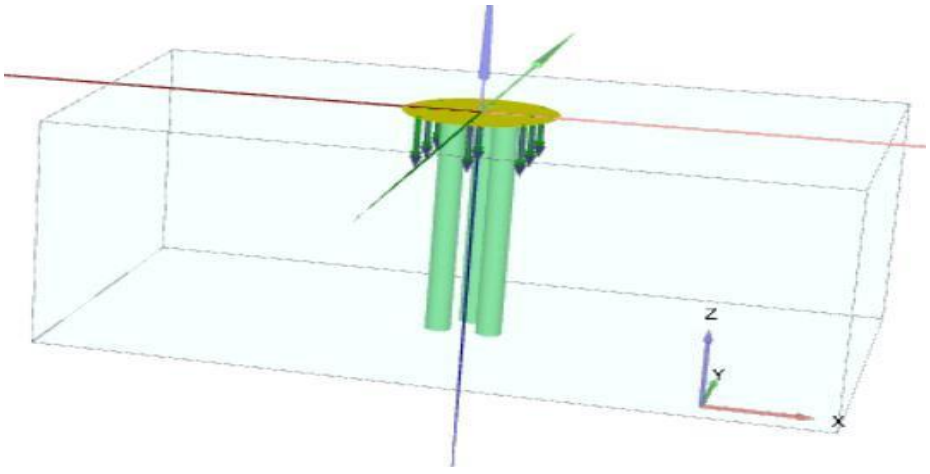

Figure 3.13. Model setup of ordinary stone column arranged in a triangular pattern for S/D = 2 for D=50mm

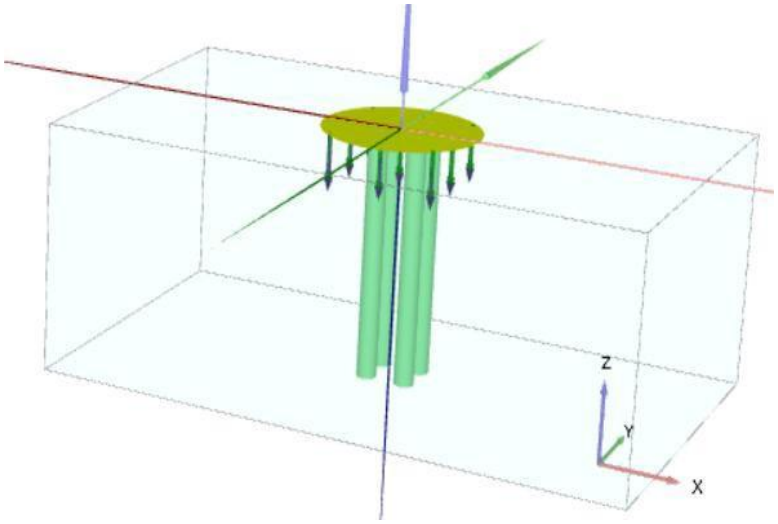

Figure 3.14. Model setup of ordinary stone column arranged in a square pattern for S/D = 2 for D = 50mm

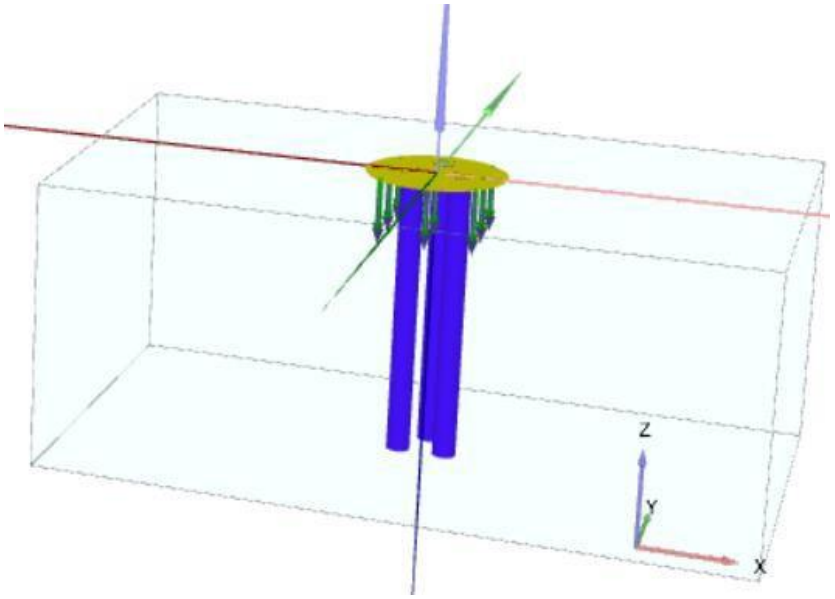

Figure 3.15. Model setup of encasement for end bearing column arranged in a triangular pattern with S/D = 2 for D=50mm

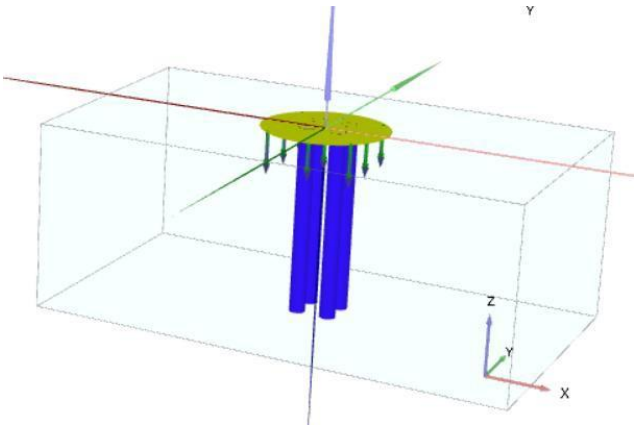

Figure 3.16. Model setup of encasement for end bearing column arranged in a square pattern with S/D=2 for D=50mm

3.12.5 Mesh Generation

Generating an appropriate finite element mesh is a critical step between defining the geometry and setting up staged construction. Once the geometry has been fully specified, it must be subdivided into finite elements to enable the numerical analysis. The mesh—an arrangement of these finite elements—must meet certain criteria to ensure smooth and accurate computations.

A high-quality mesh avoids excessively elongated or distorted elements, which could cause numerical instability. Element sizes should be sufficiently small in regions where significant stress or strain changes are expected, but not unnecessarily fine throughout the entire model, as this would lead to excessive computation times. The goal is to strike an optimal balance between accuracy and efficiency.

In PLAXIS 3D, the mesh is generated automatically, taking into account soil stratigraphy, structural elements, loads, and boundary conditions. The 3D finite element mesh for soil consists primarily of 10-node tetrahedral elements (Figure 3.17).

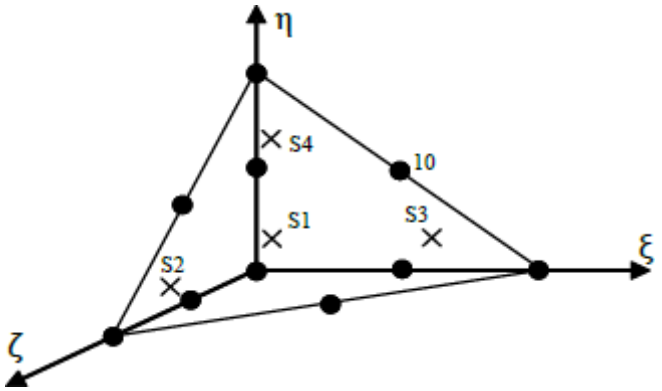

Figure 3.17. 10 - noded tetrahedral 3D soil element

The desired element dimension, represented by the global meshing parameter l_e, is required by the mesh generator. The outside geometry dimensions (x_{min}, x_{max}, y_{min}, y_{max}, z_{min}, z_{max}) are used to determine this parameter. The target element dimension is calculated using the equation below.

$$l_e = r_e \times 0.05 \times \sqrt{(x_{max} - x_{min})^2 + (y_{max} - y_{min})^2 + (z_{max} - z_{min})^2} \quad (3.5)$$

where r_e = relative element size factor; which is being determined from the element distribution. Element distribution has five global levels as represented in table 3.10.

Table 3.10. Predefined value of r_e (element distribution)

Element distribution	**r_e**
Very coarse	2.0
Coarse	1.5
Medium	1.0
Fine	0.7
Very Fine	0.5

The shape of the geometry and the selected local refinement settings determine

the exact number of finite elements in the mesh. A finer mesh is recommended in areas where significant stress concentrations or steep deformation gradients are expected, whereas other regions may not require such detail. This situation often arises in models containing corners, edges, or structural components.

PLAXIS 3D allows each geometric object to be assigned a local coarseness factor, which governs element size relative to a target size defined by the element distribution parameter. For most objects, this factor defaults to 1.0; for structural elements and loads, it is set to 0.5, which halves the element size. Acceptable values range from 0.0625 (very fine) to 8.0 (very coarse). Values above 1.0 produce locally coarser meshes, while smaller values refine the mesh. The software automatically performs additional refinements around structural elements, loads, and prescribed displacements to ensure high mesh quality.

In the present analysis, fine meshing is applied near the soil–stone column interface to accurately capture stress and deformation behaviour. This refinement enables the detection of bulging failures under load. The mesh is progressively coarser toward the lateral boundaries and finer near the interface region.

3.12.6 Staged Construction and Calculations

After discretizing the composite ground, the initial groundwater level and equilibrium stresses are defined. This is usually done by positioning the phreatic line at the specified location. Since PLAXIS operates primarily with effective stress, this parameter is particularly important for undrained soil conditions. In geotechnical analysis, specifying initial stresses is essential, as they are influenced by both the soil's self-weight and its stress history. Typically, the initial vertical effective stress ($\sigma'_{v,0}$) is related to the initial horizontal effective stress ($\sigma'_{h,0}$) through the coefficient of lateral earth pressure:

$$\sigma'_{h,0} = K_0 \times \sigma'_{v,0} \qquad (3.6)$$

In PLAXIS 3D, initial stresses can be generated using the Field Stress option,

Gravity Loading, or the K_0 procedure. In this study, the K_0 procedure was used, as it accounts for the soil's loading history. For normally consolidated soils, K_0 is commonly estimated using Jaky's empirical formula:

$$K_0 = 1 - \sin\phi \qquad (3.7)$$

PLAXIS uses this formula by default. However, extremely high or low K_0 values can produce stresses that violate the Mohr–Coulomb failure criterion. In such cases, PLAXIS automatically reduces lateral strains to satisfy the failure condition, marking these stress points as plastic. With the K_0 method, vertical stresses are determined from the soil's self-weight, while horizontal stresses are calculated using the defined K_0 value. Because this method does not generate shear stresses, it cannot ensure full stress equilibrium except for cases with horizontal surfaces, parallel soil layers, and a parallel phreatic level. For non-horizontal geometries, where shear stresses are needed for equilibrium, the K_0 procedure is not recommended.

After establishing the initial stresses with the K_0 method, another phase was introduced where all model components—soil, stone columns, and geogrid—were activated. In the subsequent phase, the prescribed displacements and corresponding boundary conditions were applied, and the analysis was performed. Both unreinforced and reinforced stone columns were evaluated for deformation and failure using plastic analysis. Plastic analysis was chosen because it develops the stiffness matrix from the original, undeformed state of the reinforced ground and is well-suited for simulating elastic–plastic deformation without considering the dissipation of excess pore water pressure. The same modelling and analysis procedure was applied for a group of stone columns.

3.13 XRD and SEM Analyses

3.13.1 General

X-ray diffraction (XRD) is an analytical technique used to determine the mineralogical composition and crystalline structure of soils by measuring the

diffraction patterns produced when a powdered sample is exposed to X-rays. The technique is based on Bragg's Law, which relates the wavelength of the incident X-rays and the angle of diffraction to the spacing between crystal lattice planes. Each mineral exhibits a characteristic set of diffraction peaksat specific angles, allowing precise identification and, in some cases, estimation of relative abundance. In geotechnical studies, XRD is widely used for identifying clay minerals such as kaolinite, illite, and smectite, which influence the soil's plasticity, swelling potential, and engineering behaviour. The method is non-destructive, requires only a small quantity of material, and provides high accuracy for crystalline phases, although it is less effective for amorphous materials. XRD analysis in this study was employed to characterise the clay fraction and assess its potential impact on the mechanical behaviour of the tested soils.

Scanning Electron Microscopy (SEM) is a high-resolution imaging technique used to examine the surface morphology and microstructure of materials, including soils, by scanning a focused beam of electrons over the sample surface. When the electrons interact with the atoms of the specimen, they produce various signals such as secondary electrons, backscattered electrons, and characteristic X-rays, which are detected and converted into detailed images. SEM provides magnifications much higher than optical microscopes, enabling observation of particle shapes, sizes, arrangements, and fabric, as well as microcracks or cementation bonds. In geotechnical engineering, SEM is particularly valuable for studying clay particle orientation, pore structure, and the effects of soil treatment or stabilization at the microscale. When combined with Energy Dispersive X-ray Spectroscopy (EDS), SEM can also provide elemental composition data to complement mineral identification from techniques such as X-ray diffraction (XRD). In this study, SEM was utilised to visualise the soil's microstructure and correlate observed features with its mechanical behaviour.

3.13.2 Process Used

In this study to identify the crystalline minerals in the soil and those utilised to create columns, such as fly ash, stone dust, and iron dust, as well as the mix design of the column, X-ray diffraction test was carried out using Bragg-Brentano in Bruker D8 advance machines to find out the crystalline materials in the soil and materials used in the formation of columns, i.e. fly ash, stone dust, iron dust and the mix design of the granular column. The SEM analysis was done using a Jeol JSM-6610 LV working under an ultra-high vacuum. The SEM images were collected in a normal plane as well as cross-section view modes. The operating voltage of SEM was 5 kV according to resolution requirements.

CHAPTER 4

RESULTS AND DISCUSSION

4.1 GENERAL

This chapter primarily focuses on evaluating the performance of encased stone columns in comparison with conventional (ordinary) stone columns. Both types of columns were installed in weak cohesive soil beds of identical properties. To assess their behaviour, single stone columns as well as column groups arranged in triangular, square, and hexagonal patterns were constructed and tested, with and without encasement. The study examined load–settlement responses for unreinforced columns and for those vertically encased with geosynthetics, both as individual units and in groups. Experimental results were analysed to determine variations in soil bearing capacity, and numerical analyses were carried out to validate these findings. In addition, Scanning Electron Microscopy (SEM) and X-ray Diffraction (XRD) tests were conducted to characterise the soil and reinforcement materials, providing further insights into their structural and mineralogical properties.

4.2 EXPERIMENTAL RESULTS: FINDINGS FROM MODEL TESTS FOR SINGLE STONE COLUMN AND GROUP OF COLUMNS

4.2.1 Analysis of the load-settlement behaviour of a clay bed

To begin with, a load test was conducted on untreated clay without any reinforcement in order to evaluate its load–settlement behaviour. The load was applied using a hydraulic jack, and the ultimate load-carrying capacity was determined at a settlement of 50 mm. A load–settlement curve was plotted for this purpose, as presented in Figure 4.1. The results indicated that the clay bed without a stone column exhibited a maximum settlement of 50 mm under an applied load of 5.9 kN.

4.2.2 Clay bed reinforced with ordinary stone column- Single Stone Column

In the current study, D = 70 mm was used. A loading plate of 300 mm diameter

was used. Area replacement ratio is defined as the area of the stone column with respect to that of the surrounding soil. The observed percentage of A_r in the present investigation was 7.09% for column having diameters of 70 mm, respectively. Figure 4.2 & 4.3 represents the load-settlement behaviour of the ordinary end bearing and floating stone column. From the Figure 4.2 and 4.3, it was observed that reinforcing the soft clay bed with ordinary stone columns increases the load carrying capacity of the composite clay bed.

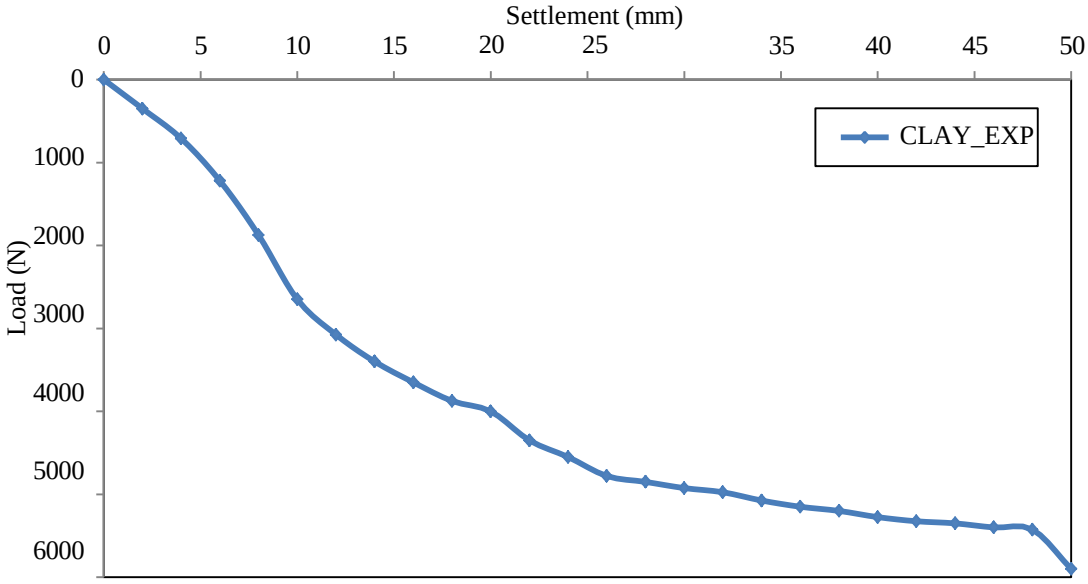

Figure 4.1 Load-Settlement variation of clay bed without any reinforcement

For the unreinforced clay bed, the load at an ultimate settlement of 50 mm was 5.9 kN, which was increased to 7.2 kN for D = 70 mm for end bearing column and 6.5 kN for D = 70 mm for floating column in the case of ordinary stone column. Replacing a portion of soil with a column made up of column mix results in creating a stiff composite soil mass, which further increases the load carrying capacity. For D = 70 mm, when an OSC is used in soft clay, the load capacity increases by 22.03% for end bearing column and 10.77% for floating column, respectively.

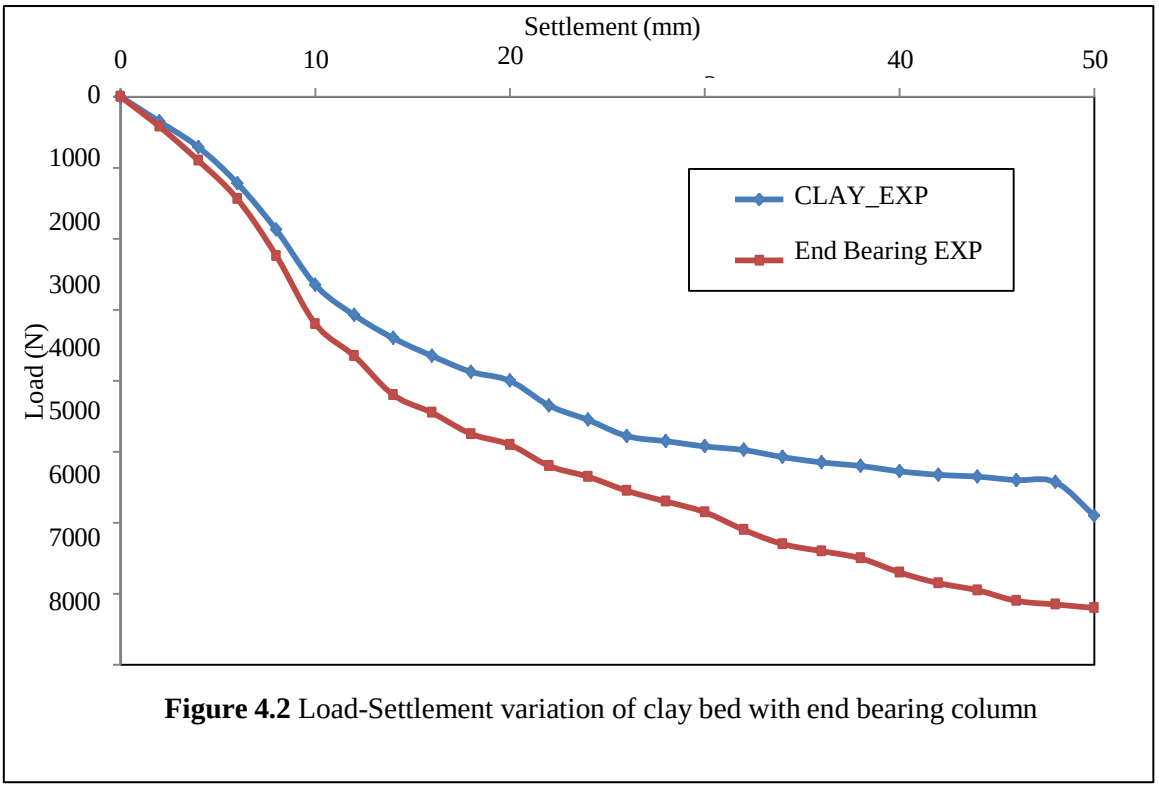

Figure 4.2 Load-Settlement variation of clay bed with end bearing column

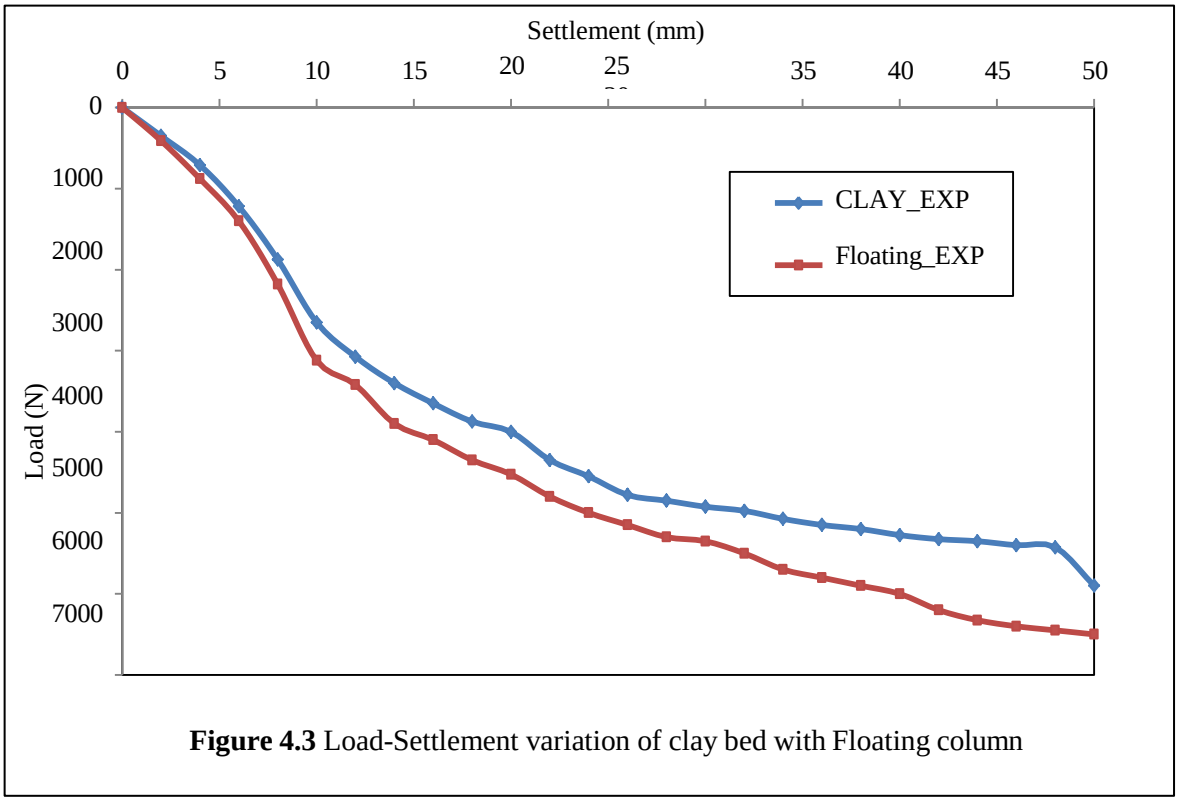

Figure 4.3 Load-Settlement variation of clay bed with Floating column

4.2.3 Clay bed reinforced with encased stone column - Single Stone Column

In very soft soil, ordinary stone columns mainly offer vertical load-bearing capacity but contribute little to lateral support, which can be problematic. To overcome this limitation, stone columns are enclosed with geosynthetic materials to provide lateral confinement. In this study, two types of encasements (geotextile and geogrid) were employed to the column length to study the effect of stiffness of the encasement material for both end bearing and floating columns.

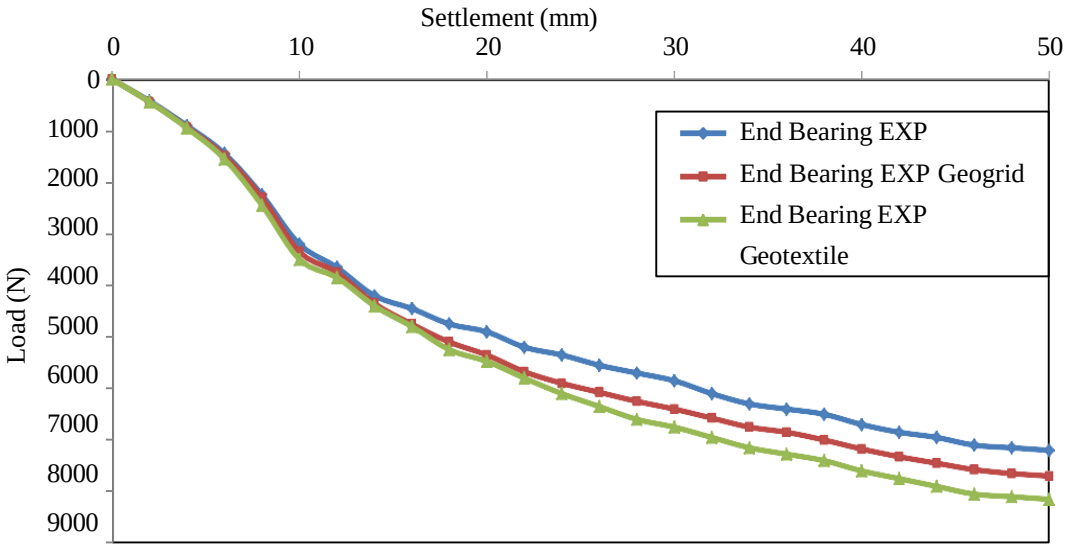

Figure 4.4 Load-settlement variation of the end bearing stone column with varying encasement

Figure 4.4 and 4.5 depicts the load-settlement behaviour of encased stone columns for end bearing and floating column with D = 70 mm for both the geosynthetics used. For D = 70 mm, the load carrying capacity for end bearing column, end bearing column encased with geogrid and end bearing column encased with geotextile was 7.2, 7.7 and 8.15 kN respectively. Similarly for floating columns, floating columns encased with geogrid and floating columns encased with geotextile was 6.5, 7.6 and 7.9 kN respectively. From the result it was observed that by providing encasement the load carrying capacity of the soil

mass increases. Further the load capacity increases by 22%, 30% and 38% for end bearing columns and 10%, 28.81% and 33.90% respectively.

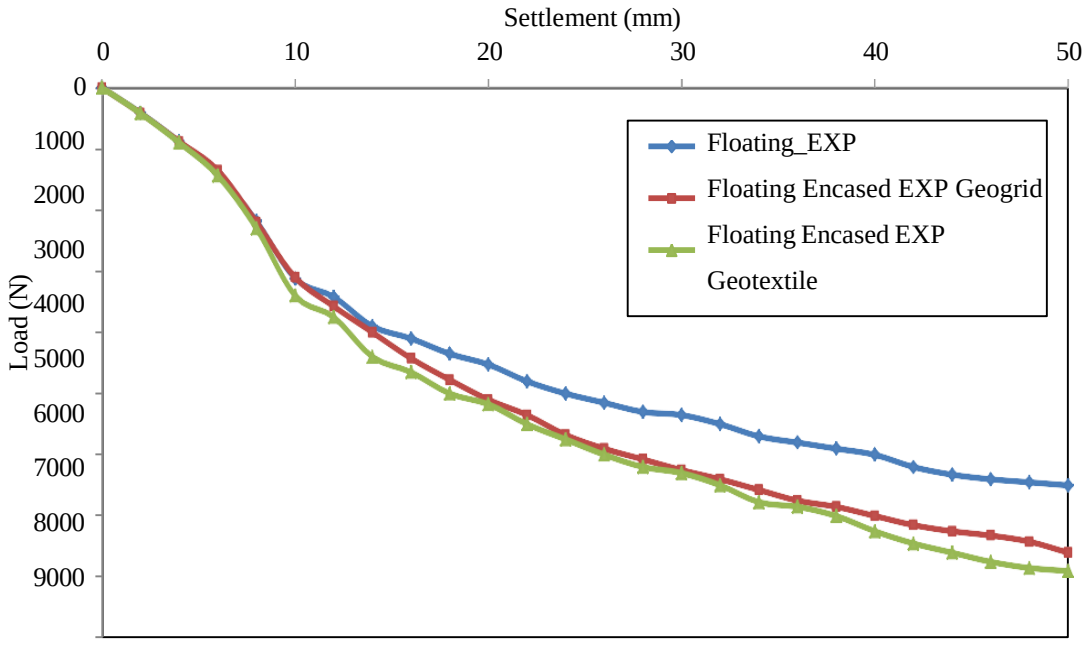

Figure 4.5 Load-settlement variation of the floating stone column with varying encasement

The beneficial role of geosynthetic encasement lies in its ability to enhance the confinement of granular columns. The encasement induces hoop stresses within the column material, which remain mobilised during loading and are not dissipated with time. This sustained confinement prevents excessive lateral deformation of the column and offsets the tendency of the surrounding expansive clay to push outward. As a result, the characteristic bulging failure commonly observed in unreinforced stone columns is significantly reduced. By controlling bulging, the encasement not only improves the overall stability of the column but also enables more efficient stress transfer from the footing through the column to the foundation stratum. A comparison between the two types of encasement used in this study further revealed that geotextile performed better for single columns, primarily due to its finer pore size, which restricted the loss of fines during loading.

The load–settlement response in Figure 4.6 highlights the significant improvement achieved through the installation of end-bearing columns and their subsequent encasement with geosynthetics. The untreated expansive clay exhibited the lowest load capacity, sustaining only about 5.9 kN at an ultimate settlement of 50 mm. With the inclusion of an end-bearing granular column, the capacity increased to 7.2 kN, representing an improvement of approximately 22% over the virgin clay bed. Further enhancement was observed when the column was encased with geogrid, where the load capacity rose to 7.7 kN, corresponding to a 31% increase compared to the unreinforced clay.

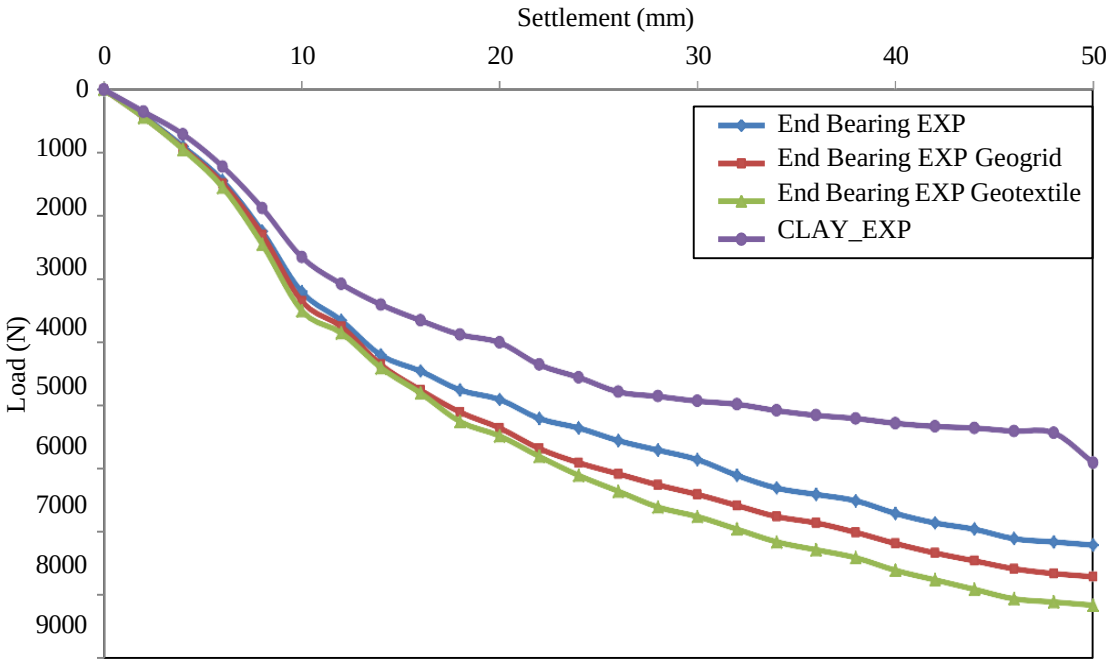

Figure 4.6 Comparison graph of end bearing column with unreinforced soil and encasement provided.

The maximum improvement was recorded for the geotextile-encased column, which sustained 8.15 kN at 50 mm settlement, nearly 38% higher than the virgin soil and around 6% greater than the geogrid-encased counterpart. These results clearly demonstrate that geosynthetic encasement effectively increases lateral confinement, reduces bulging, and enhances load transfer, with geotextile proving to be more effective than geogrid for single end-bearing column configurations.

Figure 4.7 showed the floating column configuration demonstrated a considerable improvement in load-bearing performance compared to the untreated expansive clay bed. At an ultimate settlement of 50 mm, the virgin clay sustained only about 5.9 kN, whereas the installation of a floating column increased the capacity to 6.5 kN, representing a 10% improvement. Encasement further enhanced the behaviour, with the geogrid-encased floating column carrying 7.6 kN, which is approximately 29% higher than the clay bed and 17% greater than the unencased floating column. Similarly, the geotextile-encased floating column achieved 7.9 kN, corresponding to a 34% improvement over the virgin soil and a 22% increase relative to the unencased floating column. These results highlight the effectiveness of geosynthetic encasement in mitigating bulging and enhancing confinement even for floating configurations. Moreover, the geotextile again outperformed the geogrid, owing to its superior fines retention capacity, thereby sustaining higher hoop stresses and enabling more efficient load transfer to the surrounding soil.

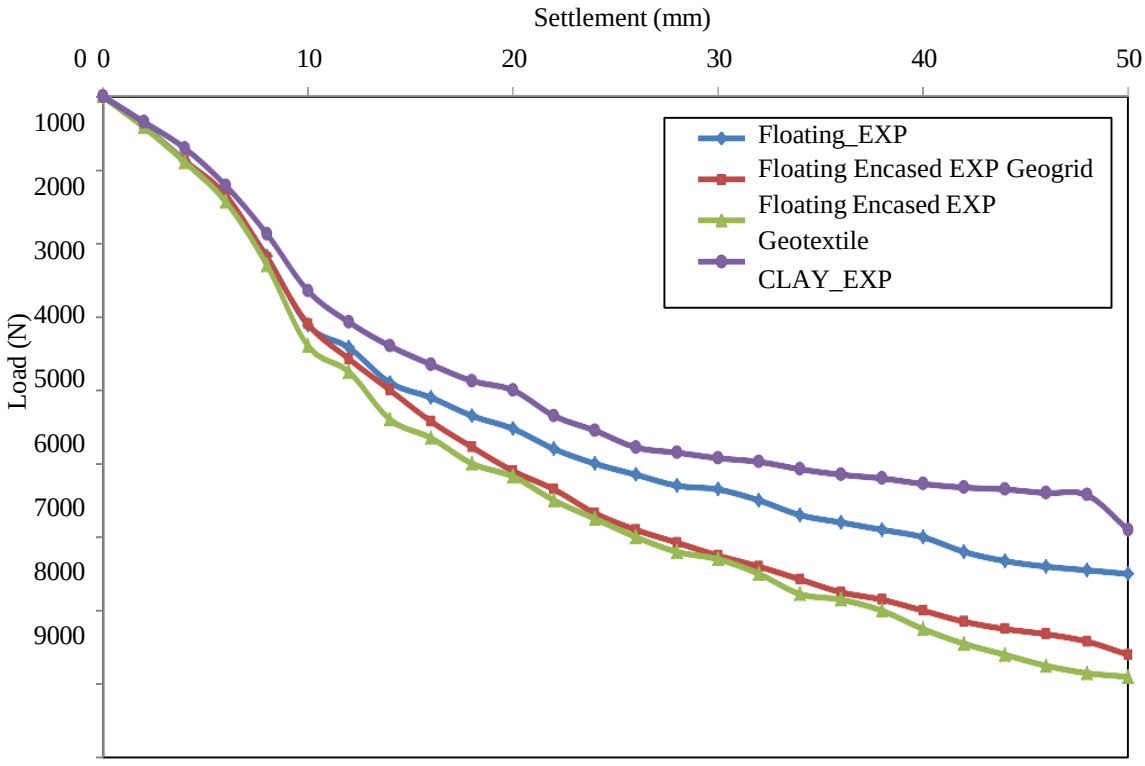

Figure 4.7 Comparison graph of floating column with unreinforced soil and encasement provided.

4.2.4 Clay bed reinforced with ordinary stone column- Group of stone columns

Triangular pattern (3 stone columns), square pattern (4 stone columns) and hexagonal pattern (6 stone columns) were used for the group analysis with varying spacing(S)/diameter (D) ratio. The S/D ratio for triangle and square pattern was 2, 2 and for hexagonal pattern 3 was used for the analysis. Figure 4.8 and 4.9 represent load-settlement behaviour of group of stone column arranged in triangular, square and hexagonal pattern for different S/D ratio for D = 50 mm, respectively. The ultimate load bearing capacity for 50 mm settlement of triangular pattern for S/D = 2, was found as 9.10 kN for end bearing column and 9.6 kN for floating column respectively. The ultimate load bearing capacity for 50 mm settlement of square pattern for S/D = 2 was found as 9.6 kN for end bearing column and 8.10 kN for floating column respectively. Similarly, for D = 50 mm, the ultimate load bearing capacity of hexagonal pattern for S/D = 3 was found as 7.9 kN for end bearing column and 7.3 for floating column respectively.

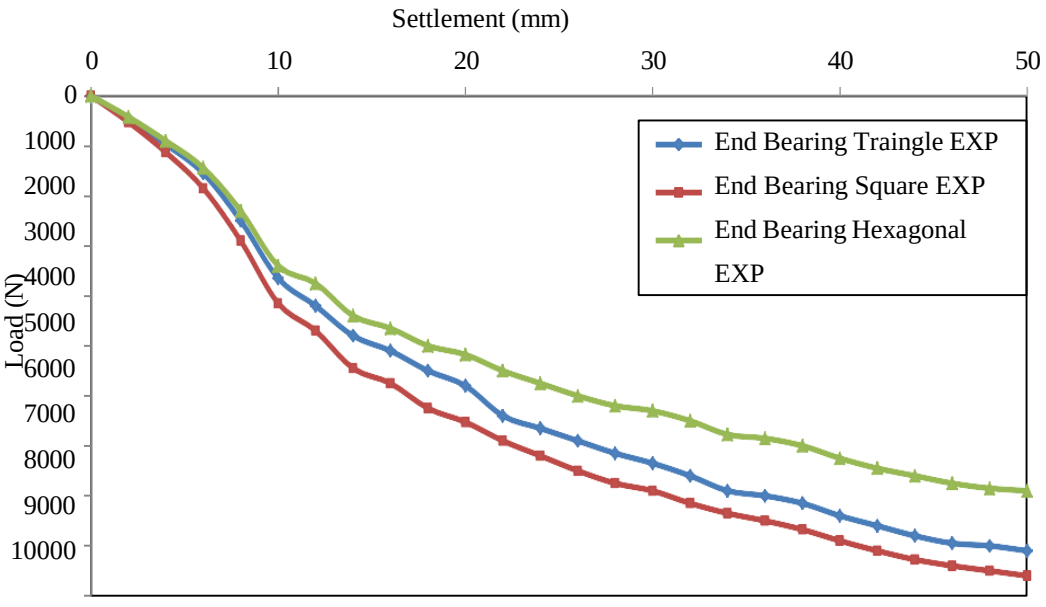

Figure 4.8 Load settlement variations of different patterns for unencased end bearing columns

As shown in figure 4.8 and 4.9, the influence of column arrangement on load–settlement behaviour was evident from the group tests. For both end-bearing and floating conditions, the Triangular arrangement consistently demonstrated the highest load-carrying capacity, followed by the square arrangement, while the Hexagonal arrangement showed the least improvement. In end-bearing groups, the triangular configuration sustained greater loads due to its closer spacing and enhanced confinement, which allowed more efficient stress transfer to the rigid base. A similar trend was observed in floating groups, although their overall capacity was slightly lower than that of end-bearing groups because of the absence of a firm stratum.

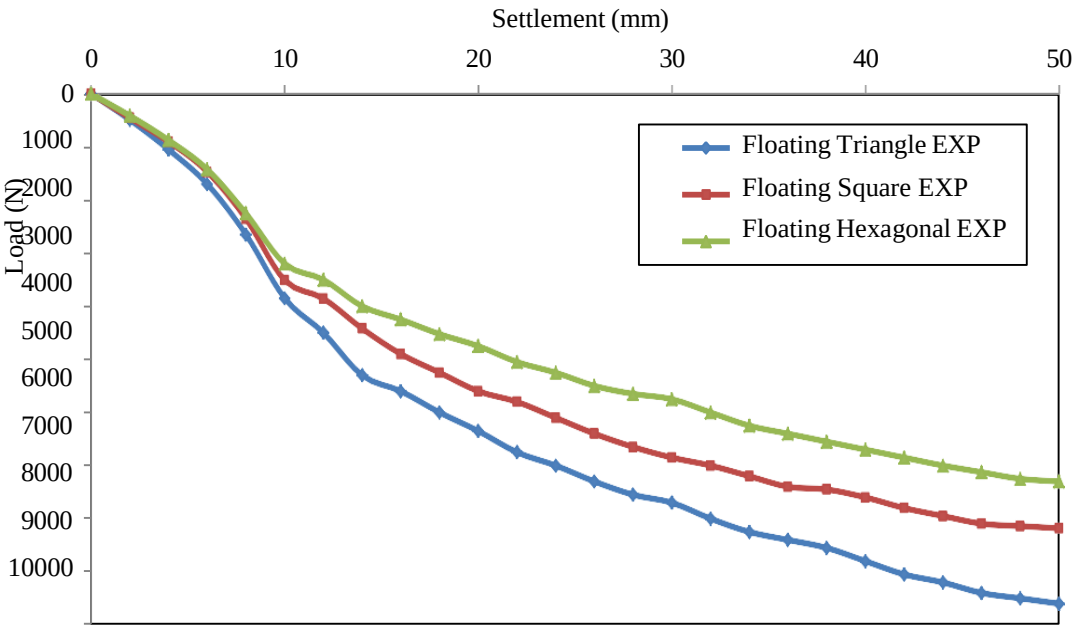

Figure 4.9 Load settlement variations of different patterns for unencased floating columns

Nevertheless, the relative improvement achieved by adopting the triangular arrangement was more pronounced in floating columns, as the efficient stress distribution helped to offset the lack of end restraint. These results clearly emphasise the importance of optimising group geometry, with the triangular configuration offering the most effective arrangement for reducing settlement and enhancing stability in both end-bearing and floating column systems.

4.2.5 Clay bed reinforced with encased stone column- Stone Columns in Group

Similar to the single stone column analysis, group analysis was also done for encased stone columns. In the group analysis also encasement provided to full length of column for both end bearing and floating columns was used. Also, both type of geosynthetics was used and compared for the analyses.

4.2.5.1 Triangular pattern with encased stone column

Figure 4.10 depicts the load-settlement behaviour of end bearing encased stone columns arranged in triangular pattern for S/D = 2 for D = 50 mm. Similarly, Figures 4.11 show the load-settlement behaviour of floating encased columns arranged in triangular pattern for S/D = 2 for D = 50 mm, respectively. For D = 50 mm, the ultimate load bearing capacity for end bearing encased stone columns of triangular pattern for S/D = 2 was found as 9.2 kN for geogrid and 9.8 kN for geotextile respectively. Similarly the ultimate load bearing capacity for floating encased stone columns of triangular pattern for S/D = 2 was found as 8.8 kN for geogrid and 9.2 kN for geotextile respectively.

The results indicate that for D = 50 mm and S/D = 2 in triangular pattern, both end bearing and floating encased stone columns exhibit improved load–settlement performance with encasement. Among the end bearing columns, the ultimate load carrying capacity was higher for geotextile encasement (9.8 kN) compared to geogrid (9.2 kN), showing a 6.52% increase.

Similarly, for floating columns, geotextile also outperformed geogrid, providing a capacity of 9.2 kN against 8.8 kN, which corresponds to a 4.55% increase. Overall, geotextile encasement proved more effective than geogrid, and end bearing columns showed slightly higher load resistance compared to floating columns under identical conditions.

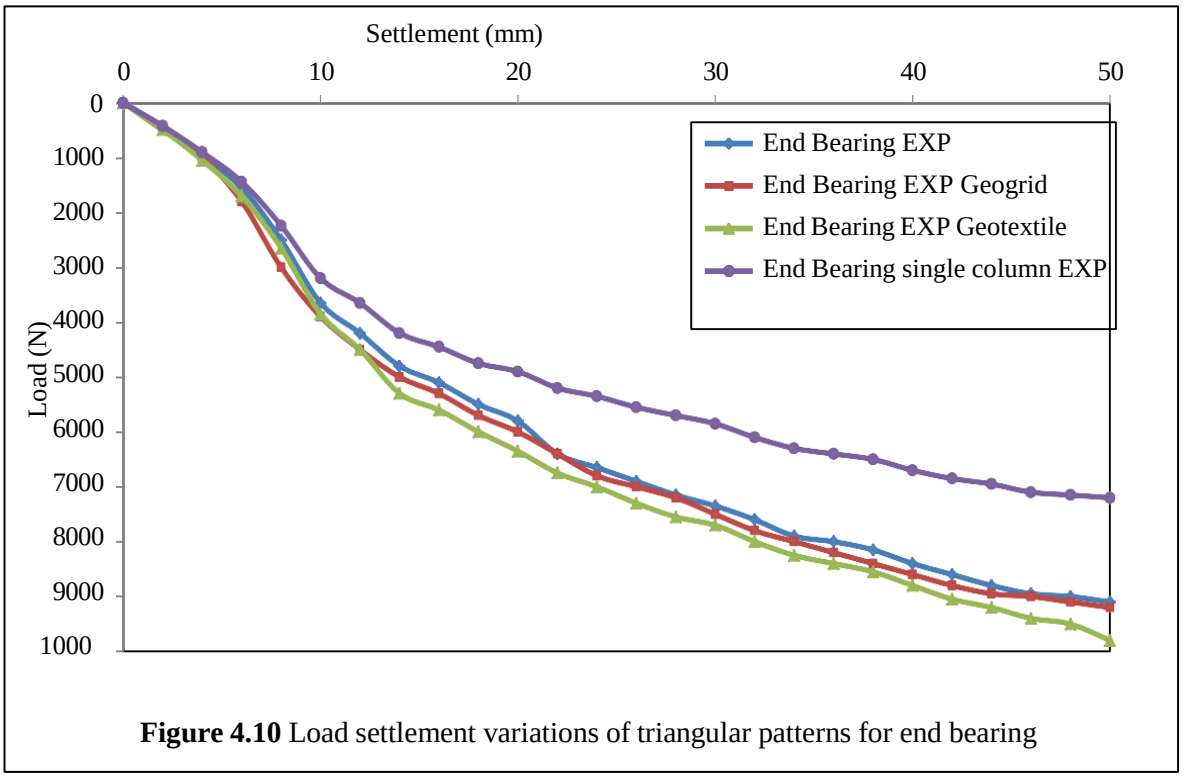

Figure 4.10 Load settlement variations of triangular patterns for end bearing

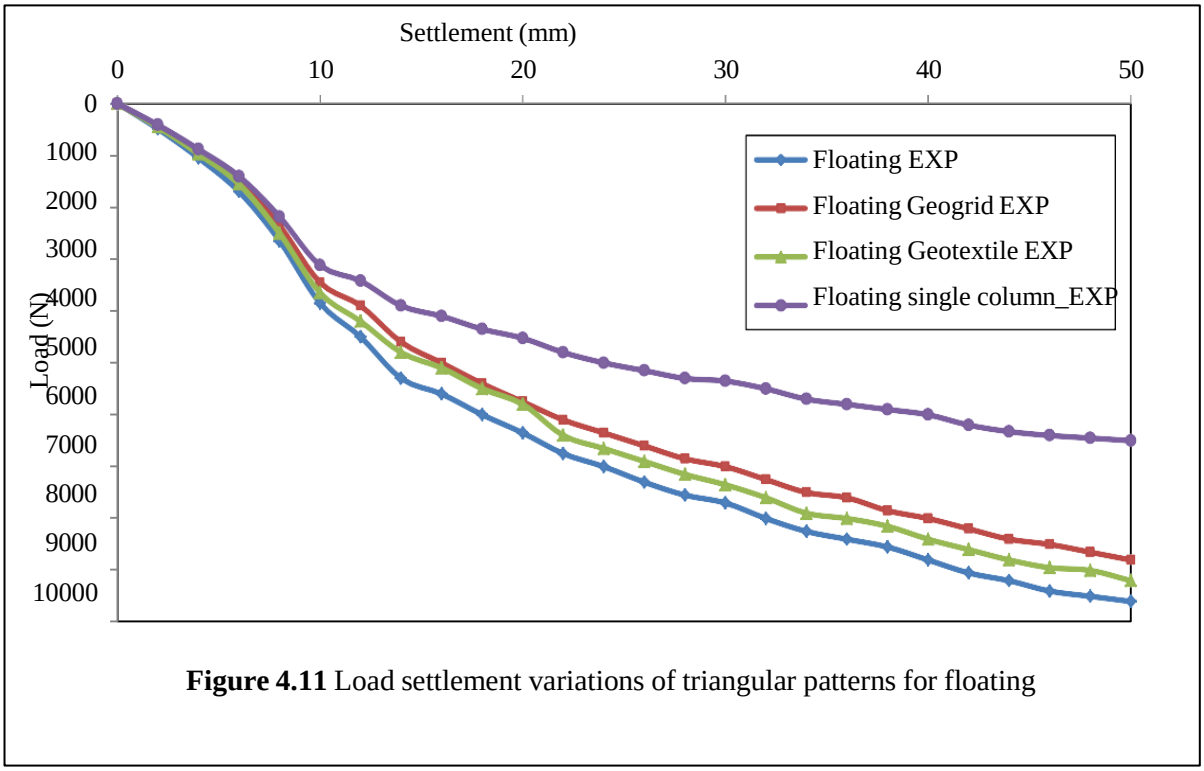

Figure 4.11 Load settlement variations of triangular patterns for floating

4.2.5.2 Square pattern with encased stone column

Figure 4.12 depicts the load-settlement behaviour of end bearing encased stone columns arranged in square pattern for S/D = 2 for D = 50 mm. Similarly,

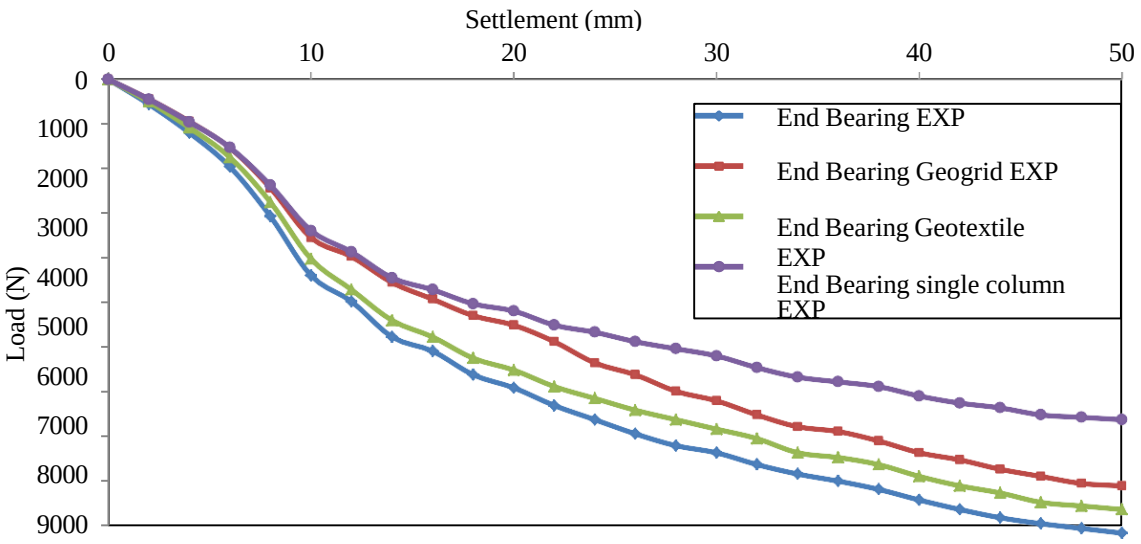

Figure 4.12 Load settlement variations of square patterns for end bearing

Figures 4.13 show the load-settlement behaviour of floating encased columns arranged in square pattern for S/D = 2 for D = 50 mm, respectively. For D = 50 mm, the ultimate load bearing capacity for end bearing encased stone columns of square pattern for S/D = 2 was found as 8.60 kN for geogrid and 9.10 kN for geotextile respectively. Similarly the ultimate load bearing capacity for floating encased stone columns of square pattern for S/D = 2 was found as 8.60 kN for geogrid and 8.70 kN for geotextile respectively.

The results for D = 50 mm and S/D = 2 in square pattern show that both end bearing and floating encased stone columns improved their load–settlement behaviour with geotextile compared to geogrid. For the end bearing arrangement, the ultimate load carrying capacity was 9.10 kN with geotextile against 8.60 kN with geogrid, reflecting a 5.81% increase. In the case of floating columns, the ultimate load capacity was 8.70 kN with geotextile and 8.60 kN with geogrid, showing only a 1.16% increase. Thus, geotextile encasement proved to be more effective, particularly for end bearing columns, while the improvement for floating columns in square pattern was marginal.

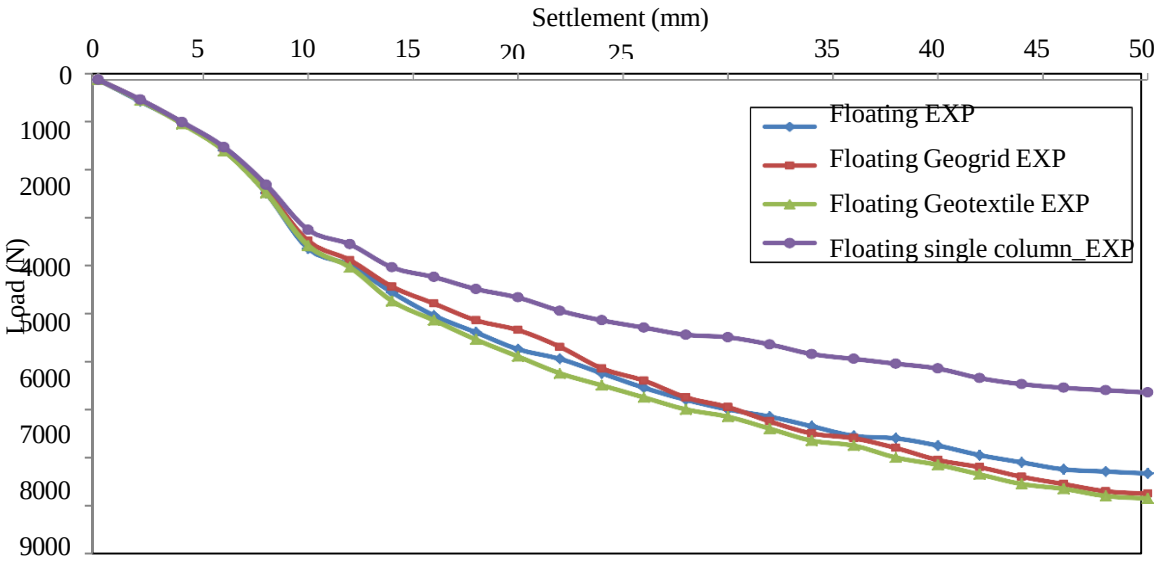

Figure 4.13 Load settlement variations of square patterns for floating

4.2.5.3 Hexagonal pattern with encased stone column

Figure 4.14 depicts the load-settlement behaviour of end bearing encased stone columns arranged in hexagonal pattern for S/D = 3 for D = 50 mm. Similarly, Figures 4.15 show the load-settlement behaviour of floating encased columns arranged in hexagonal pattern for S/D = 3 for D = 50 mm, respectively. For D = 50 mm, the ultimate load bearing capacity for end bearing encased stone columns of hexagonal pattern for S/D = 3 was found as 7.9 kN for geogrid and 8.5 kN for geotextile respectively. Similarly the ultimate load bearing capacity for floating encased stone columns of hexagonal pattern for S/D = 3 was found as 7.9 kN for geogrid and 9.1 kN for geotextile respectively.

The results for D = 50 mm and S/D = 3 in hexagonal pattern indicate that both end bearing and floating encased stone columns exhibited higher load–settlement performance with geotextile compared to geogrid. For the end bearing arrangement, the ultimate load carrying capacity was 8.5 kN with geotextile and 7.9 kN with geogrid, showing a 7.59% increase. In the case of floating columns, the ultimate load capacity was 9.1 kN with geotextile against 7.9 kN with geogrid, corresponding to a 15.19% increase. Hence, geotextile encasement provided notable improvement in both cases, with the

effect being more pronounced in floating stone columns.

The comparison of group arrangements with single columns clearly demonstrates the advantage of pattern configuration and encasement. For single columns, the load carrying capacity was limited, and failure was governed mainly by bulging in end bearing columns and punching in short floating columns. In group arrangements, however, the ultimate load carrying capacity improved due to mutual confinement between adjacent columns, which restricted excessive lateral deformation. The comparative study of triangular, square, and hexagonal patterns for D = 50 mm revealed that geotextile encasement consistently outperformed geogrid in enhancing the load–settlement behaviour of both end bearing and floating stone columns.

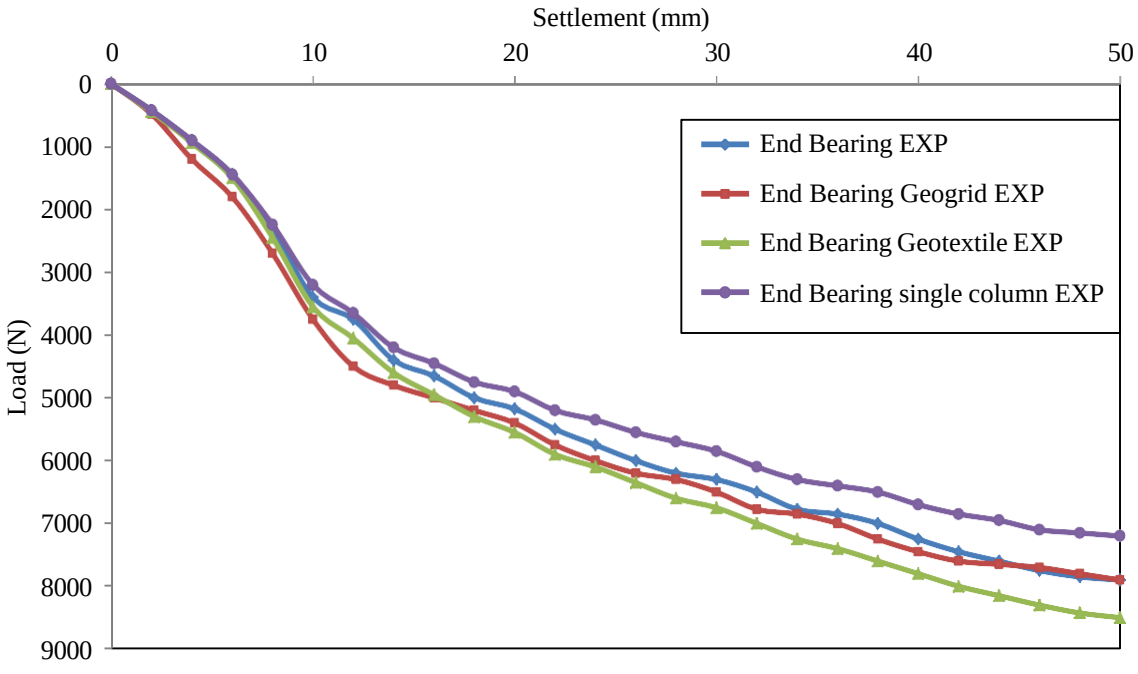

Figure 4.14 Load settlement variations of hexagonal patterns for end bearing

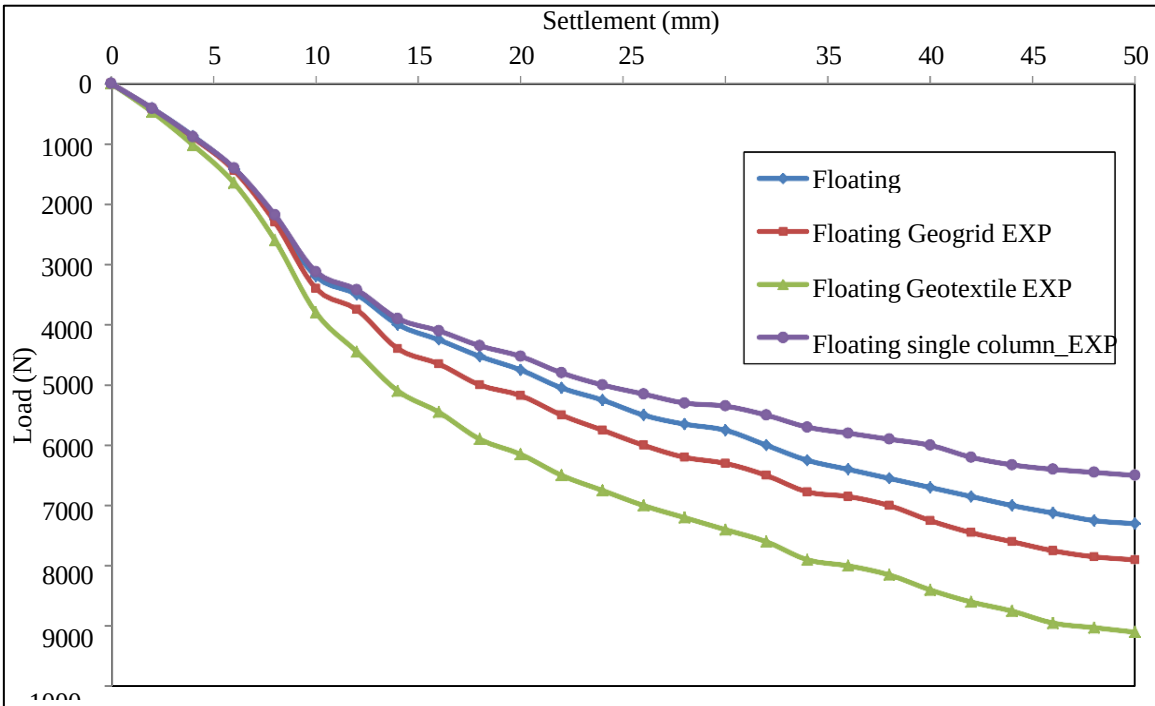

Figure 4.15 Load settlement variations of hexagonal patterns for floating

In triangular arrangement, geotextile provided a 6.52% improvement over geogrid for end bearing columns and 4.55% for floating columns. In the square pattern, the improvement was 5.81% for end bearing columns and only 1.16% for floating columns, indicating a relatively marginal effect. In contrast, the hexagonal arrangement showed the improvement, with 7.59% for end bearing and a pronounced 15.19% for floating columns. Among the patterns, triangular and hexagonal arrangements showed superior performance compared to the square pattern, with geotextile encasement consistently enhancing the load capacity beyond that of geogrid. Overall, group encased columns, particularly in triangular and hexagonal configurations, not only outperformed their geogrid counterparts but also exhibited substantial gains over single columns, highlighting the combined benefits of encasement and group action.

4.2 Column exhumation

To better understand the failure mechanism of the stone columns, column exhumation was carried out after the completion of load tests. The surrounding soil was carefully removed to expose the stone column, which allowed direct observation of its deformation pattern. The exhumation revealed noticeable

bulging of the column, confirming it as the predominant mode of failure under vertical loading due to inadequate lateral confinement provided by the surrounding clay. This visual evidence complemented the load–settlement response obtained during testing and provided a clearer understanding of the stress redistribution and interaction between the column and the surrounding soil.

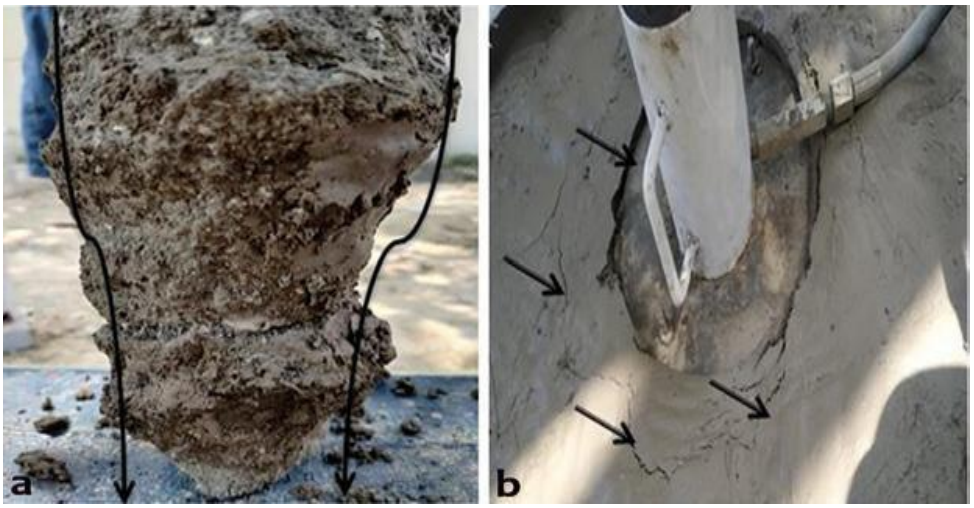

Figure 4.16 (a) Exhumed single column showed bulging failure; (b) failure cracks developed on the bed.

The Figure 4.16 shows two experimental observations related to the failure mechanism of stone columns under load. The image on the left Figure 4.16 (a) depicts an extracted stone column after load testing, where bulging of the column can be clearly seen. This bulging, highlighted by the drawn outline, is a typical failure mode of stone columns under vertical loading and indicates lateral expansion of the column as it deforms outward due to applied pressure, reflecting the mobilization of lateral stresses within the surrounding clay soil. The image on the right figure 4.16 (b) presents the surface cracks in the surrounding clay bed during loading. The arrows point to the formation and propagation of cracks radiating outward from the loaded area, which highlight the redistribution of stresses and the progressive failure of the clay matrix around the column. These observations confirm that, apart from bulging, surface

cracking is also a visible manifestation of failure. Overall, Figure (a) demonstrates bulging failure of the stone column, while Figure (b) shows the surface cracking of the surrounding soil, together providing clear evidence of the stress response and failure mechanisms during the load–settlement tests

Figure 4.17 illustrates the failure mechanism of stone columns subjected to punching failure. As shown in Figure 4.17 (a), a distinct bulb formation is observed at the base of the column after exhumation, which is a characteristic sign of punching failure where the column penetrates into the underlying soil mass instead of undergoing bulging. Figure 4.17 (b) shows the surface condition during loading, where visible cracks have developed around the loaded area as a result of the punching action. These cracks indicate the transfer of stresses to the surrounding soil and the progressive failure of the clay bed. Together, these observations confirm punching as the governing failure mechanism in this case, characterized by bulb development at the column base and surface cracking in the clay.

The exhumation studies revealed that the mode of failure of stone columns depends on their type. For end bearing columns, bulging was identified as the predominant failure mechanism.

Figure 4.17 (a) Bulb is developed at the base of the column due to punching failure; (b) cracks developed at the surface due to punching

In this case, the column exhibited lateral expansion along its length due to insufficient confinement from the surrounding clay, which was evident from the outward deformation of the column and the associated surface cracks. In contrast, floating columns primarily failed by punching, as indicated by the formation of a bulb at the base of the column due to downward penetration into the underlying soil. This was accompanied by the development of cracks concentrated around the loaded area. Hence, bulging is characteristic of end bearing columns, while punching is more common in floating columns, highlighting the variation in load transfer and soil–column interaction mechanisms.

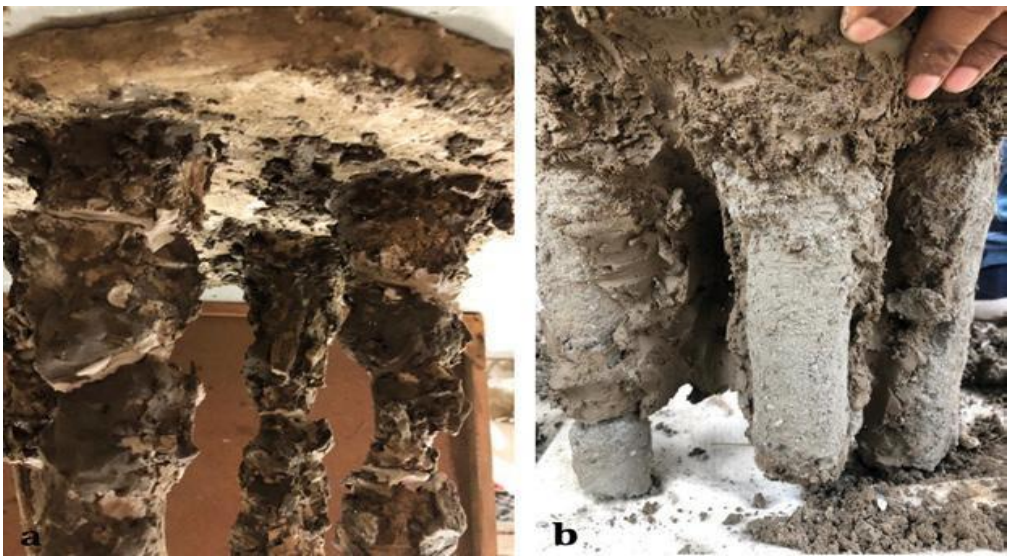

Figure. 4.18: (a) Exhumed square pattern column; (b) exhumed hexagonal column.

Figure 4.18 shows the exhumation of group stone columns after load testing. In Figure 4.18 (a), the columns are observed after removal of the overlying soil, clearly showing the interaction between adjacent columns. The bulging of individual columns along their length can be noticed, which indicates lateral deformation due to the applied vertical loading. In Figure 4.18 (b), a closer view of the group of columns is presented, highlighting the reduced lateral expansion as a result of group confinement. The presence of surrounding columns restricts excessive bulging of individual columns, thereby improving the stability and

performance of the group system compared to single columns. These observations confirm that stone columns in group arrangement not only experience bulging but also benefit from mutual confinement, which enhances their overall load carrying capacity.

The overall results highlight that the arrangement pattern of stone columns plays a significant role in governing their load–settlement behaviour and failure mechanism. For the triangular pattern, higher load carrying capacities were recorded, particularly with geotextile encasement, and exhumation revealed pronounced bulging controlled by mutual confinement among columns. In the square pattern, the load capacity was slightly lower compared to the triangular pattern, with exhumed columns showing noticeable bulging due to relatively less confinement. The hexagonal pattern exhibited comparatively better confinement and interaction among columns, as observed during exhumation, resulting in more uniform deformation and improved stability. Overall, the triangular and hexagonal arrangements performed better than the square pattern, with geotextile encasement consistently enhancing performance across all configurations.

The comparison between single and group stone columns clearly demonstrates the beneficial effect of group action on load–settlement performance. In single column tests, failure was primarily governed by bulging or punching, depending on the column type, and lateral deformation was more pronounced due to limited confinement from the surrounding soil. In contrast, exhumation of group columns, revealed reduced bulging and more uniform deformation. This improvement can be attributed to the mutual confinement provided by adjacent columns, which restricts excessive lateral expansion and distributes the applied load more effectively. Consequently, group columns not only enhance the overall load carrying capacity but also exhibit greater stability compared to single columns.

4.4 NUMERICAL RESULTS: SINGLE STONE COLUMN and GROUP OF STONE COLUMNS

4.4.1 Validation

The validation of the numerical models was carried out by simulating the load–settlement response observed in the model tests of Murtaza and Samadhiya, (2016). Their laboratory experiments, based on the unit cell concept, investigated the behaviour of individual stone columns embedded in soft clay. Tests were performed on columns with diameters of 75 mm and 90 mm, subjected to two types of loading: (a) loading applied only to the column and (b) loading applied across the entire unit cell area. Both end-bearing and floating column conditions were examined.

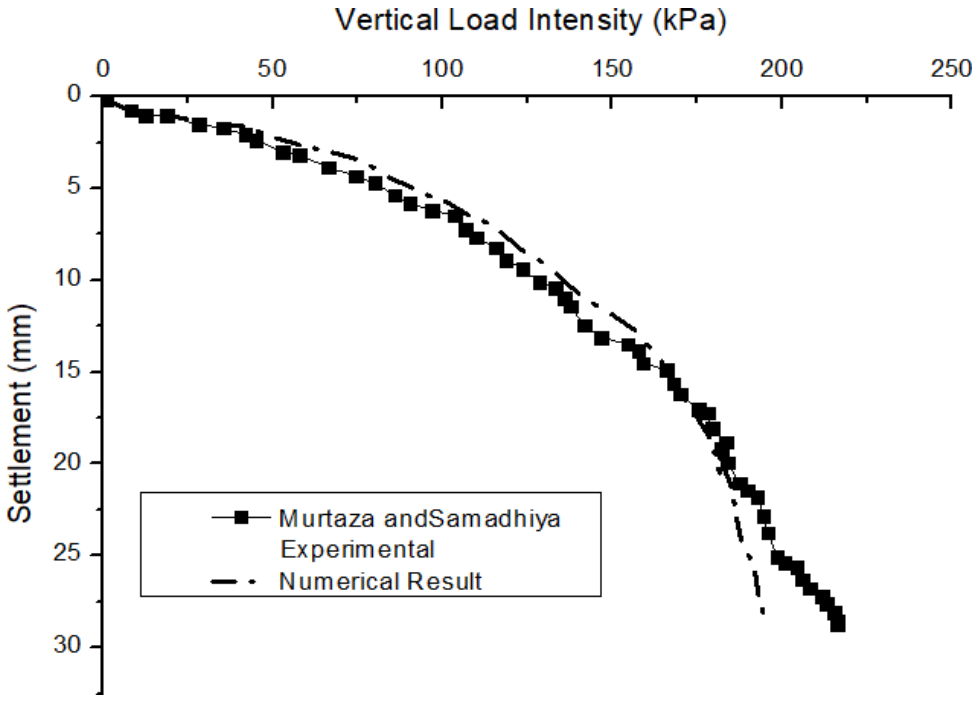

Figure 4.19. Comparison of vertical load intensity settlement behaviour of end bearing column

In the present study, validation was specifically focused on the case of column area loading for both end-bearing and floating conditions. A single 75 mm diameter column, with a length of 525 mm, was considered. The column was

encased with a geotextile having a tensile strength of 4.4 kN/m. The material properties adopted for the numerical model were consistent with those reported by Murtaza and Samadhiya. Figure 4.19 compares the vertical load–settlement response of end-bearing granular piles obtained from the present study with the experimental results. The comparison shows that settlement differed by less than 3% in most cases, with a maximum variation of about 15% occurring at settlements between 20–30 mm. These results demonstrate that the proposed model is in close agreement with experimental findings, confirming the suitability of the modelling approach for simulating the behaviour of soft clay reinforced with encased stone columns.

4.4.2 Analysis of the load-settlement behaviour of a clay bed

A numerical analysis was carried out to evaluate the load–settlement behaviour of an unreinforced clay bed. The load–settlement response of untreated soft clay is presented in Figure 4.20. At an ultimate settlement of 50 mm, the clay bed exhibited a load-carrying capacity of 5.4 kN.

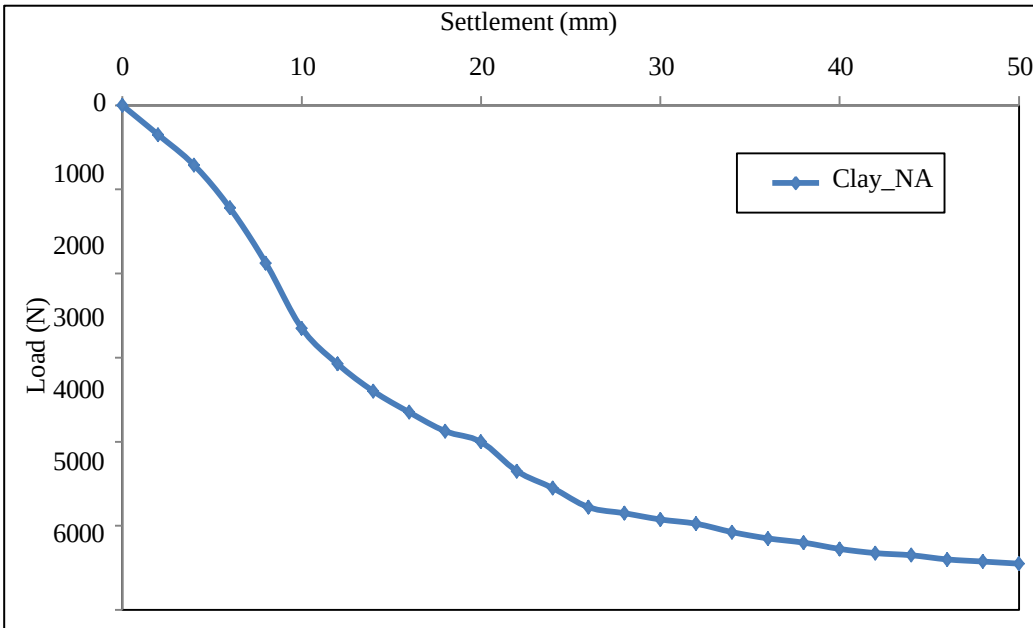

Figure 4.20 Load-Settlement variation of clay bed without any reinforcement

4.4.3 Clay bed reinforced with ordinary stone column- Single Stone Column

Similar to the experimental investigation, the 70 mm diameters of stone column was used for numerical analysis. A loading plate of 300 mm diameter was used. The observed percentage of A_r in the present investigation was 7.09% for columns having diameters of 70 mm, respectively. Figure 4.21 and 4.22 represents the load-settlement behaviour of the ordinary end bearing stone column and floating column. For the unreinforced clay bed, the load at an ultimate settlement of 50 mm was 5.4 kN, which was increased to 7.15 kN for end bearing column, corresponding to an increase of approximately 32.41% compared to the unreinforced bed and 6.30 kN in the case of floating stone column analysed numerically which represents an enhancement of about 16.67%. Similar trend as that obtained from experimental result was observe that reinforcing the soft clay bed with ordinary stone columns increases the load carrying capacity of the composite clay bed.

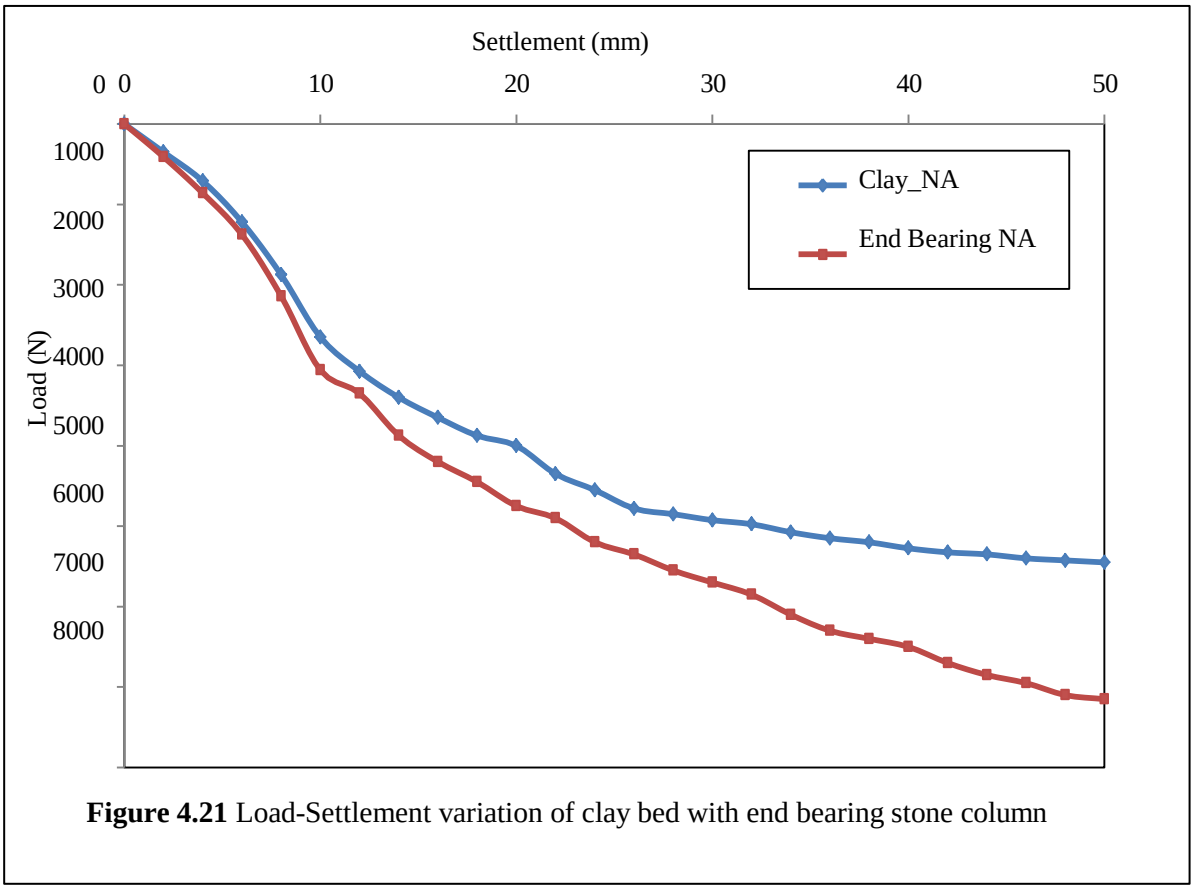

Figure 4.21 Load-Settlement variation of clay bed with end bearing stone column

The results indicates a significant enhancement in the load-carrying capacity of the composite clay bed due to the inclusion of stone columns, with the end bearing column performing better than the floating column. The trend obtained is consistent with the experimental investigation, further validating the effectiveness of stone columns in improving the strength and settlement response of soft clay soils.

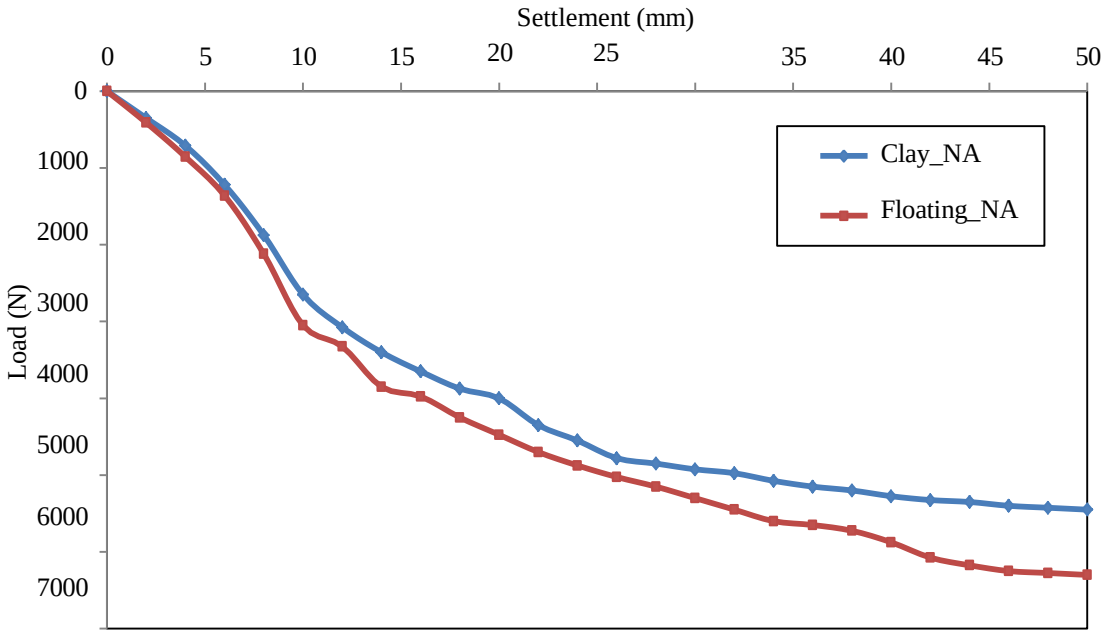

Figure 4.22 Load-Settlement variation of clay bed with floating stone column

4.4.4 Clay bed reinforced with encased stone column- Single Stone Column

To comprehend the behaviour of the encased stone column, like experimental analysis where two varieties of geosynthetics were used, in the numerical analysis also, geogrid and geotextile was used to determine the behaviour of composite soil bed. The analysis was carried out for both end bearing and floating columns.

Figure 4.23 and 4.24 depicts the load-settlement behaviour of encased stone columns for end bearing and floating column with D = 70 mm for both the geosynthetics used. For the unreinforced clay bed, the load carrying capacity at

an ultimate settlement of 50 mm was observed to be 5.4 kN. The provision of stone columns significantly improved the strength of the composite ground. For end bearing columns, the load carrying capacity increased to 7.15 kN, representing an improvement of 32.41% over the unreinforced bed. Further enhancement was achieved by encasement, where end bearing columns reinforced with geogrid and geotextile exhibited capacities of 7.52 kN and 7.85 kN, corresponding to 39.26% and 45.37% improvements, respectively.

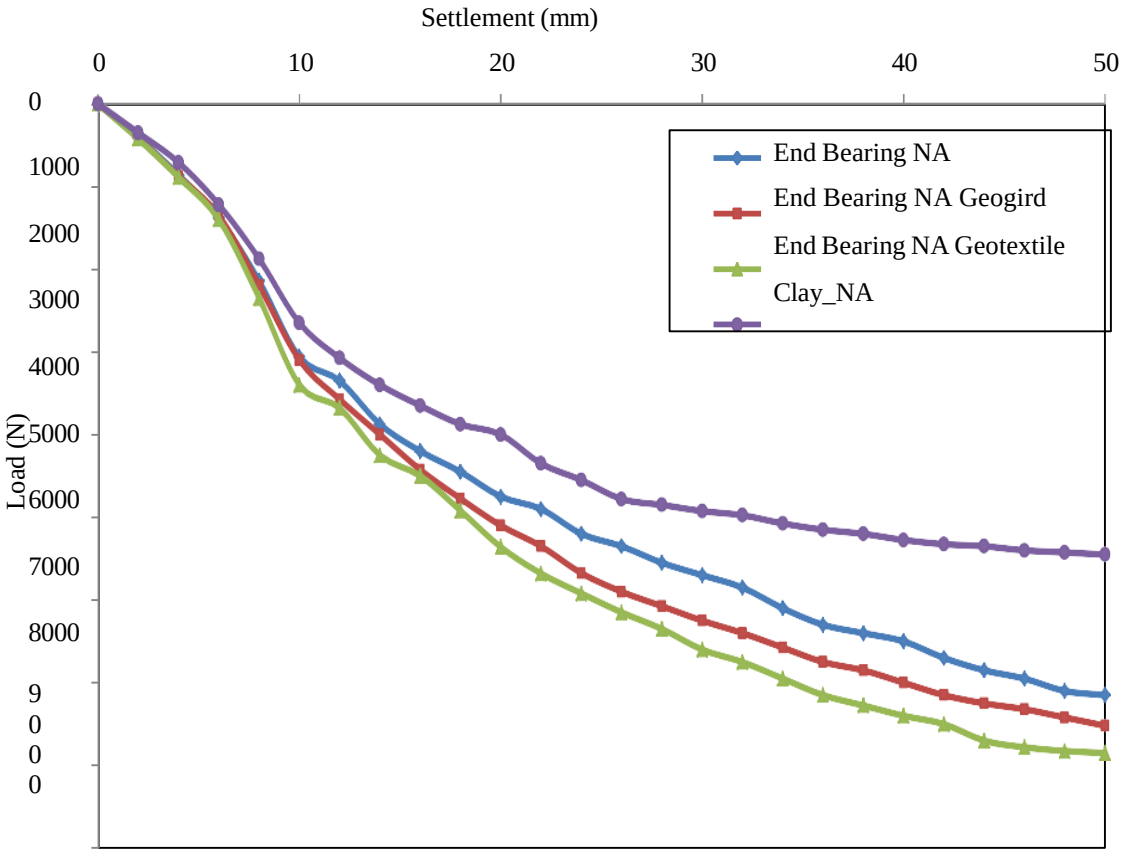

Figure 4.23 Load-settlement variation of the end bearing stone column with varying encasement

Similarly, floating columns also improved the capacity to 6.30 kN (16.67% increase), while geogrid and geotextile encasement raised the values to 7.25 kN and 7.45 kN, giving 34.26% and 37.96% improvements. These results highlight that column encasement with geosynthetics, particularly geotextile, provides substantial gains in load carrying performance, with end bearing columns

showing superior improvement compared to floating columns.

The load–settlement response of both end bearing and floating stone columns clearly indicates that the untreated clay bed exhibited the lowest load carrying capacity and the highest settlement, reflecting its weak performance under applied loading. The inclusion of stone columns significantly improved the behavior, with end bearing columns performing better than floating ones due to direct load transfer to the firm stratum. Further enhancement was observed with geosynthetic encasement, where both geogrid and geotextile provided additional confinement, leading to higher load resistance and reduced settlement. Between the two, geotextile encasement consistently outperformed geogrid, demonstrating greater efficiency in restricting lateral bulging of the column. Overall, end bearing stone columns with geotextile encasement showed the highest load carrying capacity, while floating stone columns with geogrid encasement offered comparatively lower but still notable improvement over untreated clay.

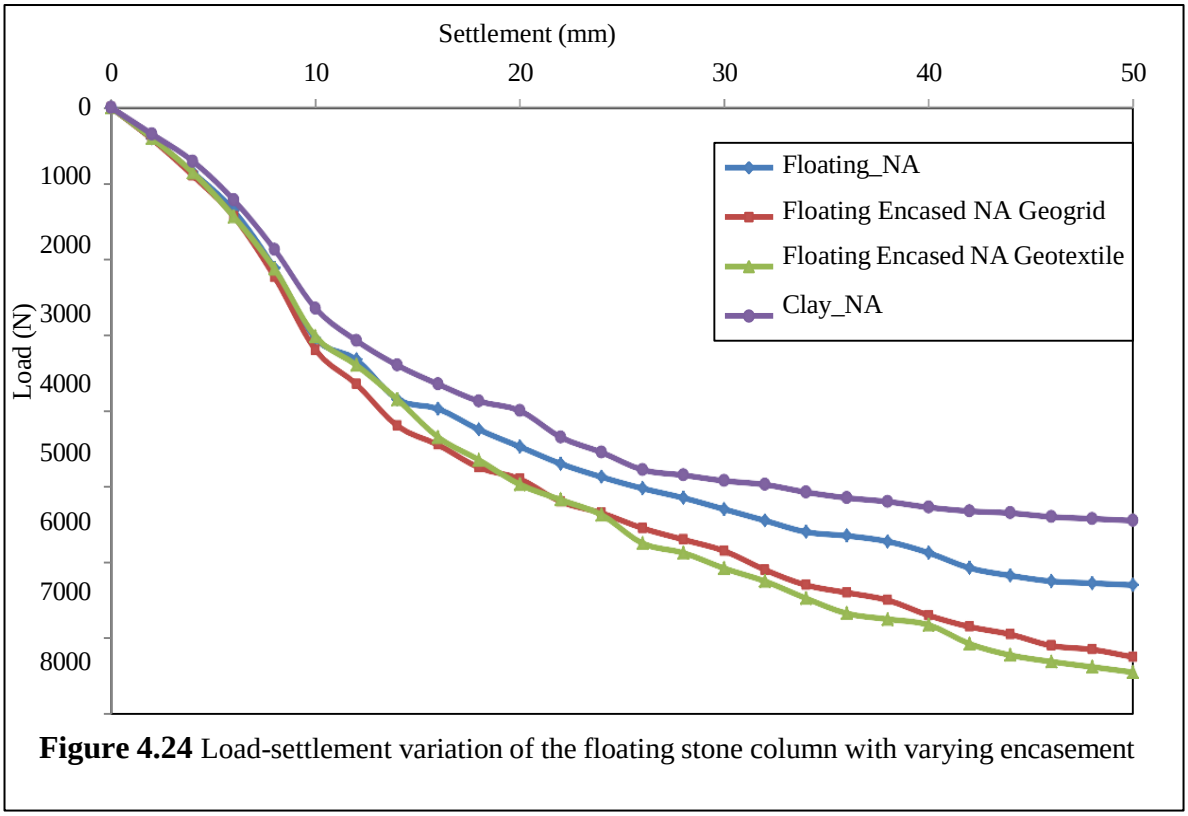

Figure 4.24 Load-settlement variation of the floating stone column with varying encasement

This confirms that reinforcement not only increases the stiffness of the composite ground system but also ensures more reliable and durable performance under loading conditions.

The displacement contours of different stone column configurations highlight the distinct deformation patterns under loading. In the case of the Ordinary Stone Column (OSC) (Figure 4.25 a), the displacement is uniformly distributed along the column, with the magnitude being the least among all configurations. This indicates better confinement and lower lateral bulging, thereby ensuring improved stability of the column within the clay bed.

For the End Bearing Column (Figure 4.25 b), the bulging phenomenon is clearly visible in the middle zone of the column. The column transfers load effectively to the underlying firm stratum; however, due to the soft clay surrounding it, a significant lateral displacement occurs in the bulging zone. This behavior confirms that end bearing columns are more effective in enhancing load capacity but remain vulnerable to bulging unless encased with reinforcement.

In contrast, the Floating Column (Figure 4.25 c) shows pronounced settlement and displacement near the bottom portion of the column. Since it does not rest on a firm stratum, the column depends primarily on skin friction for load transfer. This leads to a concentration of stresses near the tip and results in higher deformation compared to the other two cases. Consequently, floating columns are less efficient in reducing settlement and require reinforcement or group installation for improved performance.

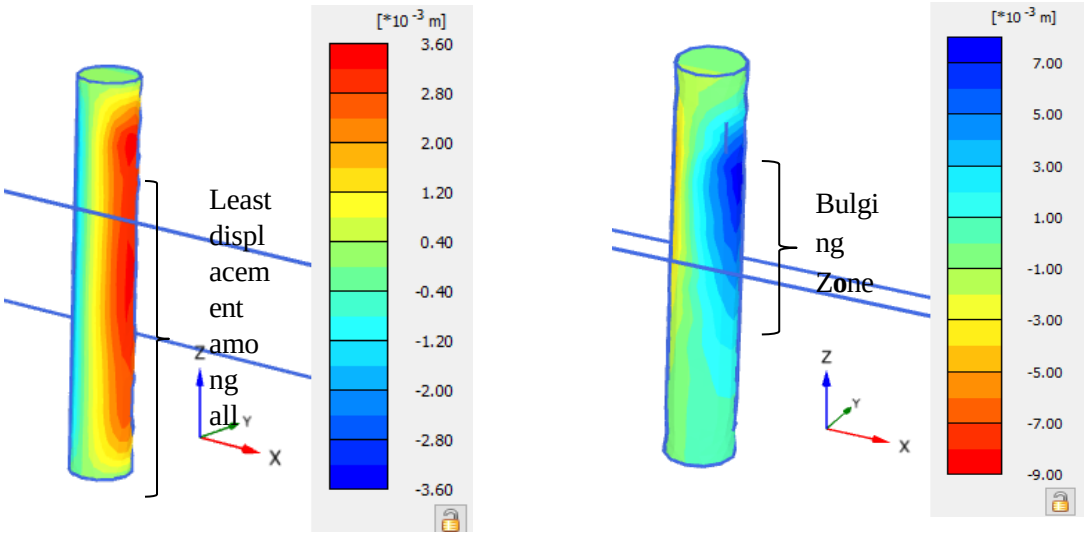

Figure 4.25. (a) OSC (b) End bearing column

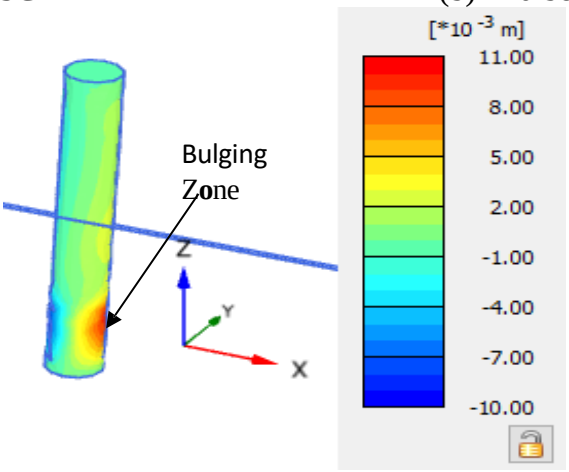

(c) Floating column

4.4.5 Clay bed reinforced with ordinary stone column- Group of stone columns

The group analysis of stone columns arranged in triangular, square and hexagonal patterns with varying S/D ratios shown in Figure 4.26 and 4.27 revealed considerable improvement in the load carrying capacity of the composite ground. For triangular configuration (S/D = 2), the ultimate load at 50 mm settlement was 8.75 kN for end bearing columns and 9.10 kN for floating columns, corresponding to improvements of 61.94% and 68.52% over the unreinforced clay bed. In the case of the square pattern (S/D = 2), end bearing columns exhibited the highest capacity of 9.15 kN, which is 69.44% greater than

the unreinforced bed, whereas the floating columns carried 7.45 kN, marking a 37.96% increase. For the hexagonal configuration (S/D = 3), the capacities reduced to 7.65 kN and 6.45 kN for end bearing and floating columns, yielding 41.67% and 19.44% improvements, respectively. These results indicate that the square pattern provides the maximum improvement in load carrying capacity for end bearing columns**,** whereas the triangular pattern favours floating columns, while the hexagonal arrangement shows comparatively lower efficiency due to the larger spacing between columns.

Thus, it can be concluded that closer spacing and compact arrangements such as triangular and square patterns are more efficient in improving the load carrying performance of stone column–reinforced ground, whereas wider spacing, as in the hexagonal pattern, results in comparatively lower improvement. Moreover, end bearing columns perform better in square arrangements, while floating columns benefit more from triangular configurations.

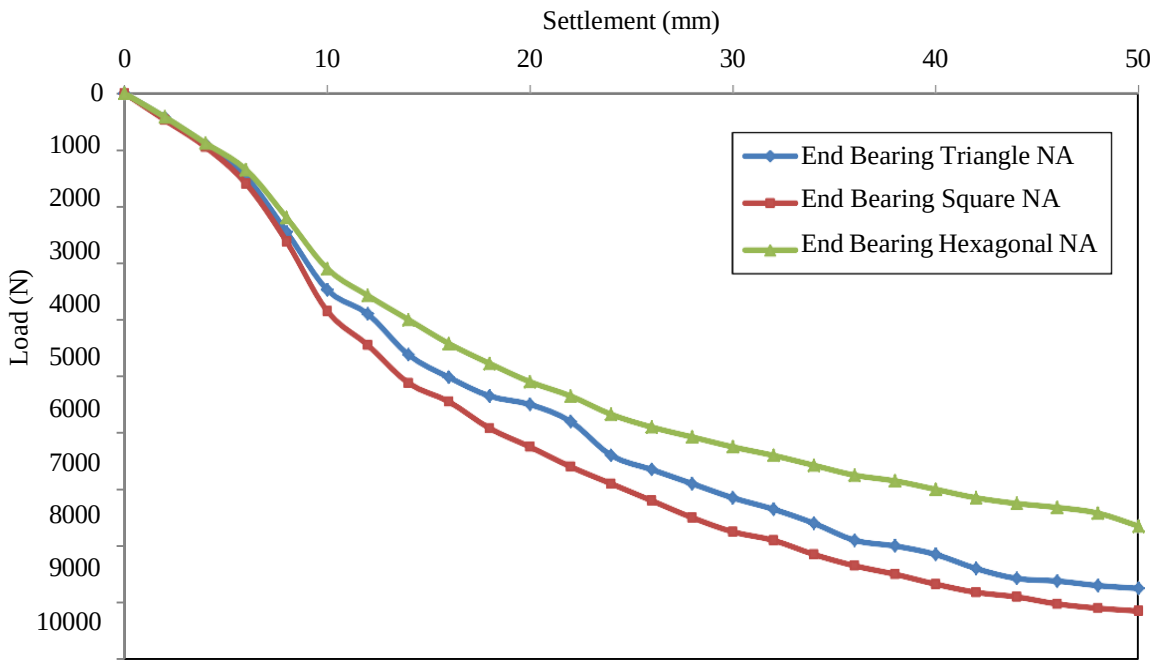

Figure 4.26 Load settlement variations of different patterns for unencased end bearing columns

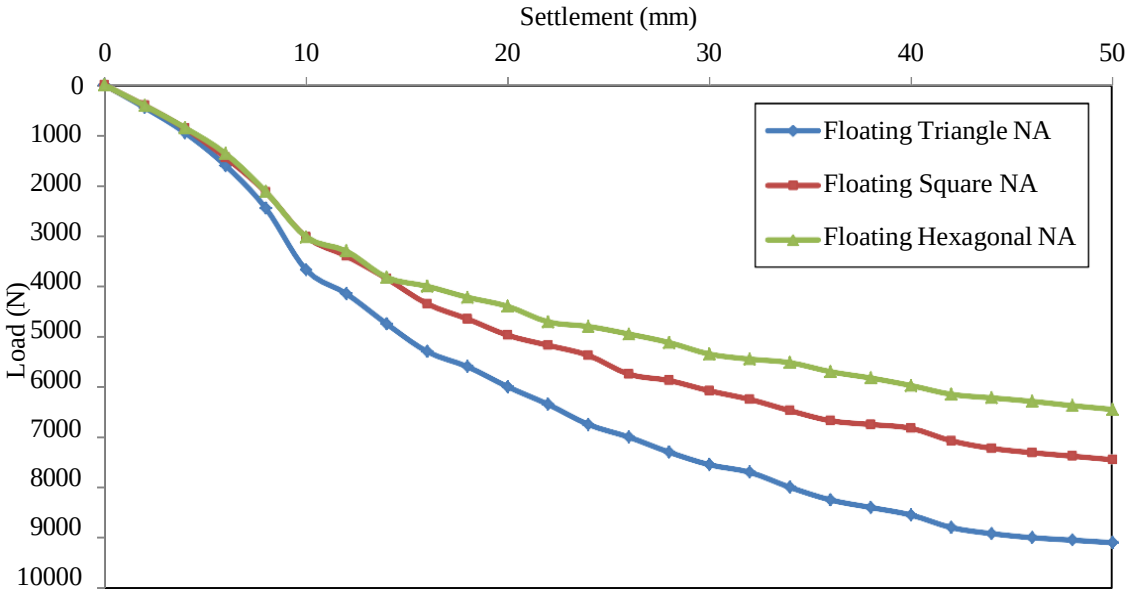

Figure 4.27 Load settlement variations of different patterns for unencased floating

4.4.6 Reinforcing clay bed with encased stone column- Group of Stone Columns

Similar to the single stone column analysis, group analysis was also done for encased stone columns. In the group analysis also encasement provided to full length of column for both end bearing and floating columns was used. Also, both type of geosynthetics was used and compared for the analyses.

4.4.6.1 Triangular pattern with encased stone column

Figure 4.28 depicts the load-settlement behaviour of end bearing encased stone columns arranged in triangular pattern for S/D = 2 for D = 50 mm. Similarly, Figures 4.29 show the load-settlement behaviour of floating encased columns arranged in triangular pattern for S/D = 2 for D = 50 mm, respectively. For D = 50 mm, the ultimate load bearing capacity for end bearing encased stone columns of triangular pattern for S/D = 2 was found as 8.75 kN for geogrid and 9.3 kN for geotextile respectively indicating that geotextile provides superior confinement and enhances the overall stiffness of the composite system. Similarly the ultimate load bearing capacity for floating encased stone columns of triangular pattern for S/D = 2 was found as 8.65 kN for geogrid and 8.75 kN for geotextile respectively, showing comparable performance, though geotextile again provided a marginally higher improvement. Overall, the results confirm

that encasement enhances the efficiency of stone columns**,** with geotextile proving more effective than geogrid, and the triangular arrangement offering favorable load-settlement response for both end bearing and floating columns.

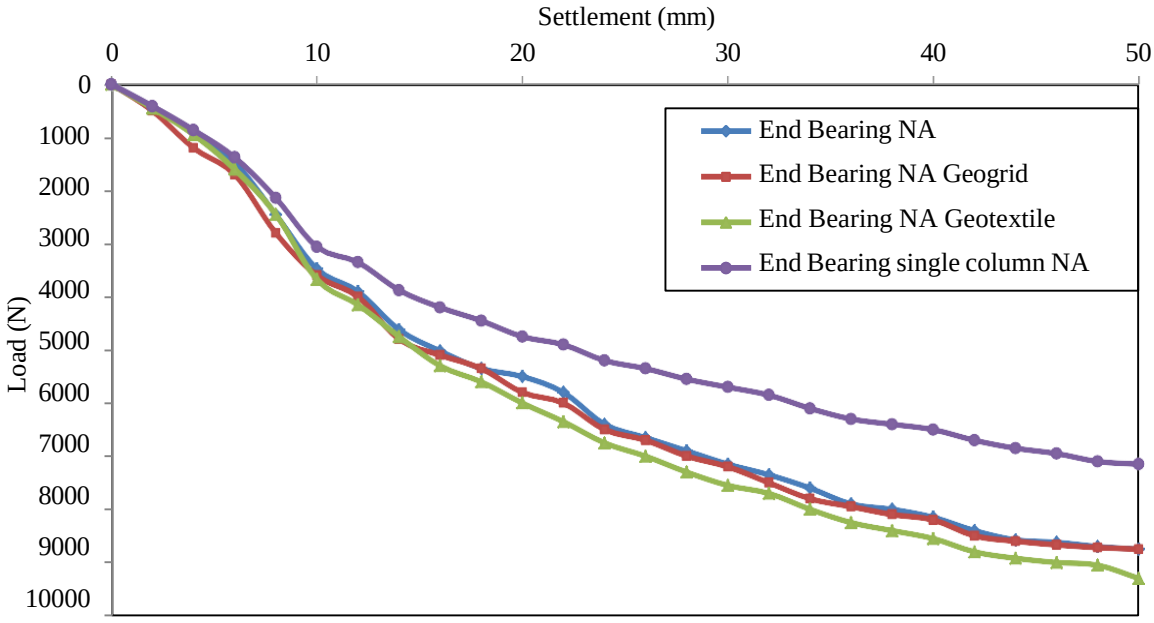

Figure 4.28 Load settlement variations of triangular patterns for end bearing

The study clearly demonstrates that encasement significantly enhances the performance of stone columns in triangular arrangements (S/D = 2, D = 50 mm). End bearing columns showed the highest improvement, with geogrid and geotextile encasement increasing the load carrying capacity by 62.04% and 72.22%**,** respectively, over the unreinforced clay bed. Floating columns also benefitted, with improvements of 60.19% for geogrid and 62.04% for geotextile encasement. These observations confirm that geotextile performs better than geogrid, providing superior confinement and higher load resistance. Furthermore, the results highlight that end bearing columns gain more advantage from encasement than floating columns, making them the most efficient configuration for improving ground strength.

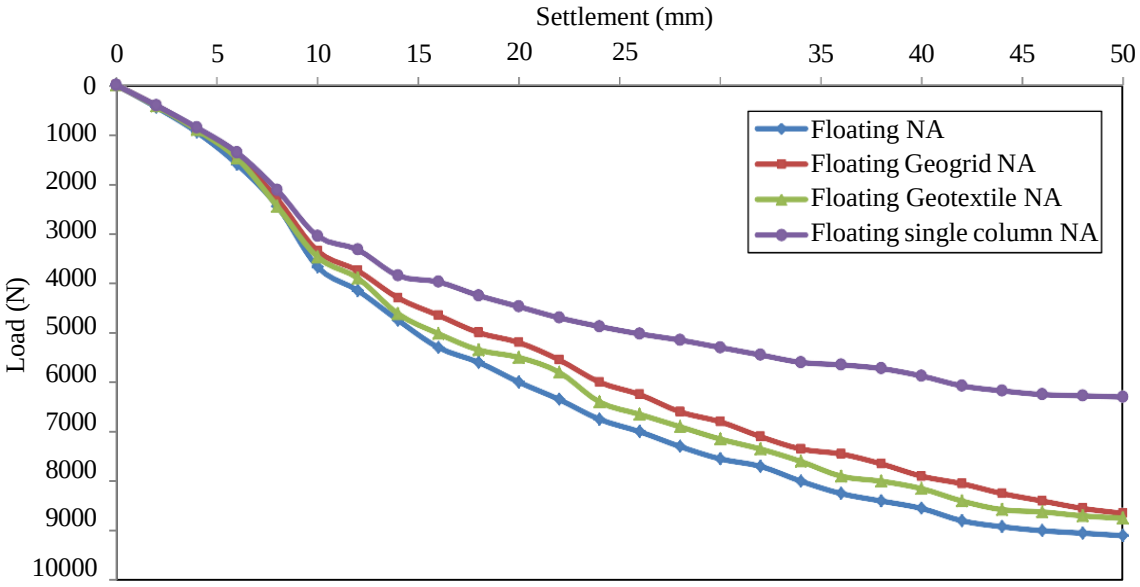

Figure 4.29 Load settlement variations of triangular patterns for floating columns

4.4.6.2 Square pattern with encased stone column

Figure 4.30 depicts the load-settlement behaviour of end bearing encased stone columns arranged in square pattern for S/D = 2 for D = 50 mm. Similarly, Figures 4.31 show the load-settlement behaviour of floating encased columns arranged in square pattern for S/D = 2 for D = 50 mm, respectively. For D = 50 mm, the ultimate load bearing capacity for end bearing encased stone columns of square pattern for S/D = 2 was found as 8.15 kN for geogrid and 8.70 kN for geotextile respectively. Similarly the ultimate load bearing capacity for floating encased stone columns of square pattern for S/D = 2 was found as 7.35 kN for geogrid and 8.4 kN for geotextile respectively.

The results of the square pattern arrangement (S/D = 2, D = 50 mm) show that encasement considerably improves the load carrying capacity of stone columns compared to the unreinforced clay bed. For end bearing columns, the capacity increased to 8.15 kN with geogrid (50.93% improvement) and further to 8.70 kN with geotextile (61.11% improvement), indicating that geotextile provides superior confinement. Floating columns also benefitted, with capacities of 7.35 kN for geogrid (36.11% increase) and 8.40 kN for geotextile (55.56% increase). These observations confirm that geotextile performs better than

geogrid in enhancing load resistance, and that end bearing columns derive greater benefit from encasement than floating columns in square arrangements.

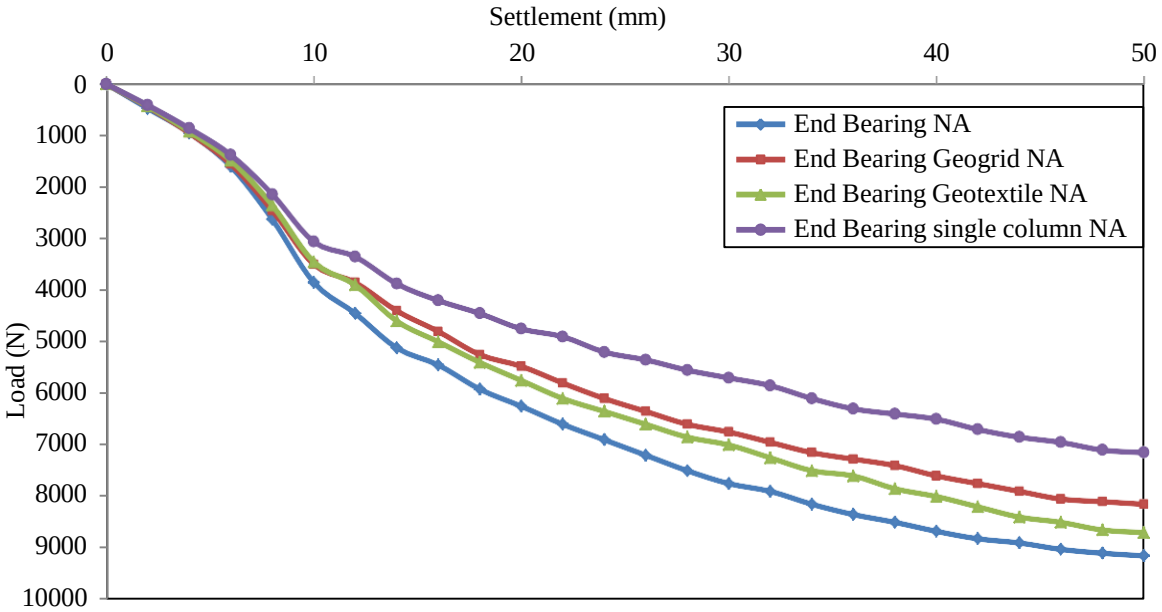

Figure 4.30 Load settlement variations of square patterns for end bearing columns

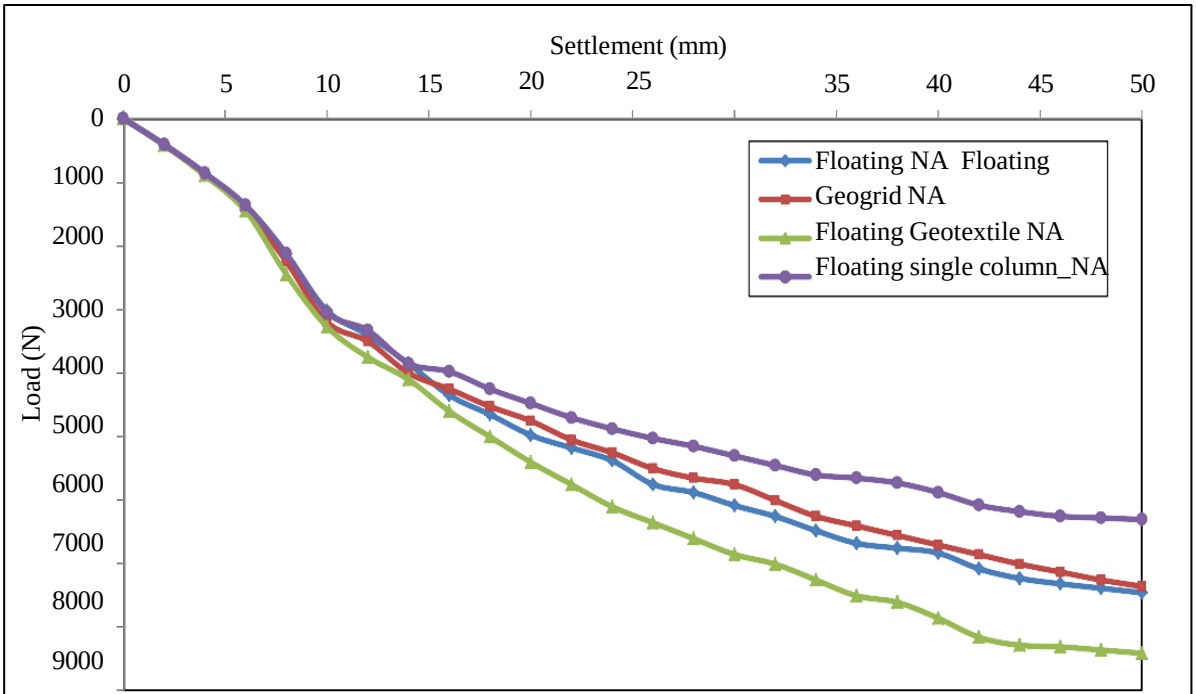

Figure 4.31 Load settlement variations of square patterns for floating columns

The observations indicate that encasement of stone columns in square arrangements with S/D = 2 significantly improve the load carrying capacity compared to the unreinforced clay bed.

End bearing columns showed greater improvement than floating columns, with geotextile encasement proving more effective than geogrid in both cases. This confirms that geotextile provides better confinement and strength enhancement, while end bearing encased columns are the most efficient configuration for improving ground performance in square patterns.

4.4.6.3 Hexagonal pattern with encased stone column

Figure 4.32 depicts the load-settlement behaviour of end bearing encased stone columns arranged in hexagonal pattern for S/D = 3 for D = 50 mm. Similarly, Figures 4.33 show the load-settlement behaviour of floating encased columns arranged in hexagonal pattern for S/D = 3 for D = 50 mm, respectively. For D = 50 mm, the ultimate load bearing capacity for end bearing encased stone columns of hexagonal pattern for S/D = 3 was found as 7.45 kN for geogrid and 8.22 kN for geotextile respectively. Similarly the ultimate load bearing capacity for floating encased stone columns of hexagonal pattern for S/D = 3 was found as 8.42 kN for geogrid and 7.45 kN for geotextile respectively.

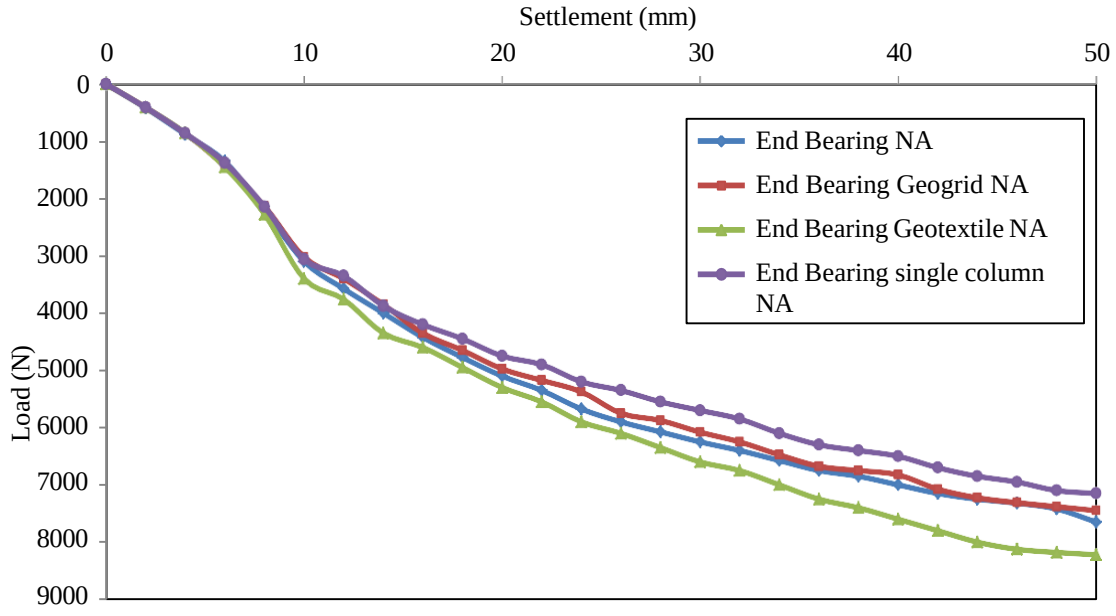

Figure 4.32 Load settlement variations of hexagonal patterns for end bearing

The results of the hexagonal pattern arrangement with S/D = 3 and D = 50 mm show that encasement improves the load carrying capacity of stone columns, though the improvement is less pronounced than in triangular and square patterns. For end bearing columns, geogrid and geotextile encasement increased the capacity to 7.45 kN (37.96% improvement) and 8.22 kN (52.22% improvement), respectively, with geotextile again showing better confinement. For floating columns, the behaviour was less consistent, with geogrid providing the highest improvement of 55.93%, while geotextile resulted in only a 37.96% increase. Overall, geotextile is more effective for end bearing columns, while geogrid provides better results for floating columns in the hexagonal arrangement. The larger spacing in the hexagonal pattern reduces group efficiency, making it less effective than triangular or square configurations.

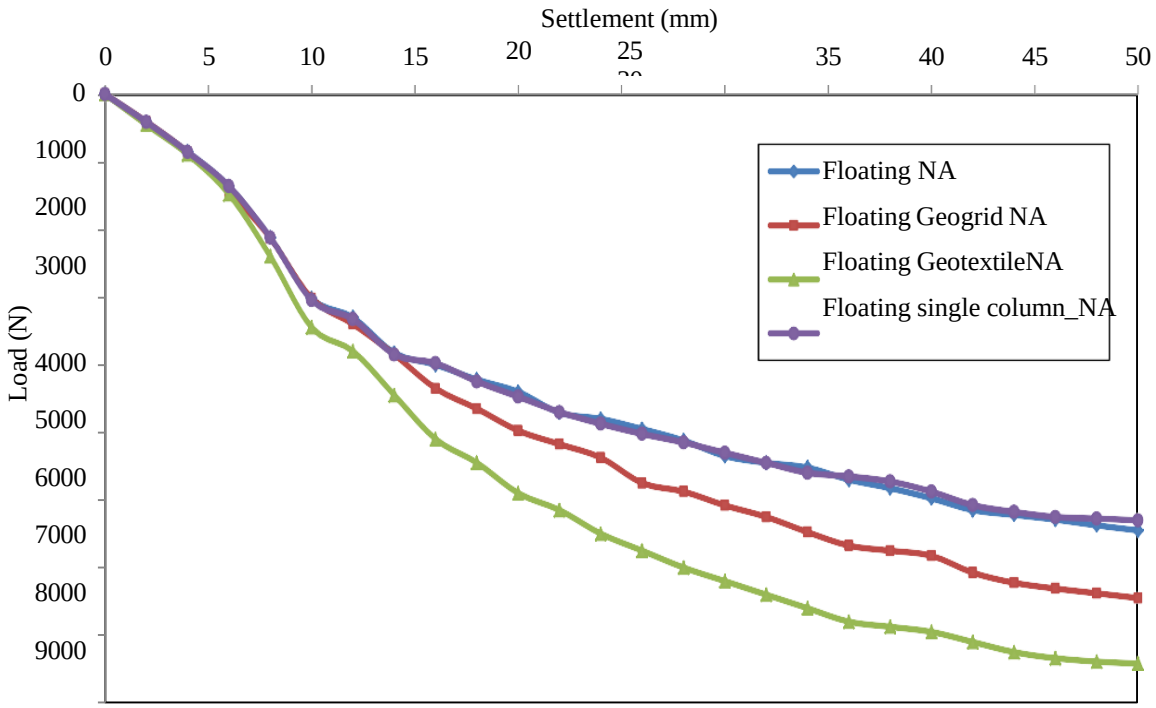

Figure 4.33 Load settlement variations of hexagonal patterns for floating

The comparative study of encased stone-column groups shows a clear pattern: closer, more compact arrangements (S/D = 2) and geotextile encasement produce the largest gains in load carrying capacity, while wider spacing (S/D = 3) reduces group efficiency. Overall, the triangular and square patterns

outperform the hexagonal pattern. The best result in the tested cases is the triangular pattern with geotextile encasement for end bearing columns (9.30 kN; 72.22% increase over the unreinforced clay bed), followed by triangular geogrid and geotextile encasements for floating columns (60–62% increases). Square patterns also give large improvements, particularly for end bearing columns with geotextile (8.70 kN; 61.11% increase) and for floating columns with geotextile (8.40 kN; 55.56% increase). The hexagonal pattern (S/D = 3) is the least effective overall because the larger spacing reduces interaction between columns; although some encasement cases (for example, floating with geogrid at 8.42 kN, 55.93%) still show moderate gains, they do not match the top performances of triangular or square layouts.

Two consistent findings emerge: (1) encasement materially increases capacity for both end bearing and floating columns, and (2) geotextile generally provides superior confinement and higher increases than geogrid—particularly for end bearing columns—while geogrid occasionally gives competitive results for some floating-column cases. End bearing encased columns benefit more from encasement than floating encased columns in most tested configurations.

The overall experimental and numerical investigations confirm that stone column installation significantly enhances the load carrying capacity of soft clay beds, with end bearing columns consistently performing better than floating columns. Both approaches showed good agreement in terms of load–settlement response, validating the reliability of the numerical model in capturing field behaviour. The inclusion of geosynthetic encasement further improved performance by providing lateral confinement and reducing bulging, thereby increasing stiffness and strength of the composite ground. Between the two types of geosynthetics, geotextile consistently yielded greater improvement than geogrid, particularly for end bearing columns, while geogrid occasionally gave comparable performance for floating columns.

In group configurations, triangular and square patterns with closer spacing (S/D

= 2) demonstrated superior efficiency compared to hexagonal patterns with wider spacing (S/D = 3). The highest improvements were observed for end bearing columns encased with geotextile in triangular and square arrangements, showing increases of more than 70% over the unreinforced clay bed. Floating columns also benefited substantially, though to a lesser degree than end bearing columns.

Overall, the study concludes that both experimental and numerical analyses highlight the effectiveness of stone columns in strengthening soft soils, with encasement—especially with geotextile—providing the greatest benefit. End bearing encased columns in compact group layouts emerge as the most efficient configuration for enhancing the load carrying capacity of soft clay deposits.

4.4.7 Swelling Behavior in numerical modelling

In the present study, the swelling behaviour of expansive soil was incorporated in the numerical modelling to simulate realistic field conditions and to evaluate its influence on ground deformation. Expansive soils exhibit significant volume change characteristics due to moisture variation, leading to swelling during wetting and shrinkage during drying, which adversely affects foundation performance. The numerical analysis was carried out using PLAXIS 3D with the Mohr–Coulomb constitutive model, wherein the swelling behaviour was represented through compressibility parameters such as compressibility index (Cc = 0.50) and swelling index (Cs = 0.10), along with Young's modulus (E = 10 MPa) and Poisson's ratio (ν = 0.35). The inclusion of the swelling index enabled the simulation of volumetric expansion during unloading or reduction in effective stress, thereby capturing the swelling tendency of expansive soil. The results indicate that untreated expansive soil exhibits significant swelling behaviour, reflected in the form of higher settlement and heave tendency due to increased void ratio and reduced effective stress. A comparative evaluation shows that the settlement of untreated soil increased from 14.0 mm (without swelling) to 18.5 mm (with swelling), representing an increase of approximately

32%, which highlights the severity of swelling effects. However, the inclusion of stone columns significantly modifies this behaviour. The settlement in reinforced soil increased only from 10.5 mm to 12.2 mm (≈16%) for ordinary stone columns, from 8.6 mm to 9.8 mm (≈14%) for encased columns, and from 7.5 mm to 8.6 mm (≈15%) for stone columns with iron dust. This clearly demonstrates that the presence of stone columns reduces the impact of swelling by nearly 50% compared to untreated soil. The reduction in swelling-induced deformation is attributed to the provision of drainage paths, increased composite stiffness, and lateral confinement of the surrounding soil. Furthermore, geosynthetic encasement enhances confinement, while the addition of iron dust improves stiffness and inter-particle interaction, resulting in better control of swelling behaviour. The overall settlement reduction achieved due to reinforcement was found to be approximately 34% for ordinary stone columns, 47% for encased columns, and up to 54% for stone columns with iron dust under swelling conditions. These findings are consistent with studies reported by Black et al. (2007) and Bergado et al., (1994) who observed improved stiffness and reduced compressibility due to stone column inclusion, as well as Madhav and Vitkar (1978), who highlighted the effectiveness of reinforcement in controlling swelling behaviour. Thus, the incorporation of swelling parameters in numerical modelling provides a realistic representation of expansive soil behaviour and confirms that stone column reinforcement is highly effective in mitigating swelling-induced deformation while improving bearing capacity and overall ground performance.

Table 4.1. Comparison of results with and without swelling

Condition	Settlement without Swelling (mm)	Settlement with Swelling (mm)	% Increase due to Swelling
Untreated soil	14.5	18.5	32%
Stone column	10.5	12.2	16%
Stone column with encasement	8.6	9.8	14%
Stone column + iron dust	7.5	8.6	15%

4.4.8 Load Bearing Capacity compared by conventional formulae (e.g., Terzaghi's formula, Mayerhoff formula and IS code formula)

Plate diameter, B = 300 mm = 0.3 m

Radius = 0.15 m

Area $A=\pi(0.15)^2 = 0.0707\ m^2$

Cohesion, c = 32.37 kPac = 32.37

Friction angle, $\phi=18.2^{o}$

Unit weight (from Table 3.1) $\gamma \approx 18\ kN/m^3$

Depth of footing ≈ 0 (surface loading condition in model test)

Experimental load = 5.9 kN

$$q_{exp} = 5.9/0.707 = 83.5\ kPa$$

1)Terzaghi's bearing capacity equation formula for circular footing

$$q_{ult} = 1.3cN_c + \gamma D_f N_q + 0.3\ \gamma B N_\gamma$$

footing is at surface $D_f = 0$ $N_c = 17$, $N_q = 7$, $N_\gamma = 5$

$$q_{ult} = 724\ kPa$$

Ultimate load $Q_{ult} = 5.12$ kN

2) Mayerhof's equation

$$q_{ult} = cN_cS_cd_c + \gamma D_f N_q S_q d_q + 0.5\ \gamma B N_\gamma S_\gamma d_\gamma$$

for circular footing, $S_c = 1.3$, $S_q = 1.2$, $S_\gamma = 0.6$, $D_f = 0$

$$q_{ult} = cN_cS_cd_c + 0.5\ \gamma B N_\gamma S_\gamma d_\gamma = 720.7\ kPa$$

Ultimate load $Q_{ult} = 5.09$ kN

3) IS code formula:

for circular footing

$$q_{ult} = cN_cS_c + \gamma D_f N_q S_q + 0.5\ \gamma B N_\gamma S_\gamma$$

$S_c = 1.3$, $S_q = 1.2$, $S_\gamma = 0.6$, $D_f = 0$

$$q_{ult} = cN_cS_c + 0.5\ \gamma BN_\gamma S_\gamma = 720\ kPa$$

Ultimate load $Q_{ult} = 5.1$ kN

In the plate load test the ultimate load at which the sample fails is 5.9 kN is obtained. The ultimate load as obtained from Terzaghi's formula, Mayerhoff formula and IS code formula are 5.12 kN, 5.09 kN and 5.1 kN respectively. The theoretical values obtained are close to the experimental results. This agreement indicates that the shear strength parameters c = 32.37 kPa & $\phi = 18.2^0$ obtained from laboratory testing realistically represented the behaviour of the prepared clay bed. Similar consistency between analytical predictions and plate load test results in expensive clay has been reported in the literature by Jie Han (2015), who noted that classical bearing capacity equations provide reasonable estimates when laboratory-determined parameters are used. Furthermore, model studies by Madhav and Miura (1994), as well as Murugesan and Rajagopal (2009), demonstrated that good correlation between theoretical and experimental values confirms proper soil characterization and minimal scale effects. Therefore, the agreement in the present study validates the reliability of the experimental procedure, the selected soil parameters, and the numerical modelling approach adopted in the present study.

4.5 Comparative Analysis of Experimental and Numerical Outcomes of Tests Performed on Single Stone Column and Group of Stone Columns

A comparison with the numerical data obtained by Plaxis 3D was also conducted to validate the experimental results. The failure mechanism was similar in both cases, which can be very well observed from Figures 4.25. The deformation was higher in unreinforced soil than reinforced soil (OSC). However, the failure of the OSC was due to bulging, which was controlled by providing an encasement around the OSC. The encasement provided vertically of geotextile and geogrid. Both the experimental and numerical analyses exhibited the same trend regarding failure mechanisms.

Table 4.2: Comparison of stone column load capabilities measured

experimentally and numerically for single column

Dia of the stone column	Type of Column	Experimental Results (kN)	Numerical Results (kN)	Coefficient of variation (%)
D=70mm	End Bearing	7.2	7.15	0.49
	Floating	6.5	6.3	2.21
	End Bearing encased with geogrid	7.7	7.52	1.67
	End bearing encased with geotextile	8.15	7.85	2.65
	Floating with Geogrid	7.6	7.25	3.33
	Floating with Geotextile	7.9	7.45	4.15

Table 4.1 shows the comparison of experimental and numerical results for stone columns of 70 mm diameter shows a close agreement, as reflected by the low coefficients of variation. For the end bearing column, the experimental load capacity was 7.2 kN against 7.15 kN from numerical analysis, giving a variation of only 0.49%. Similarly, the floating column recorded 6.5 kN experimentally and 6.3 kN numerically with a variation of 2.21%. The inclusion of geogrid and geotextile encasement further improved the load capacity of both end bearing and floating columns, with experimental values consistently slightly higher than the numerical predictions. For end bearing columns, geogrid and geotextile encasement increased the load to 7.7 kN and 8.15 kN, respectively, with variations of 1.67% and 2.65%. For floating columns, geogrid and geotextile encasement enhanced the capacity to 7.6 kN and 7.9 kN, with variations of

3.33% and 4.15%. Overall, the results confirm that the numerical model reliably simulates the experimental behaviour of stone columns, while also demonstrating the effectiveness of geosynthetic encasement, particularly geotextile, in improving load carrying capacity.

Table 4.3: Comparison of stone column load capabilities measured experimentally and numerically for group column in triangular pattern (s/d = 2)

Dia of the stone column	Type of Column	Experimental Results (kN)	Numerical Results (kN)	Coefficient of variation (%)
D=50mm	End Bearing	9.10	8.75	2.77
	Floating	9.6	9.1	3.78
	End Bearing encased with geogrid	9.2	8.75	3.55
	End bearing encased with geotextile	9.8	9.3	3.70
	Floating with Geogrid	8.8	8.65	1.22
	Floating with Geotextile	9.2	8.75	3.55

The comparison of experimental and numerical results for stone columns of 50 mm diameter shows good agreement, with coefficients of variation generally below 4% showed in Table 4.2. For the end bearing column, the experimental load capacity was 9.10 kN compared to 8.75 kN from numerical analysis, yielding a variation of 2.77%. The floating column showed a slightly higher experimental capacity of 9.6 kN against 9.1 kN numerically, with a variation of 3.78%. With geogrid encasement, the load capacity of end bearing and floating columns was 9.2 kN and 8.8 kN, respectively, while geotextile encasement further enhanced the performance to 9.8 kN for end bearing and 9.2 kN for

floating columns. The variations for these encased conditions ranged between 1.22% and 3.70%, confirming close correspondence between experimental and numerical outcomes. Overall, the results validate the reliability of the numerical model in simulating load–settlement behaviour, while also demonstrating that geotextile encasement provides a more significant improvement in load carrying capacity compared to geogrid.

Table 4.4: Comparison of stone column load capabilities measured experimentally and numerically for group column in square pattern (s/d = 2)

Dia of the stone column	Type of Column	Experimental Results (kN)	Numerical Results (kN)	Coefficient of variation (%)
D=50mm	End Bearing	9.60	9.15	3.39
	Floating	8.10	7.45	5.91
	End Bearing encased with geogrid	8.60	8.15	3.8
	End bearing encased with geotextile	9.10	8.70	3.18
	Floating with Geogrid	8.6	7.35	11.08
	Floating with Geotextile	8.7	8.4	2.48

The results for stone columns of 50 mm diameter showed in Table 4.3 show a consistent correlation between experimental and numerical findings, with coefficients of variation generally within an acceptable range. For the plain end bearing column, the experimental load capacity was 9.60 kN compared to 9.15 kN numerically, yielding a variation of 3.39%. The floating column exhibited a lower experimental capacity of 8.10 kN against 7.45 kN numerically, with a

variation of 5.91%. With geogrid encasement, the end bearing and floating columns showed capacities of 8.60 kN and 8.60 kN experimentally, which were slightly lower than the plain end bearing case, while the numerical values were 8.15 kN and 7.35 kN, giving variations of 3.80% and 11.08%, respectively. Geotextile encasement improved the performance, raising the capacity to 9.10 kN for end bearing and 8.70 kN for floating columns, with variations of 3.18% and 2.48%. These results confirm that the numerical model provides reliable predictions of experimental behaviour. Furthermore, geotextile encasement proved more effective than geogrid in enhancing column performance, with the plain end bearing column achieving the highest load carrying capacity overall.

Table 4.5: Comparison of stone column load capabilities measured experimentally and numerically for group column in hexagonal pattern (s/d = 3)

Dia of the stone column	Type of Column	Experimental Results (kN)	Numerical Results (kN)	Coefficient of variation (%)
D=50mm	End Bearing	7.9	7.65	2.27
	Floating	7.3	6.45	8.74
	End Bearing encased with geogrid	7.9	7.45	4.15
	End bearing encased with geotextile	8.5	8.22	2.37
	Floating with Geotextile	9.10	8.42	5.49
	Floating with Geogrid	7.9	7.45	4.15

For the stone columns of 50 mm diameter, the comparison between

experimental and numerical results shows close agreement with relatively small coefficients of variation, indicating the reliability of the numerical model as shown in table 4. The plain end bearing column exhibited an experimental load capacity of 7.9 kN compared to 7.65 kN numerically, with a variation of 2.27%. The floating column, however, recorded a lower capacity of 7.3 kN experimentally and 6.45 kN numerically, showing a higher variation of 8.74%. With geogrid encasement, both end bearing and floating columns displayed a capacity of 7.9 kN experimentally and 7.45 kN numerically, each with a variation of 4.15%. Geotextile encasement proved more effective, as the end bearing column reached 8.5 kN experimentally and 8.22 kN numerically (2.37% variation), while the floating column achieved the highest capacity of 9.10 kN experimentally and 8.42 kN numerically (5.49% variation). Overall, geotextile encasement significantly enhanced the performance of both end bearing and floating columns, particularly in the floating case, while geogrid encasement showed relatively modest improvement.

The load-carrying capacity of stone columns varies significantly with column type, diameter, and reinforcement. For a diameter of 50 mm, end bearing columns exhibit higher load capacity (7.9 kN) compared to floating columns (7.3 kN), highlighting the efficiency of direct end bearing in transferring loads to the underlying firm layer. Reinforcement further enhances performance, as end bearing columns encased with geotextile show a notable increase in load capacity to 8.5 kN, representing approximately a 7.6% improvement over unreinforced columns, while geogrid encasement provides a marginal increase of about 0.0–0.6%. Interestingly, when comparing diameters, the 50 mm end bearing columns carry slightly more load than the 70 mm columns (7.9 kN vs 7.2 kN), indicating potential experimental variability or the influence of soil conditions. Numerical analyses closely replicate the experimental results, generally slightly underestimating the load values, with low coefficients of variation, demonstrating good agreement between models and experiments. Floating columns consistently exhibit lower load capacity and higher deviations, reflecting their reliance on frictional resistance rather than end bearing. Overall,

end bearing columns encased with geotextile consistently provide superior load-carrying performance, illustrating the combined effects of column type, diameter, and reinforcement in improving the strength and stability of soft soil foundations.

The novelty of the present study lies in the integrated experimental and numerical investigation of stone columns installed in expansive soil incorporating industrial waste materials such as iron dust along with sand, and reinforced using geosynthetic encasement (geotextile and geogrid). The research also evaluates the influence of column diameter, column arrangement (single and group columns), and different encasement materials on the performance of stone columns in expansive soil. The findings demonstrate that the inclusion of iron dust and geosynthetic encasement significantly enhances the load carrying capacity and stiffness of stone columns, thereby providing an effective and sustainable ground improvement technique for problematic expansive soils. Nelson and Miller (1992) and Chen (1988), Madhav and Miura (1994), Shahu and Reddy (2011).

4.6 X-ray diffraction (XRD) and Scanning Electron Microscope (SEM) Analyses

4.6.1 General

X-ray diffraction test was carried out using Bragg-Brentano in Bruker D8 advance machines to find out the crystalline materials in the soil and materials used in the formation of columns, i.e. fly ash, stone dust, iron dust and the mix design of the granular column. The Scanning Electron Microscope (SEM) analysis was done using a Jeol JSM-6610 LV working under an ultra-high vacuum. The SEM images were collected in a normal plane as well as cross-section view modes. The operating voltage of SEM was 5 kV according to resolution requirements.

4.6.2 X-ray diffraction (XRD)

The XRD analysis was carried out to identify the mineralogical composition of

the expansive soil and the additives used in column construction. The diffraction pattern of expansive soil shows a strong crystalline peak around 2θ ≈ 27–28°, confirming the dominance of quartz, along with smaller peaks associated with clay minerals such as montmorillonite and kaolinite, which are responsible for its expansive behaviour. In the case of fly ash, the broad hump in the range of 20–35° 2θ indicates the presence of an amorphous glassy phase, along with minor crystalline peaks of quartz and mullite, reflecting its pozzolanic nature. Stone dust exhibits sharp and well-defined crystalline peaks, particularly around 27–28° 2θ, confirming the presence of quartz and feldspar minerals, which contribute to its inert and stable behaviour. The additional mix shows a relatively diffused pattern with lower intensity peaks, suggesting partial amorphous characteristics and mineral dispersion. Finally, the XRD spectrum of the multi-blended column mix displays a combination of crystalline peaks from quartz and feldspar along with amorphous humps, indicating the integration of soil, fly ash, and stone dust. This confirms that the blended column mix achieves both reactive and inert mineral phases, enhancing pozzolanic activity and improving soil stabilization potential.

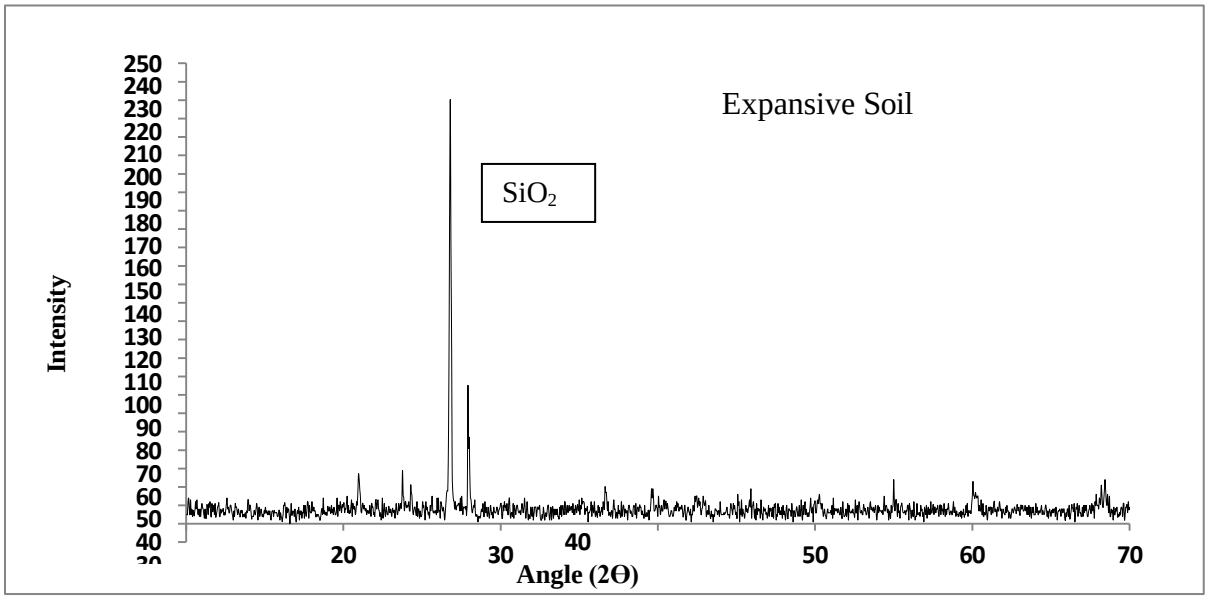

Figure 4.34: (a) XRD image of expansive soil.

The XRD pattern of expansive soil shows dominant peaks corresponding to montmorillonite, kaolinite, illite, and quartz minerals. The presence of

montmorillonite confirms the highly expansive nature of the soil due to its high water absorption and swelling characteristics. Clay minerals observed in the XRD image indicate high compressibility, excessive shrink–swell behaviour, and low bearing capacity of the untreated soil. Quartz peaks represent the silica content present in the soil matrix but contribute less to swelling behaviour.

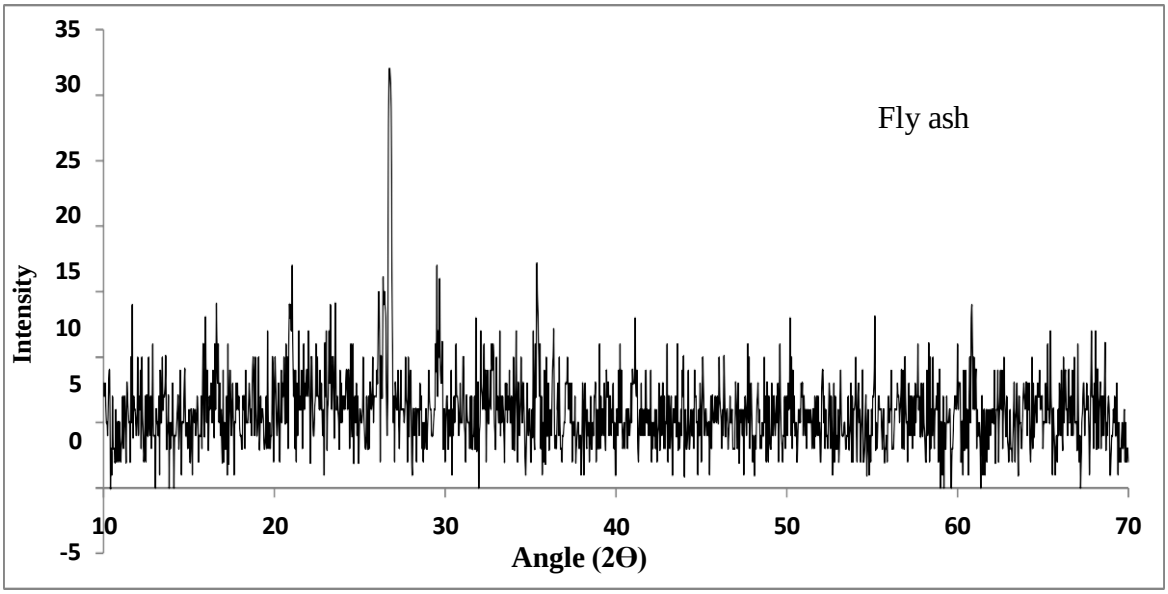

b) XRD image of Fly ash.

The XRD image of fly ash shows the presence of quartz, mullite, hematite, and calcite minerals. The silica- and alumina-rich compounds present in fly ash promote pozzolanic reactions when mixed with soil, leading to the formation of cementitious compounds. These reactions improve bonding between soil particles, increase stiffness, and reduce the plasticity and swelling behaviour of expansive soil. The reduction in intensity of clay mineral peaks further indicates improvement in soil stabilization.

The XRD pattern of stone dust mainly consists of quartz, calcite, and feldspar minerals. The high quartz content contributes to improved frictional resistance and stiffness, while calcite enhances bonding and densification within the soil matrix. The mineralogical composition observed in the XRD image explains the increase in shear strength, bearing capacity, and reduction in settlement behaviour due to the addition of stone dust.

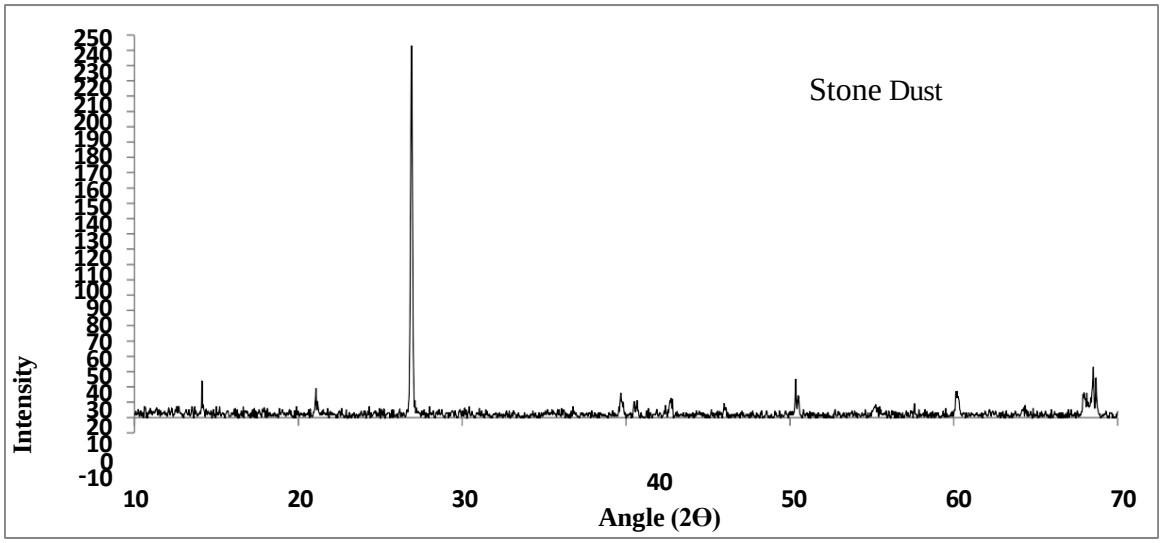

c) XRD image of Stone Dust

The XRD image of iron dust shows prominent peaks of hematite (Fe_2O_3), magnetite (Fe_3O_4), and other iron oxide compounds. These minerals contribute to cementation and stronger inter-particle bonding within the soil system. The formation of dense and stable mineral phases reduces pore spaces and compressibility while increasing stiffness and load-bearing capacity. The reduced activity of expansive clay minerals observed in the XRD pattern confirms the stabilization effect of iron dust.

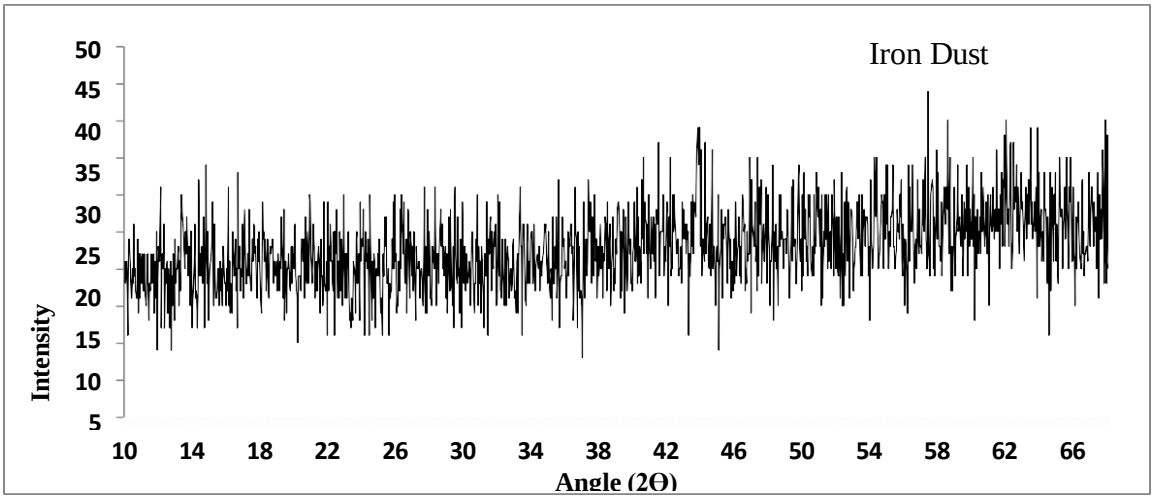

d) XRD image of Iron Dust

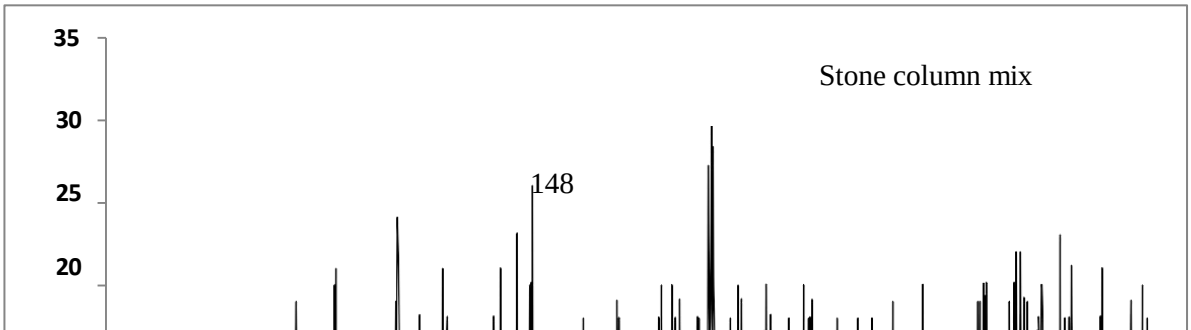

e) XRD image of column mix with iron dust

The XRD pattern of the stone column mix exhibits combined peaks of quartz, calcite, silica-rich compounds, and iron oxide minerals. The presence of quartz indicates the formation of a strong granular skeleton, which improves shear resistance and load transfer characteristics. Calcite and silica compounds contribute to densification and cementitious bonding, while iron oxide minerals enhance confinement and stiffness of the stone column system. The reduction in swelling clay mineral peaks and the formation of stable mineral phases confirm the improvement in stability, bearing capacity, and settlement behaviour of the reinforced expansive soil system.

The XRD analysis confirms the mineralogical modification and stabilization of expansive soil due to the addition of fly ash, stone dust, iron dust, and stone column materials. The untreated expansive soil exhibited dominant swelling clay minerals such as montmorillonite, which are mainly responsible for high swelling potential, compressibility, and low strength characteristics. After stabilization, the intensity of expansive clay mineral peaks decreased significantly, while stable minerals such as quartz, calcite, mullite, hematite, and iron oxide compounds became more prominent.

The formation of silica-rich and cementitious compounds improved inter-particle bonding, densification, and stiffness of the soil matrix. Quartz and calcite enhanced frictional resistance and load transfer characteristics, whereas iron oxide compounds contributed to stronger confinement and improved bearing capacity. The reduction in swelling minerals and the formation of stable mineral phases indicate improved engineering behaviour of the reinforced soil system.

Overall, the XRD results validate the experimental findings by confirming increased strength, reduced swelling behaviour, lower compressibility, improved settlement characteristics, and enhanced stability of expansive soil reinforced with stone columns and stabilizing additives.

4.6.3 Scanning Electron Microscope (SEM)

The SEM micrographs (Figure 4.35 a–e) illustrate the microstructural variations in the tested soil samples. Images (a) and (c) exhibit aggregated clay particles forming dense flocculated clusters with visible inter-particle voids, indicating a relatively compact fabric that contributes to higher strength and lower compressibility. In contrast, image (b) shows a more dispersed arrangement of fine particles with an open structure, reflecting weaker inter-particle bonding and higher porosity, which can reduce load-bearing capacity. Image (d) reveals a distinct plate-like or flaky morphology, characteristic of clay minerals such as kaolinite or montmorillonite, which are known for their tendency to absorb water and undergo volume changes. Image (e) presents a mixed microstructure comprising aggregated lumps interspersed with pores, suggesting partial cementation and heterogeneous packing. Overall, the SEM observations highlight the differences in soil fabric, where denser and more aggregated structures correspond to improved load resistance, while loose and flaky arrangements result in higher compressibility and reduced stability.

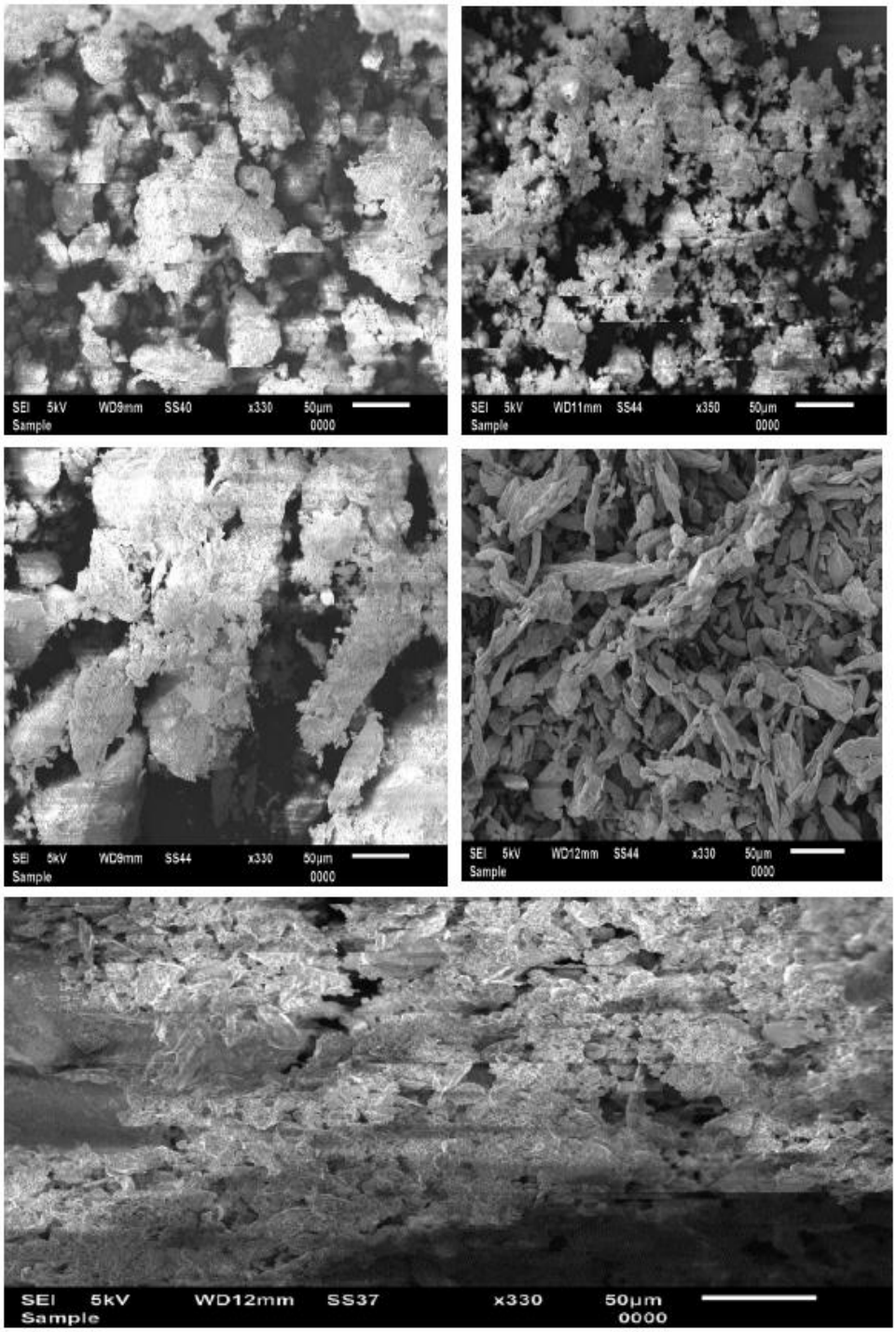

Figure 4.35 SEM images of (a) expansive soil, (b) fly ash, (c) stone dust, (d) iron dust and (e) column mixes with iron dust

The SEM image of expansive soil shows flaky and plate-like clay particles with large voids, microcracks, and weak inter-particle bonding. This loose and dispersed microstructure indicates the high swelling and shrinkage

characteristics of expansive soil, which are responsible for low shear strength, high compressibility, excessive settlement, and poor load-bearing capacity. The presence of cracks and pores confirms the unstable nature of untreated expansive soil.

The SEM image of fly ash reveals mostly spherical and smooth particles along with hollow cenospheres uniformly distributed within the matrix. These spherical particles help in filling the voids between soil particles and improve packing density. The microstructure indicates the pozzolanic nature of fly ash, which promotes cementitious bonding and enhances stiffness and strength while reducing the plasticity and swelling behaviour of expansive soil.

The SEM image of stone dust shows angular and rough-textured granular particles arranged in a dense structure with reduced pore spaces. The angularity of particles improves interlocking and frictional resistance between particles, resulting in increased shear strength and stiffness. The dense packing observed in the SEM image explains the reduction in compressibility and settlement behaviour of the stabilized soil.

The SEM image of iron dust exhibits dense metallic particles with rough surfaces and compact agglomerated structures. Fine iron particles occupy the void spaces between soil grains, producing a denser soil matrix and stronger particle bonding. This compact microstructure indicates improved stiffness, enhanced load-bearing capacity, and reduced swelling behaviour due to better confinement and reduced pore spaces within the soil system.

The SEM image of the stone column mix shows a highly dense and compact granular structure with strong interlocking between particles and minimal void spaces. Improved bonding between soil particles, stone aggregates, and stabilizing materials is clearly observed. The compact arrangement confirms enhanced confinement and efficient load transfer within the stone column system. The reduction in microcracks and pore spaces explains the improvement

in bearing capacity, stiffness, and settlement behaviour of the reinforced expansive soil system.

The SEM analysis clearly demonstrates the microstructural improvement of expansive soil after the addition of fly ash, stone dust, iron dust, and stone column materials. The untreated expansive soil exhibited a loose and dispersed structure with flaky clay particles, large voids, and microcracks, indicating weak bonding, high compressibility, and high swelling potential. After stabilization and reinforcement, the soil structure became denser and more compact with improved particle arrangement and reduced pore spaces.

The addition of fly ash promoted cementitious bonding and void filling due to its spherical particles, while stone dust improved interlocking and frictional resistance because of its angular granular structure. Iron dust further enhanced densification and stiffness by filling voids and forming a compact agglomerated matrix. The stone column mix showed a highly dense and well-confined granular structure with strong particle interaction and reduced microcracks.

The SEM images confirm improved bonding, enhanced confinement, reduced swelling behaviour, lower compressibility, and better load transfer characteristics in the reinforced soil system. Overall, the SEM results validate the experimental findings by demonstrating significant improvement in bearing capacity, stiffness, settlement behaviour, and overall stability of expansive soil reinforced with stone columns and stabilizing additives.

Together, the XRD and SEM analyses provide complementary insights: SEM highlights the morphological arrangements and bonding of soil particles, while XRD confirms the mineralogical composition and reactivity of the materials. The combined results validate that the inclusion of fly ash and stone dust in the column mix improves the microstructural integrity and mineralogical interactions, thereby enhancing the overall load-bearing performance of the soil–column system.

CHAPTER 5
CONCLUSIONS

5.1 GENERAL

This chapter presents the key findings from the testing and finite element analysis, along with a concise overview of the investigation. It also offers recommendations for future research.

5.2 CONCLUSIONS

1. Stone columns for ground improvement tested in this study were made utilising industrial waste products such as iron dust and fly ash; sand was replaced with stone dust.
2. End bearing column shows failure in bulging while floating columns failed in punching failure.
3. In groups of columns three loading arrangements were tested, i.e. triangular, square and hexagonal. Triangular loading gives the best results compared to the two other loading arrangements with or without encasement.
4. Single columns are less efficient than to groups of columns. The loading arrangement in triangular groups gives optimum efficiency.
5. The column's bearing capacity is improved by the use of encasement using geosynthetics and reduces the settlement as compared to columns without encasement.
6. Geotextile shows better results than geogrid due to its grid size as the material used for column casting is fine grained. The slurry spills out or extrudes into the surrounding soil replaced for the column casting.
7. The experimental results were validated using the software Plaxis 3D; The numerical modelling results obtained from PLAXIS 3D showed good agreement with the experimental findings for both single and group stone columns.
8. The load–settlement behaviour predicted numerically closely followed

the trends observed in the laboratory model tests under different loading and encasement conditions.

9. The numerical model successfully captured the improvement in load-carrying capacity and reduction in settlement achieved by ordinary and geosynthetic-encased stone columns.
10. Minor variations between the experimental and numerical results were observed due to assumptions related to material homogeneity, boundary conditions, and idealized soil behaviour adopted in the finite element modelling.
11. The variation between experimental and numerical results was generally within an acceptable engineering range of approximately 5–15%, indicating satisfactory accuracy of the numerical simulations.
12. The comparison confirms that PLAXIS 3D can be effectively used to simulate the behaviour of stone columns in expansive soil and to validate laboratory model test results.
13. XRD on powdered materials shows a predominance of quartz in both the expansive soil and the multi-blended material mix. The SEM analyses were performed on powdered materials. We analysed the microstructure and crystal structures of expansive soil, fly ash, stone dust, iron dust and the column mix of fly ash, iron dust, stone dust and cement as a binder.

5.3 AREA OF FUTURE RESEARCH

The present stage of development in this field shows notable gaps that are important for achieving a deeper understanding of the behavior of stone column–reinforced ground and for accurately forecasting its response to applied loads. Further research can be undertaken on the following topics:

1. In present study waste materials like fly ash, stone dust, and iron dust are used to form a column mix. There is less study on the use of the waste materials in the stone columns constructions. As there is scarcity of land and need to utilize the industrial and agricultural waste can be studied in future experiments using either small-scale or field-scale testing.

2. More detailed investigations is done on the different diameter of the columns, spacing of the columns in groups, S/D ratio.
3. While the present study examines the use of vertical encasement only, findings indicate that stone columns reinforced in vertical and horizontal directions exhibit comparable load-bearing capacity. Moreover, there is a lack of field investigations exploring the combined application of vertical and horizontal reinforcement. Future research could therefore focus on stone columns reinforced in both orientations, assessed through either small-scale or full-scale field testing.
4. In present encasement is provided to column length. In future investigations the impact of variation of encasement length can also be done. More detailed investigation is necessary.
5. Future studies could explore the performance of reinforced stone columns in multi-layered soil profiles. In many real-world scenarios, site conditions include a sand layer between clay layers or the reverse. While stone columns have been observed to perform effectively in such configurations, the application of reinforced stone columns under these conditions has received little attention and remains insufficiently analyzed.
6. The use of pressure cells enables a more detailed examination of stress concentration on both the column and the surrounding soil. This, in turn, allows for a clearer understanding of how the load is shared between the columns and the adjacent soil.
7. Only the utilization of geotextile and geogrid has been employed in the current investigation. Any other type of geosynthetic material can also be substituted. More detailed experimental investigation is necessary.

CHAPTER 6

ADDITIONAL WORK

6.1 General

Land scarcity has prompted civil engineers to develop ground improvement techniques that enable construction, for instance, on grounds with expansive soils. Stone or granular columns inserted into the soft soil are frequently used for this purpose. In this study we investigate a ground improvement technique using stone columns. Stone columns contain a mix of industrial waste like fly ash, iron dust or stone dust in replacement of sand and cement as a binder. The continuously increasing volume of waste material makes it attractive for engineers to utilise such waste for construction purposes. In the present work we tried to utilise the waste in certain mixes and cast columns with these specific mixes in expansive soil. The parameters considered were the different blends of waste material in column design, different diameters of the single stone column and bearing strength of single vs. groups of columns. The experiments were conducted in the laboratory using a mould with a diameter of 150 mm and a height of 170 mm. Granular columns using waste materials like fly ash, stone dust, iron dust, and cement as a binder were cast in moulds of 20, 30 and 50 mm diameter. The replacement technique was used for the installation of the columns in expansive soil. The column's compressive strength was compared with and without the use of iron dust. The load-deformation curve was obtained with the help of a plunger of 50 mm in the CBR machine. The encasements were made from two types of geosynthetics, i.e. geogrid and geotextile. The mix design was followed by the UCS (unconfined compressive strength) tests performed on soil samples and the granular mix of different ratios with and without iron dust. The mix used for the design of the stone column showed optimum compressive strength compared to the expansive soil. There is no noticeable benefit when columns are spaced more than three times the diameter of the column. Design charts are created based on the findings, and a design procedure is offered.

6.2 Methodology

6.2.1 Test program:

The clay chunks obtained from the paddy fields were pulverized; freed of grass, plant roots, stones, pebbles, and other unwanted materials; and kept in the sun to dry. The fine clayey soil was thoroughly mixed with the required amount of water for a soft consistency. The granular column was inserted into the highly cohesive expansive soil. The waste material used for column fill was a mix of stone dust, fly ash, ordinary Portland cement (OPC), and/or iron dust. The woven geosynthetics were used for the encasement of the granular column for single and groups of columns.

In the present study, 31 tests were conducted among which 12 tests were on a group of columns 18 on single columns of 20, 30 and 50 mm diameter of the column included 1 test on the virgin soil. The experimental program showed in table 6.1.

Table 6.1: summary of an experimental program

Test	Reinforcement type	Detailed parameters		No of tests
		Single stone column	Group stone column	
1	Natural expansive soil	-	-	1
2	Expansive Soil + stone column (end bearing without iron dust)	l = 170 mm (end bearing) Diameter = 20, 30 and 50 mm No of experiment = 3	l = 170 mm (end bearing) Diameter 30 mm, s/d = 1 No of experiment = 2	5
3	Expansive Soil + stone column (end bearing with iron dust)	l = 170 mm (end bearing) Diameter = 20, 30 and 50 mm No of experiment = 3	l = 170 mm (end bearing) Diameter = 30 mm, s/d = 1. No of experiment = 2	5
4	Expansive soil + stone column (end bearing with irondust) with geosynthetics (geogrid or geotextile)	l = 170 mm (end bearing) Diameter = 20, 30 and 50 mm No of experiment = 6	l = 170 mm (end bearing) Diameter = 30 mm, s/d = 1 No of experiment = 4	10

	encasement			
5	Expansive soil + stone column (end bearing without iron dust) with geosynthetics (geogrid or geotextile)	l = 170 mm (end bearing) Diameter = 20, 30 and 50 mm No of experiment = 6	l = 170 mm (end bearing) Diameter = 30 mm, s/d = 1 No of experiment = 4	10

6.2.2 Test setup:

All the experiments were conducted in a cylindrical mould of dimensions of 170 mm in height and 150 mm in diameter. The tank borders were designed so that induced stresses would be negligible at the edges (Shahu and Reddy 2011). The soil sample was prepared as per IS 2720-16 (2016). The 5 kg soil was filled in three layers and compacted with the help of a rammer of 25 kg with 56 blows on each layer. To avoid wall friction, the mould was lubricated inside with oil. Here 20% of the soil weight water was added to the sample, i.e. the optimum moisture content procured from a standard proctor test performed in the laboratory. The soil sample with mould soaked in water for 96 hours as per IS 2720-16 (2016). The mould was pulled out of the water and left for 10 to 15 minutes so that the excess water could be removed. The expansion ratio procured for soil sample was 1.23%. The footing load was applied by the plunger of 50 mm diameter at a maintained rate of 1.25 mm/min in the CBR machine. The deformation observed with help of a two dial gauge of sensitivity 0.02 mm placed over the testing plate and the mould. In all model studies, a footing diameter approximately equal to twice the diameter of the stone column was chosen, equating to an area replacement ratio of (A_r) 10%, 14% and 23% for single column of 20, 30 and 50 mm diameter. The ratio of area of column to the area of surrounding expansive soil defined as the area replacement ratio. The settlement measured up to 20 – 40 mm as per IS 15284-1 (2003) or when the column was fail. As a reference, the soft clay bed without a stone column loaded with a 50 mm diameter footing was performed. A load-deformation curve was obtained

between loadings via settlement.

Figure 6.1: sample soaked in water for 96 hours, **Figure 6.2:** sample after soaking for 96 hours with single end bearing column, **Figure 6.3**: failed sample after loading with single column, **Figure 6.4:** column casing with encasement using geotextile, **Figure 6.5 & Figure 6.6**: column casing with geogrid, **Figure 6.7:** placing of encasement with casing in expansive soil.

6.2.3 Forming of the granular column:

The stone columns were designed as per IS 15284-1 (2003). The end-bearing columns were designed for the present study. The single columns of 20, 30, and 50 mm diameter were cast in the centre of the cylindrical mould. For groups, double columns and triangular pattern columns of 30 mm diameter are designed. The replacement technique was used for the design of the column. The pipes of 20, 30, and 50 mm diameter were inserted into the soil bed at the desired spacing between the columns. The pipe was lubricated with oil inside and outside perimeter to avoid friction between the soil and the pipe. With the help of an auger and spatula, the soil was removed from the pipe. The desired depth of the column was checked on the scale. The column was filled with a mix of stone

dust, fly ash, and cement and 12% water compared with the mix of stone dust, fly ash, cement, and iron dust, and 12% water. After the column was prepared, the pipe was removed carefully. Water content = P/4 + 3 where P is the cement consistency of OPC used for a mix. The cement consistency is 36%, calculated by the Vicat apparatus in the laboratory. The column mix is determined by the (unconfined compressive strength) UCS test. The UCS samples of a different mix are prepared in the sampler and left for 7 days in desiccator for curing and tested as per IS 2720-10 (1991). The mix gives optimum compressive strength compared to the soil used for the column mix. The average of three samples of each mix with different percentages of fly ash, stone dust, and cement compared with mix with iron dust was prepared and tested in the laboratory.

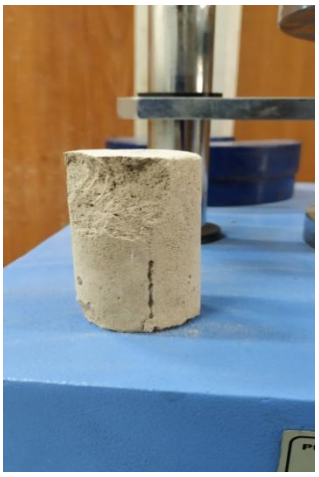

Figure 6.8: sample prepared for UCS test with the help of sampler, **Figure 6.9:** Loading cell with failed sample, **Figure 6.10:** failed sample.

For the encasement of the column, geosynthetics were applied to the perimeter of the column. The geosynthetics were rolled on the outside diameter of the pipe and inserted into the soil bed. The pipe used for column construction was lubricated inside and outside diameter so that can be easily removed. The soil was removed with the help of an auger and spatula, and then the granular mix was filled. The mix was tamped with the tamping rod. After the column was prepared, the pipe was removed carefully so that the column and the encasement were not disturbed. Two types of geosynthetics are compared in the present study, i.e. geogrid and geotextile. The geosynthetics were tied with thread so

that they were properly rolled up.

6.3 Column exhumation:

The column mix from the column was carefully removed after the test, and a thin paste of plaster of Paris was put into the void to restore the column's distorted shape. The cured plaster of Paris was then isolated for further analysis by scooping away the surrounding soil. The penetration of the bottom of the column and the length of the deformed columns were measured after the test, (Ali et al. 2012).

Figure 6.11: exhumed column with geotextile **Figure 6.12**: exhumed column with geogrid

6.4 Results and discussion

To choose the optimum mix design the strength test was done on different column mixes. The unconfined compressive strength tests results showed in Figure 6.13 and 6.14.

The average compressive strength of soil was 642 kPa. The experimental result verified with the equation (O'Flaherty et al., 1961)

$$\log CBR = 1.115 + 0.660 \log UCS \qquad (6.1)$$

a working relationship between California bearing ratio and unconfined compressive strength under varying experimental conditions. The mix of 1:3 prepared to cast the stone column i.e. 1 part cement and fly ash and 3 part stone

dust tested. The optimum results considered was 45% cement + 55% fly ash added with 3 part of stone dust used for column mix.

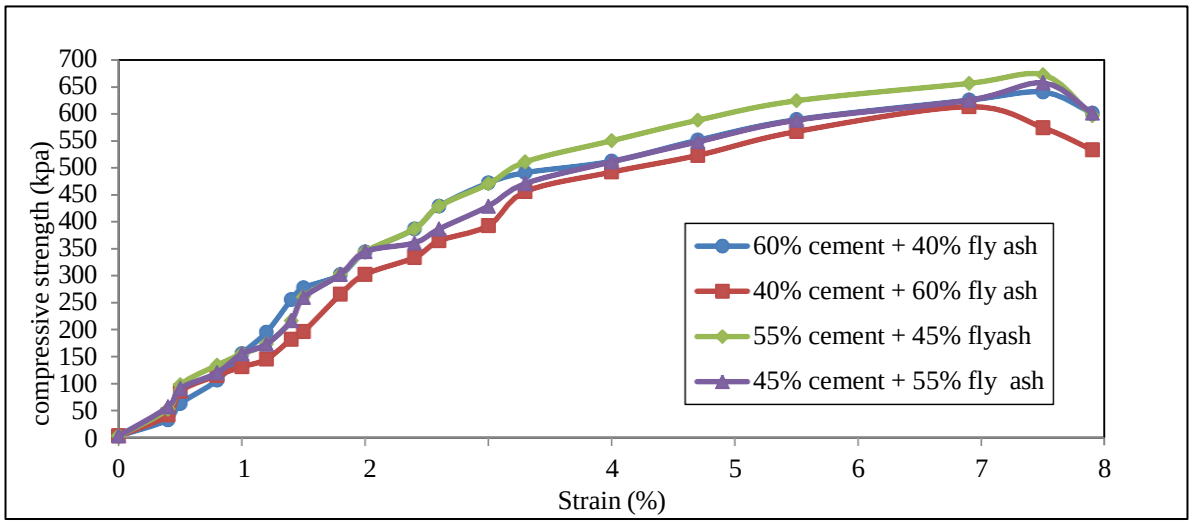

Figure 6.13: UCS tests mix designed for granular column without iron dust

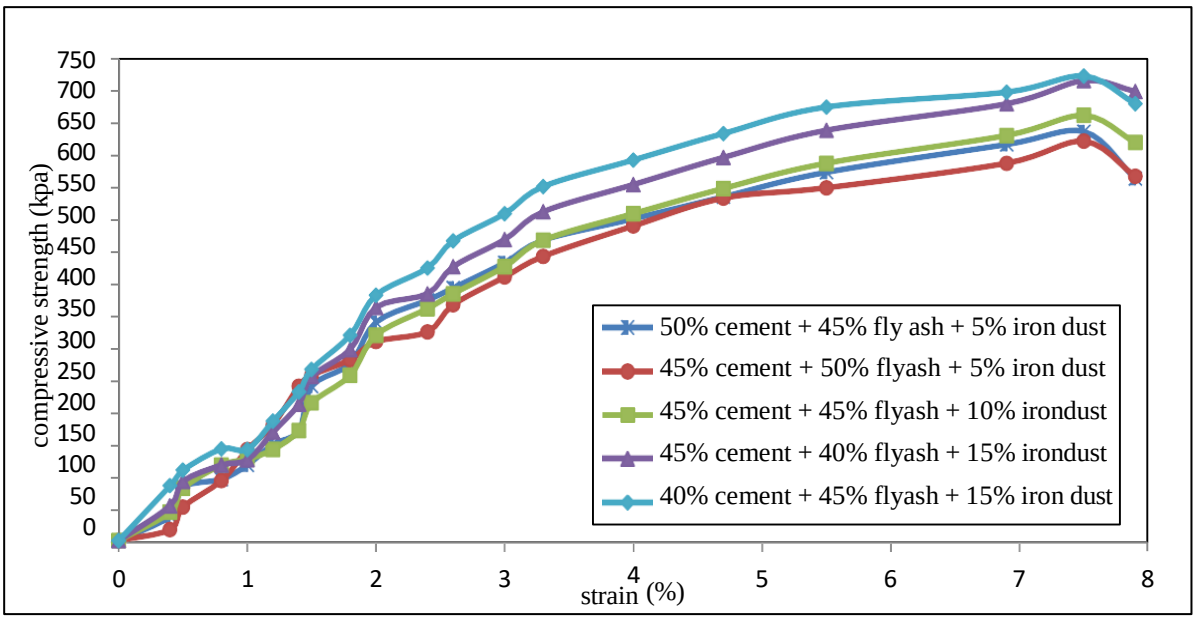

Figure 6.14: UCS tests mix designed for granular column with iron dust

The average compressive strength of the column mix without iron dust was 657 kPa. Similarly for iron dust mix 45% cement + 45% fly ash + 10% iron dust mix used for construction of column in the mould. The average compressive strength of the column mix with iron dust was 662 kPa. The mix design used for the column construction was in range of the compressive strength of the expansive

soil used and also economical to the environment.

6.4.1 Granular column without iron dust: The load was shared between the soil and the granular column designed without iron dust.

6.4.1.1 Granular unencased single column: The load settlement graph procured as shown in Fig 6.15. With the increase in load settlement also increases for certain time after that failure is shown and the readings in proving ring decreases as shown in graph. For 20 mm column failure is at 40 mm settlement while for 30 mm and 50 mm settlement is at 60 and 50 mm. Failure pattern is obtained with the help of exhumed columns using plaster of Paris. Bulging failure is obtained in end bearing columns.

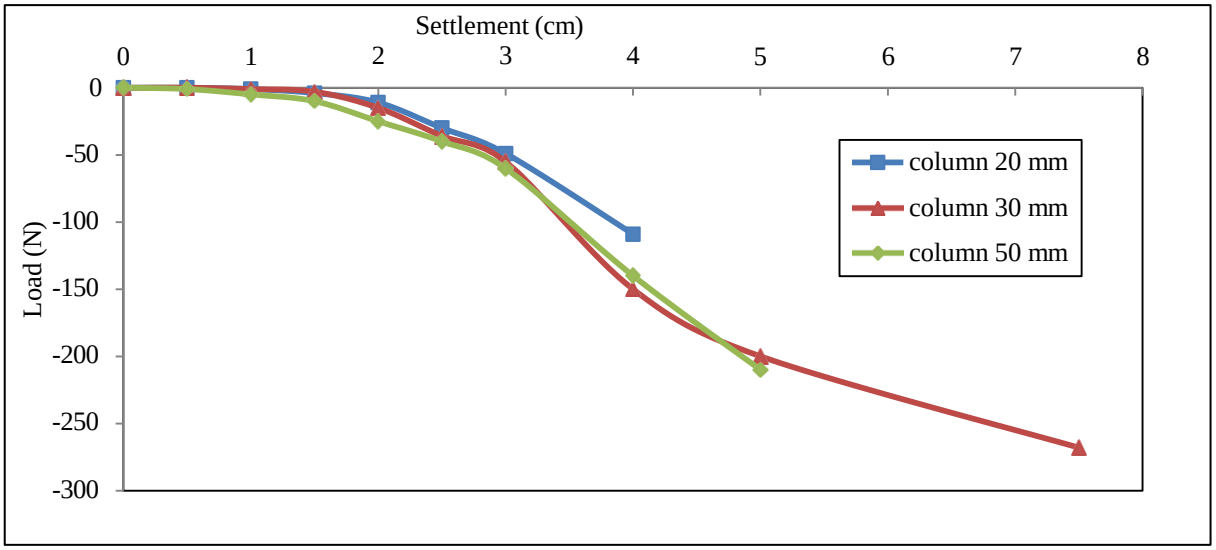

Figure 6.15: Granular unencased single column without iron dust

The load–settlement behaviour of stone columns with varying diameters (20 mm, 30 mm, and 50 mm) is presented in the graph. It is evident that the load-carrying capacity improves significantly with an increase in column diameter. The 20 mm diameter column exhibited the lowest resistance, reaching a maximum load of approximately 100 N at a settlement of about 30–40 mm, after which it failed rapidly. In contrast, the 30 mm diameter column demonstrated the highest load-bearing capacity, sustaining up to 280 N at a settlement of nearly 120 mm, indicating superior performance compared to the other

diameters. The 50 mm diameter column also showed improved behaviour compared to the 20 mm column, resisting up to 200 N at a settlement of around 50 mm before declining. These results highlight that while an increase in diameter enhances load-carrying capacity, an optimum diameter exists, with the 30 mm column emerging as the most effective in this study.

6.4.1.2 Granular encased single column: The columns are encased with using geosynthetics i.e. geotextile and geogrid shown in Figure 6.5 and 6.6. As the load increases settlement also increases with a certain amount of time. After which failure of the encased column obtained. The load bearing capacity of the column increases with the encasement of the column. Geotextile gives better results as compared to geogrid. After test completed exhumed column obtained as shown in Figure 6.12 and 6.13 for both geogrid and geotextile.

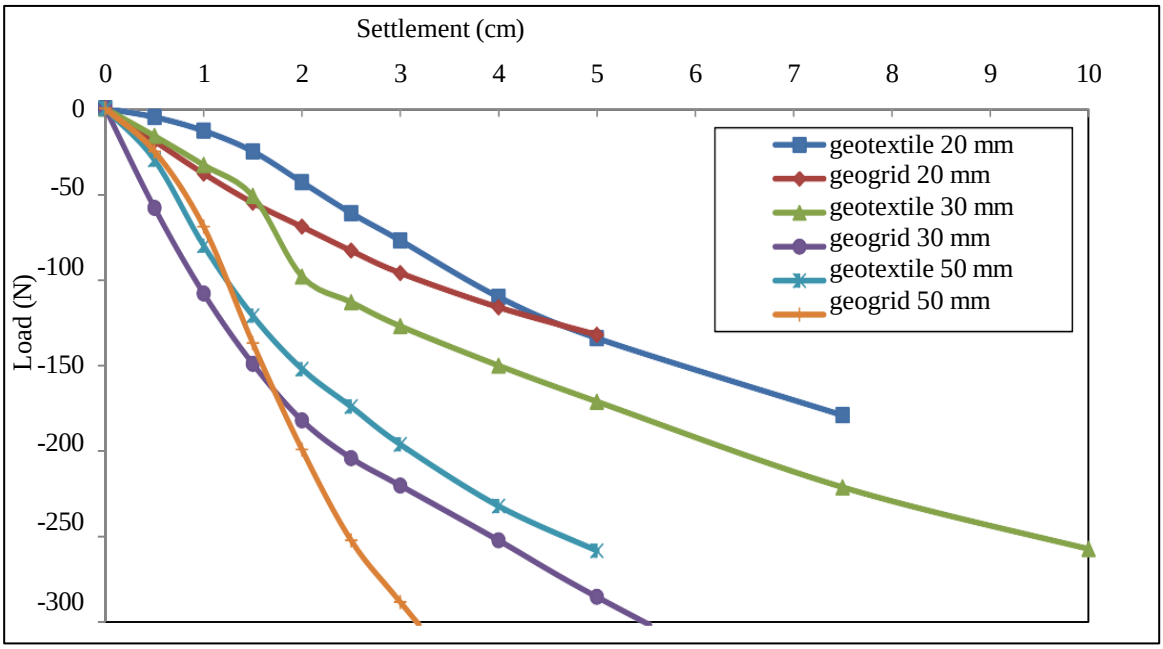

Figure 6.16: Granular encased single column without iron dust

The load–settlement behaviour of stone columns encased with geotextile and geogrid for different diameters (20 mm, 30 mm, and 50 mm) is shown in the graph, and the results clearly highlight the superiority of geotextile encasement over geogrid. For the 20 mm column, the geotextile-encased specimen exhibited

the highest load resistance and sustained loading at lower settlements, whereas the geogrid-encased column failed earlier, indicating inadequate confinement. A similar trend was observed for the 30 mm diameter columns, where the geotextile-encased column demonstrated gradual load improvement and higher performance compared to the geogrid-encased column, which showed early settlement and reduced resistance. In the case of 50 mm diameter columns, the geotextile encasement again provided greater confinement and improved load resistance, while the geogrid encasement exhibited rapid settlement and the lowest capacity among all cases. Overall, geotextile encasement proved to be significantly more effective across all diameters, with the 20 mm geotextile column even outperforming larger geogrid-encased columns. These findings emphasise that the type of encasement plays a more decisive role in enhancing column performance than the diameter alone, with geotextile providing superior confinement, reduced settlement, and greater load-carrying efficiency.

6.4.1.3 Granular column in group

In group of granular column two columns placed along the diameter of the mould and other was triangular pattern designed with s/d = 1 with or without encasement. In group of two columns the settlement for without encasement showed 220 mm and for with encasement was 200 and 230 mm for geotextile and geogrid. In case of triangular pattern, settlement showed witthout encasement 240 mm and with encasement provided using geotextile and geogrid was 260 and 230 mm. In group of columns triangular arrangement gives better results as compared to double columns. By providing encasement settlement reduces with the increase in load. In group of columns geogrid gives better results in both the geosynthetics used for the encasement.

6.4.2 Granular column with iron dust: In this case the iron dust is also added to the columns and the results are obtained.

6.4.2.1 Granular unencased single column

With the addition of iron dust the granular columns are casted using diameter of

20 mm, 30 mm and 50 mm, respectively. With the increase in load, settlement also increases upto certain time. When failure is obtained proving ring reading started reducing. The obtained results are shown in Fig 6.17. The bulging failure is obtained in end bearing columns. Exhumed columns taken with the help of plaster of Paris.

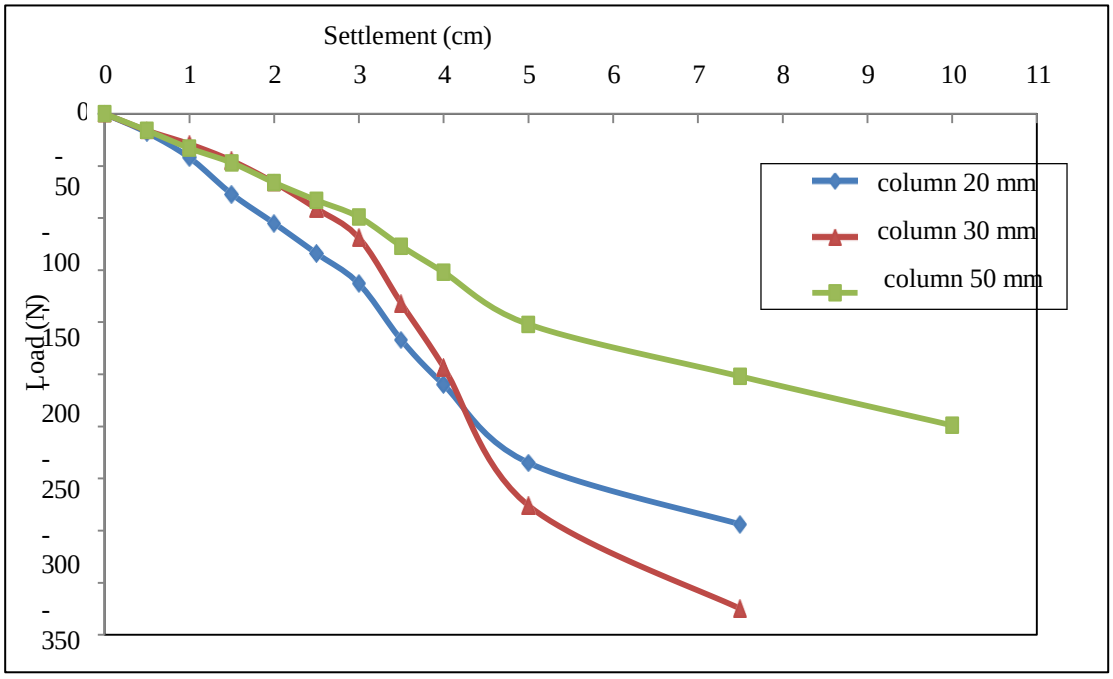

Figure 6.17: Granular unencased single column with iron dust

The load–settlement behavior of stone columns with varying diameters (20 mm, 30 mm, and 50 mm) is illustrated in the graph. It is observed that the 20 mm diameter column sustains a maximum load of about 400 N at a settlement of nearly 70 mm, showing a steeper load reduction pattern and indicating limited load-bearing capacity. In contrast, the 30 mm diameter column demonstrates superior performance, withstanding a maximum load of approximately 470 N at around 70 mm settlement, thereby highlighting it as the optimum column size in terms of load resistance. On the other hand, the 50 mm diameter column exhibits the ability to accommodate larger settlements up to 100–110 mm; however, its load-bearing capacity remains lower at around 300 N. These results clearly indicate that increasing column diameter does not linearly improve the load capacity, and while the 50 mm column provides greater settlement tolerance, the

30 mm column offers the most efficient performance in terms of maximum load resistance.

6.4.2.2 Granular encased single column

The columns are encased with using geosynthetics i.e. geotextile and geogrid shown in Fig 6.5 and 6.6. As the load increases settlement also increases with a certain amount of time. After which failure of the encased column obtained. The load bearing capacity of the column increases with the encasement of the column. Geotextile gives better results as compared to geogrid. After test completed exhumed column obtained as shown in Fig 6.12 and 6.13 for both geogrid and geotextile.

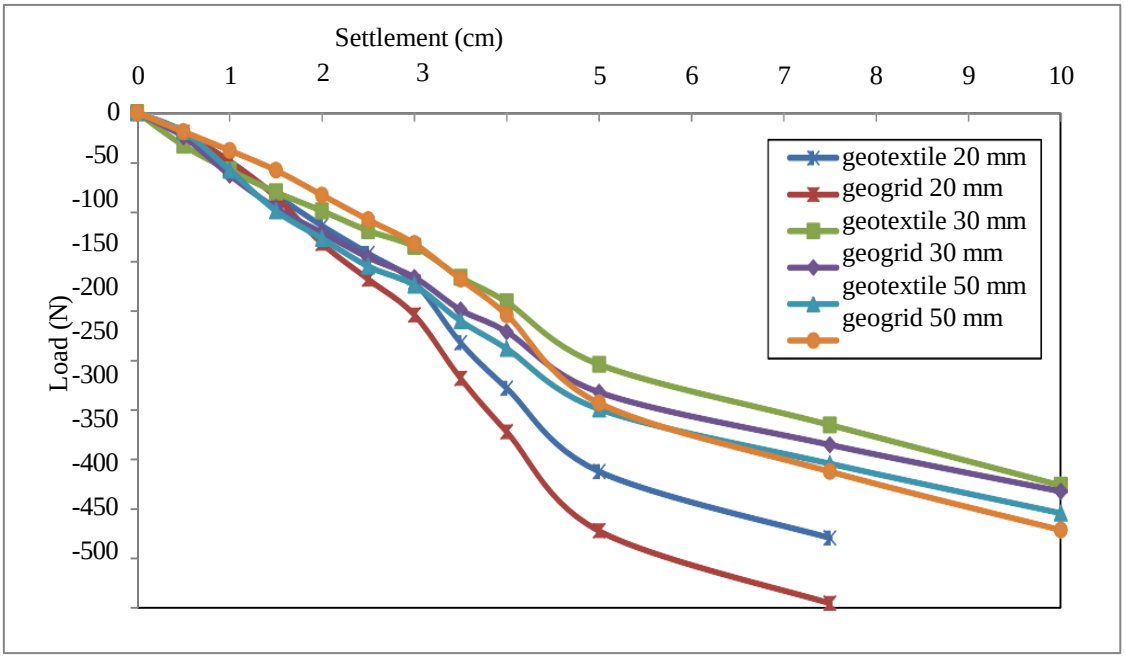

Figure 6.18: Granular unencased single column with iron dust

The graph Figure 6.18 illustrates the load–settlement response of stone columns of varying diameters (20 mm, 30 mm, and 50 mm) when encased with two different types of geosynthetics: geotextile and geogrid. The performance trends reveal that geosynthetic encasement significantly improves the load-bearing capacity of the columns compared to unreinforced ones, but the effectiveness depends on both the diameter and the type of encasement. For the 20 mm

diameter column, the geotextile-encased column carries higher loads than the geogrid-encased one, with the latter showing the lowest capacity overall (≈ –470 N at 70 mm settlement). In the case of 30 mm diameter columns, both geotextile and geogrid encasements perform better, with the geotextile-encased column achieving higher resistance (≈ –300 N at 90 mm settlement) than the geogrid counterpart. Similarly, for 50 mm diameter columns, both encasement types show improved settlement tolerance, but the geotextile-encased column again provides slightly higher load-bearing capacity throughout the settlement range. Overall, it can be concluded that geotextile encasement generally outperforms geogrid encasement across all diameters, with the most effective performance observed in the 30 mm geotextile-encased column, which shows the best balance between load resistance and settlement control. This indicates that the choice of both column diameter and encasement material plays a critical role in enhancing soil reinforcement efficiency.

The comparative evaluation of unreinforced and geosynthetic-encased columns clearly demonstrates that encasement significantly enhances the load-bearing performance. For the 20 mm column, geogrid encasement improved the load capacity by about 15%, while geotextile provided a 7.5% increase over the unreinforced case. In the 30 mm column, geotextile proved more effective with a 6.4% improvement, whereas geogrid contributed only a marginal 2.1% gain. The most notable enhancement was observed in the 50 mm column, where geotextile increased the load capacity by nearly 20% compared to 13.3% for geogrid. These results indicate that while both geotextile and geogrid contribute to improved strength and deformation control, geotextile encasement consistently outperforms geogrid, particularly for larger diameter columns. Overall, the findings highlight that geosynthetic encasement not only increases load resistance but also ensures better settlement control, with geotextile encasement emerging as the most efficient reinforcement option for optimizing column performance.

6.4.2.3 Granular column in group

For group of columns, two columns placed along the diameter of the mould and other was triangular pattern designed with s/d = 1 with or without encasement. In group of two columns of diameter 30 mm the settlement for without encasement showed 200 mm and for with encasement was 180 and 220 mm for geotextile and geogrid. In case of triangular pattern settlement showed without encasement 220 mm and with encasement provided using geotextile and geogrid was 240 and 230 mm. In group of columns triangular arrangement gives better results as compared to double columns. By providing encasement settlement reduces with the increase in load. In group of columns geogrid gives better results in both the geosynthetics used for the encasement.

From these observations, it is evident that the triangular arrangement consistently performs better than the double column arrangement, as it shows reduced settlements under similar conditions. The addition of iron dust further enhances performance, as it results in lower settlements compared to the corresponding cases without iron dust, particularly in the two-column group. Moreover, geogrid encasement demonstrates better results than geotextile in both conditions, highlighting its superior confinement capability in group column behavior. Overall, the results confirm that the combination of triangular arrangement, iron dust inclusion, and geogrid encasement provides the most effective configuration for reducing settlements and improving the efficiency of group granular columns.

6.5 Comparison in casting of granular column with or without iron dust

The results showed that with the mix of iron dust gives better results as compared to without iron dust. With using iron dust settlement reduces which cause increase in load capacity of the granular column. As the load increases, bearing capacity of the column increases for both the cases with or without encasement.

The experimental and comparative study on granular columns demonstrates that both column arrangement and encasement significantly influence load-bearing capacity and settlement behavior. For single columns, geotextile encasement

proved more effective in enhancing load resistance, with the 30 mm diameter column showing optimum performance. In contrast, for group columns, the triangular arrangement consistently outperformed the double-column arrangement, offering better settlement control and load distribution. Between the two geosynthetics, geogrid provided superior results in group columns, while geotextile showed advantages in single columns. The inclusion of iron dust further improved the performance of both single and group columns, reducing settlements and enhancing overall strength, with the effect being more pronounced in group configurations.

Overall, it can be concluded that the most effective configuration is the triangular group arrangement of granular columns with geogrid encasement and iron dust inclusion, which ensures the highest load-bearing efficiency and minimum settlement.

6.6 Conclusion

1. The stone column for the ground improvement is made utilising industrial effluents products such as, iron dust, fly ash and sand is replaced with stone dust.
2. End bearing column shows failure in bulging.
3. The 30 mm column diameter gives better results as compared to others.
4. With the use of iron dust bearing capacity increases more as compared to without iron dust.

3. In group of columns two loading arrangements are used i.e. double columns placed along with the diameter of the mould and triangular pattern columns. In both the above triangular loading gives the best results compared to two column loading arrangements with or without encasement.
4. The efficiency of the single column is less as compared to the group of columns. The triangular loading arrangement in groups gives approachable efficiency.

5. The column's bearing capacity is improved by the use of encasement using geosynthetics and reduces the settlement as compared to without encasement.
6. Geotextile shows better results as compared to geogrid due to its grid size as the material is fine used for column casting. The refined substance spills out or gets punched in the surrounding soil replaced for the column casting.

REFERENCES

Abid, M., Rahman, M., & Islam, S. (2023). Numerical investigation of geosynthetic-encased stone columns in unsaturated soils. E3S Web of Conferences, 436, 12001.

Aboshi, H., Ichimoto, E., Enoki, M., and Harada, K. (1979). The composer-A method to improve characteristics of soft clays by inclusion of large diameter sand columns. Proceedings of the International Conference on Soil Reinforcement, Paris, 1, 211-216.

Abusharar, S. W., and Han, J. (2011). Two-dimensional deep-seated slope stability analysis of embankments over stone column-improved soft clay. Engineering Geology, 120(1–4), 103–110. https://doi.org/10.1016/j.enggeo.2011.04.002

Alexiew, D., Daniel B., and Steve L. (2005). Geotextile encased columns (GEC): load capacity, geotextile selection, and pre-design graphs. Contemporary Issues in Foundation Engineering. 1-14

Alexiew, D., and Thomson, G. (2013). Foundations on geotextile encased granular columns: Overview, experience, and perspectives. Proceedings of International Symposium on Advances in Foundation Engineering (ISAFE 2013).

Ali, K., Shahu, J. T., and Sharma, K. G., 2012. Model tests on geosynthetic-reinforced stone columns: a comparative study. Geosynthetics International, 19(4), 292–305.

Ali, K., Shahu, J.T., and Sharma, K.G. (2014). "Model tests on single and group of stone columns with different geosynthetic reinforcement arrangement". Geosynth. Int. 21(2). 103-118

Ambily, A. P., and Gandhi, S. R. (2007). Behavior of stone columns based on experimental and FEM analysis. Journal of Geotechnical and Geoenvironmental Engineering, 133(4), 405-415.

Bahi, M., & Houhou, M. (2025). Three-dimensional parametric analysis of

embankments supported by geosynthetic-encased stone columns. World Journal of Engineering.

Balaam, N. P., Poulos, H. G., and Brown, P. T. (1978). Settlement analysis of soft clays reinforced with granular piles. Proc., 5th Asian Conf. on Soil Engineering, Bangkok, Thailand, 81–92.

Barksdale, R. D., and Bachus, R. C. (1983). Design and construction of stone columns: Volume 1. Rep. No.FHWA/RD-83/026, Federal Highway Administration, Washington DC, US.

Barksdale, R. D. (1987). Applications of the state of the art of stone columns-liquefaction, local bearing failure, and example calculations, Technical Report. REMR-GT-7, The Georgia Institute of Technology, Atlanta, USA.Basarkar, S. S., Panse, V., and Wankhade,R. R. (2009). Ground Strengthening by Vibro- Stone Columns–A Case Study. Proc. Indian Geotechnical Conference (IGC-2009). Guntur, India. 2009.

Basack, S., Indraratna, B., Rujikiatkamjorn, C., and Siahaan, F. (2017). Modeling the Stone Column Behavior in Soft Ground with Special Emphasis on Lateral Deformation. Journal of Geotechnical and Geoenvironmental Engineering, 143(6). https://doi.org/10.1061/(asce)gt.1943-5606.0001652

Bauer, G.E., and Joulani, N (1996), Laboratory and Analytical Investigation of Sleeve Reinforced Stone Columns. Geosynthetics: application, design and construction, pp. 463-466.

Bergado, D.T., Chai, J.C., Alfaro, M.C., & Balasubramaniam, A.S. (1994). Improvement Techniques of Soft Ground in Subsiding and Lowland Environment.

Black, J. A., Sivakumar, V., and Bell, A. (2011). The settlement performance of stone column foundations. Geotechnique, 61(11), 909–922. https://doi.org/10.1680/geot.9.P.01.

Bouassida, M., De Buhan, P., and Dormieux, L. (1995). Bearing capacity of a

foundation resting on a soil reinforced by a group of columns. Geotechnique, 45(1), 25–34. https://doi.org/10.1680/geot.1995.45.1.25.

Bowels, J. E. (1996). Foundation analysis and design. 5th ed. Mc Graw HillBook Company, p 1175, ISBN 0-07-118844-4. http://doi.org/10.1061/9780784408650.

Brauns, J. (1978). Reinforcing soft cohesive soil with granular piles. Geotechnique, ol. 55, 263-271.

Baruah, D., & Sahu, A. K. (2015). Comparative study of load deformation behavior of silty clay bed reinforced with stone column of different depth and gradation. Proceedings of the International Conference on Engineering Geology in the New Millennium, New Delhi.

Castro, J., and Sagaseta, C. (2009). Consolidation around stone columns: Influence of column deformation. International Journal for Numerical and Analytical Methods in Geomechanics, 33, 851-877.

Castro, J., Cimentada, A., daCosta, A. D., Cañizal, J., and Sagaseta, C. (2013). Consolidation and deformation around stone columns: Comparison of theoretical and laboratory results. Computers and Geotechnics, 49, 326-337.

Castro, J., Karstunen, M., and Sivasithamparam, N., (2014). Influence of stone column installation on settlement reduction. Computers and Geotechnics, 59, 87-97.

Chandrawanshi, S.(2018). Settlement Behaviour of Very Soft Soil Reinforced With Stone Columns: An Experimental Study. Ph.D. Thesis, Maulana Azad National Institute of Technology, India.

Charles, J. A., and Watts, K. A. (1983). Compressibility of soft clay reinforced with stone columns. Proc. 8th European Conference Soil Mechanics and Foundation Engineering, Helsinki, 347-352.

Chen, J. F., Wang, X. T., Xue, J. F., Zeng, Y. and Feng, S. Z. (2018). Uniaxial compression behavior of geotextile encased stone columns. Geotextiles and

Geomembranes, 46(3), 277–283. https://doi.org/10.1016/j.geotexmem.2018.01.003

Choobbasti, A. J., Zahmatkesh, A. and Noorzad, R. (2011). Performance of Stone Columns in Soft Clay: Numerical Evaluation. Geotechnical and Geological Engineering, 29(5), 675–684.

Cimentada, A., da Costa, A., Cañizal, J. and Sagaseta, C. (2011). Laboratory study on radial consolidation and deformation in clay reinforced with stone columns. Canadian Geotechnical Journal, 48(1), 36–52. https://doi.org/10.1139/T10-043.

Das, B.M. (2010). Principle of Foundation Engineering. CL-engineering, Amata Nakron industrial Estate, 7th Edition, March 2010.

Das, A. K., and Deb, K. (2018). Experimental and 3D Numerical Study on Time-Dependent Behavior of Stone Column–Supported Embankments. International Journal of Geomechanics, 18(4), 04018011

Das Manita and Dey Ashim Kanti (2020). Use of Soil–Cement Bed to Improve Bearing Capacity of Stone Columns" International Journal of Geomechanics, 20(6) https://doi.org/10.1061/(ASCE)GM.1943-5622.0001655

Datye, K. R., and Nagaraju, S. S. (1981). Design approach and field control for stone columns. Proc., 10th Int. conf. on Soil Mech. and Found. Eng., Stockholm, Vol. 3, 637-640.

Dayte, K. R., and Madhav, M. R. (1988). Case Histories of Foundations With Stone Columns. International Conference on Case Histories in Geotechnical Engineering. 5.

Deb, K., Samadhiya, N. K., and Namdeo, J. B. (2011). Laboratory model studies on unreinforced and geogrid-reinforced sand bed over stone column-improved soft clay. Geotextiles and Geomembranes, 29(2), 190-196

Deb, K., and Behera, A. (2017). Rate of Consolidation of Stone Column–Improved Ground Considering Variable Permeability and Compressibility in Smear Zone. International Journal of Geomechanics, 17(6). https://doi.org/10.1061/(asce)gm.1943-5622.0000830.

Deb, K., and Shiyamalaa, S. (2015). Effect of Clogging on Rate of Consolidation of Stone Column–Improved Ground by Considering Particle Migration. International Journal of Geomechanics, 16(1), 1-10.

Debnath, P., Dey, A. K., (2017). Bearing capacity of geogrid reinforced sand over encased stone columns in soft clay. Geotextiles and Geomembranes, 45(6), 653-664.

Deshpande P.M. and Vyas A.V. (1996), Interactive Encased Stone Column Foundation. Sixth Intl. Conf. and Exhibition on Piling and Deep Foundation, DFI'96, ISSMFE, pp. 1-19.

Dutta, S., Nadaf, M. B., Lal Birali, R. R., and Mandal, J. N. (2016). Encased stone columns for soft ground improvement. In Geo-Chicago 2016 (pp. 746-755)

Elsawy, M. B. D. (2013). Behaviour of soft ground improved by conventional and geogrid-encased stone columns, based on FEM study. Geosynthetics International, 20(4), 276–285. https://doi.org/10.1680/gein.13.00017.

Etse, G., and Willam, K. (1999). Failure Analysis of Elastoviscoplastic Material Models. Journal of Engineering Mechanics, 125(1), 60–69. https://doi.org/10.1061/(asce)0733-9399(1999)125:1(60)

Fansuri, M., Abdullah, R., & Setiawan, H. (2025). Comparative seismic performance of ordinary and geosynthetic-encased stone columns for liquefaction mitigation. Geomechanics and Geoengineering

Fattah, M. Y., and Majeed, Q. G. (2012). Finite Element Analysis of Geogrid Encased Stone Columns. Geotechnical and Geological Engineering, 30(4), 713–726. https://doi.org/10.1007/s10706-011-9488-8

Fattah, Mohammed Y., Bushra Zabar S., and Hanan Hassan A. (2014). An experimental analysis of embankment on stone columns. Journal of Engineering 20(7), 62-84.

Gniel, J., and Bouazza, A. (2009). Improvement of soft soils using geogrid encased

stone columns. Geotextiles and Geomembranes, 27(3), 167-175

Han, J. (2015). Principles and Practices of Ground Improvement, John Wiley & Sons, New Jersey.

Han, J., and Ye, S.L. (2001). Simplified Method for Consolidation Rate of Stone Column Reinforced Foundations. Journal of Geotechnical and Geoenvironmental Engineering, 127(7), 597–603.

Han, J., and Ye, S. L. (2002). A Theoretical Solution for Consolidation Rates of Stone Column-Reinforced Foundations Accounting for Smear and Well Resistance Effects. International Journal of Geomechanics, 2(2), 135–151. https://doi.org/10.1061/(asce)1532-3641(2002)2:2(135).

Hanna, A. M., Etezad, M., Ayadat, T., (2013). Mode of Failure of a Group of Stone Columns in Soft Soil. International Journal of Geomechanics, ASCE , 13(1), 87-96.

Hasan, M., Samadhiya, N. K., (2016). Experimental and numerical analysis of geosynthetic-reinforced floating granular piles in soft clays. International Journal of Geosynthetics and Ground Engineering, 2(3), 22.

Hasan, M., and Samadhiya,N. K.(2017). Performance of geosynthetic-reinforced granular piles in soft clays: Model tests and numerical analysis. Computers and Geotechnics 87: 178- 187.

Hassanzadeh, A., Rezaei, M., & Farahani, H. (2026). Wall mesh-encased stone columns using recycled rubber concrete and asphalt aggregates. Scientific Reports, 16, 38535.

Huasmann, M.R. (1990). Engineering Principles of Ground Modification, McGraw-Hill, New York.

Hughes, J. M. O., and Withers, N. J. (1974). Reinforcing of soft cohesive soils with stone columns. Ground Engineering 7(3), 42-49.

Hughes, J. M. O., Withers, N. J., and Greenwood, D. A. (1975). A field trial of the

reinforcing effect of a stone column in soil. Geotechnique, 25(1), 31-44.

Indraratna, B., Basack, S. and Rujikiatkamjorn, C. (2013). Numerical solution to stone column reinforced soft ground considering arching, clogging and smear effects. Journal of Geotechnical and Geoenvironmental Engineering 139(3): 377-394.

IS 15284 (Part 1)-2003. Indian standard code of practice for design and construction for ground improvement guidelines. Part 1: Stone columns. Bureau of Indian Standards, New Delhi, India.

IS 2720 -1983. Indian standard methods of test for soils. Bureau of Indian Standards, New Delhi, India.

Jadid, M. N. (2013). A Practical Approach For Computing Soil Bearing Capacity Under Shallow Foundations Using Vibro-Replacement Method. International Refereed Journal of Engineering and Science, 2(5), 54–62.

Ji, W., Zhao, H., & Sun, Y. (2024). Numerical evaluation of shear strength behaviour of geosynthetic-encased stone columns. Geotechnical Engineering International, 31(3), 358–371.

Kang, D., Kim, S., & Lee, J. (2023). Bearing capacity and failure mechanisms of multilayer geosynthetic-encased stone columns under static and dynamic loading. Sustainability, 15(6), 5205.

Kolekar, Y. A., and Dasaka, S. M. (2014). Ariability in the soil properties of the consolidated clay beds. International Journal of Geotechnical Engineering, 8(4), 365-371.

Kumar, S. G., Robinson, R. G., Rajagopal, K. (2014). Improvement of soft clays by combined vacuum consolidation and geosynthetic encased stone columns. Indian Geotechnical Journal, 44(1), 59-67.

Kumar, R., and Jain, P. K. (2013). Expansive Soft Soil Improvement by Geogrid Encased Granular Pile. International Journal on Emerging Technologies, 4(1), 55-

61.

Kumar, R., Sharma, P., & Verma, S. (2023). Numerical analysis of dual-layer geosynthetic-encased stone columns installed in soft soil. Advances in Civil Engineering https://doi.org/10.1155/2023/5039439.

Liu, Y., Zhang, X., & Chen, L. (2023). Static and dynamic load transfer behaviour of geosynthetic-encased stone columns. Sustainability, 15(2), 1108.

Lu, X., Chen, Y., & Zhao, T. (2026). DEM–FDM coupled numerical investigation on geosynthetic-encased stone columns considering gravel size and geogrid aperture. Applied Sciences, 16(3), 1610.

Madhav, M. R., and Miura, N. (1994). Stone Columns. Panel Rep., 13th Int. Conference on Soil Mechanics and Foundation Engineering, New Delhi, Jan., pp. 163-64.

Madhav, M.R., & Vitkar, P.P. (1978). Strip Footing on Weak Clay Stabilized with a Granular Trench or Pile. Canadian Geotechnical Journal, 15(4), 605–609. https://doi.org/10.1139/t78-066

Madun, A., Meghzili, S. A., Tajudin, S. A. A., Yusof, M. F., Zainalabidin, M. H., Al-Gheethi, A. A., Dan, M. F. M., and Ismail, M. A. M. (2018). Mathematical solution of the stone column effect on the load bearing capacity and settlement using numerical analysis. Journal of Physics: Conference Series, 995(1). https://doi.org/10.1088/1742-6596/995/1/012036.

Malarvizhi, S. N., and Ilamparuthi, K. (2004). Load versus settlement of clay bed stabilized with stone and reinforced stone columns. The Asian Regional Conf. on Geosynthetics, Seoul, 322-329.

Malarvizhi, S. N., and Ilamparuthi, K. (2007). Comparative study on the behavior of encased stone column and conventional stone column. Soils and Foundations, 47(5), 873- 885.

McCabe, B. A., Nimmons, G. J., and Egan, D. (2009).A review of field performance of stone columns in soft soils. Proceedings of the Institution of Civil Engineers-Geotechnical Engineering, 162(6), 323-334.

McKelvey, D., and Sivakumar V. (2000). A review of the performance vibro stone column foundations. Proc. of 3rd International Conference onGround Improvement Techniques. Singapore: CI-Premier Ltd, Singapore.

McKelvey, D., Sivakumar V., and Bell, A. (2004). Modelling vibrated stone columns in soft clay. Proceedings of the Institution of Civil Engineers-Geotechnical Engineering 157(3): 137-149

Mehrannia, N., Farzin, K., and Navid, G.(2018). Experimental study on soil improvement with stone columns and granular blankets. Journal of Central South University 25.4: 866- 878.

Miranda, M., and Da Costa, A. (2016). Laboratory analysis of encased stone columns. Geotextiles and Geomembranes, 44(3), 269–277. https://doi.org/10.1016/j.geotexmem.2015.12.001.

Miranda, M., Da Costa, A., Castro, J., & Sagaseta, C., 2017. Influence of geotextile encasement on the behaviour of stone columns: Laboratory study. Geotextiles and Geomembranes, 45(1), 14-22.

Mohamed, H., Ali, M., & Hassan, R. (2023). Numerical investigation of geosynthetic-encased stone columns using PLAXIS 3D. Innovative Infrastructure Solutions, 8, 215.

Mohammed, A., Karim, M., & Hasan, T. (2025). Experimental and numerical studies on geosynthetic-encased stone columns in saturated and unsaturated soils. Transportation Geotechnics 52. https://doi.org/10.1016/j.trgeo.2025.101566

Mohanty, P., and Samanta, M. (2015). Experimental and numerical studies on response of the stone column in layered soil. International Journal of Geosynthetics and Ground Engineering 1.3: 27.

Murugesan, S., and Rajagopal, K. (2006). Geosynthetic-encased stone columns: numerical evaluation. Geotextiles and Geomembranes, 24(6), 349–358.

Murugesan, S., and K. Rajagopal (2009). Experimental and numerical investigations on the behaviour of geosynthetic encased stone columns. Indian Geotechnical Conference.

Murugesan, S., and Rajagopal, K. (2010). Studies on the behavior of single and group of geosynthetic encased stone columns. Journal of Geotechnical and Geoenvironmental Engineering, 136(1), 129-139

Muir Wood, D., Wenzheng Hu, and David FT Nash. (2000). Group effects in stone column foundations: model tests. Geotechnique 50.6: 689-698.

Najjar, S. S., (2013). A state-of-the-art review of stone/sand-column reinforced clay systems. Geotechnical and Geological Engineering, 31(2), 355-386

Nazaruddin, A. T., Shakri, M. S., and Hafez, M. A. (2013). A laboratory study on bearing capacity of treated stone column. Electronic Journal of Geotechnical Engineering, 18 Y, 5871–5880

Needleman, A. (1988). Material rate dependence and mesh sensitivity in localization problems. Computer Methods in Applied Mechanics and Engineering, 67(1), 69–85. https://doi.org/10.1016/0045-7825(88)90069-2

Ng, K. S., and Tan, S. A. (2014). Design and analyses of floating stone columns. Soils and Foundations, 54(3), 478–487.

Pandey, A., Kumar, A., & Singh, B. (2022). A review on performance of ordinary and geosynthetic-encased stone columns in soft soils. Geotechnical and Geological Engineering, 40, 4567–4592.

Priebe, H.J. (1976). To estimate the usage behavior of a building site improved by plugging. Civil engineering, (53), 160-162.

Priebe, H. J. (1995). The design of vibro replacement. Ground Engineering 28 (10):

31.

Priebe, H. J. (2005). Design of vibro replacement: The application of Priebe's method to extremely soft soils, 'floating' foundations and proof against slope or embankment failure. Ground Engineering January (2005), 25-27

Rahman, M., Hossain, S., & Karim, A. (2026). Simplified analytical approach for evaluating geotextile-encased stone columns. Scientific Reports, 16, 34737.

Rajesh, S. (2017). Time-dependent behaviour of fully and partially penetrated geosynthetic encased stone columns. Geosynthetics International, 24(1), 60–71. https://doi.org/10.1680/jgein.16.00015.

Rajesh, S., and Jain, P. (2015). Influence of permeability of soft clay on the efficiency of stone columns and geosynthetic-encased stone columns - A numerical study. International Journal of Geotechnical Engineering, 9(5), 483–493. https://doi.org/10.1179/1939787914Y.0000000088.

Raithel, M., and Kempfert, H. G. (2000). Calculation models for dam foundations with geosynthetic coated sand columns. Proceedings of International Conference on Geotechnical and Geological Engineering, GeoEng 2000, Melbourne, Australia, 347–352.

Raithel M., Kirchner A., Schade C. and Leusink E. (2005), Foundation of Constructions on Very Soft Soils with Geotextile Encased Columns - State of the Art. Geofrontiers 2005, GSP 131 Innovations in grouting and soil improvement, pp. 1-11.

Rangeard, D., Phan, P. T., Martinez, J., and Lambert, S. (2016). Mechanical behavior of fine-grained soil reinforced by sand columns: An experimental laboratory study. Geotechnical Testing Journal, 39(4), 648-657

Ranjan, G., and Rao, B. G. (1983). Skirted granular piles for ground improvement. Proc., VIII European Conf. on Soil Mech. and Found. Eng., Halainki

Ranjan, G.,and Rao, A.S.R. (2000). Basic and applied soil mechanics. Second edition, New Age International (P) Ltd. Publisher, Daryahang, New Delhi.

Rao, B. G. (1982). Behavior of skirted granular pile foundation. PhD thesis, University of Roorkee, Roorkee, India.

Rao, N., Madhiyan, S. M., and Prasad, Y. (1992). Influence of bearing area on the behavior of stone columns. Indian Geotechnical Conf, 235–237.

Richard D.S. and Yogesh P. (2005), Repairing Railway Spur Roadbed Failure Using Geotextile-Encased Columns . 05-0881, Kleinfelder, Inc. Annual TRB Meeting 2005.

Saxena, A., Patel, R., & Jain, N. (2024). Performance of recycled aggregate-filled ordinary and geosynthetic-encased stone columns. International Journal of Geo-Engineering, 15, 8.

Schreyer, H. L., and Neilsen, M. K. (1996). Analytical and numerical tests for loss of material stability. International Journal for Numerical Methods in Engineering, 39(10), 1721–1736.

Serridge, C. (2005). Achieving sustainability in vibro stone column techniques. Proceedings of the Institution of Civil Engineers -Engineering Sustainability, 158(4), 211-222.

Shahu, J. T., and Reddy, Y. R. (2011). Clayey Soil Reinforced with Stone Column Group: Model Tests and Analyses. Journal of Geotechnical and Geoenvironmental Engineering, 137(12), 1265–1274.

Shenkman, R., and Ponomaryov, A. (2016). Experimental and Numerical Studies of Geotextile Encased Stone Columns in Geological Conditions of Perm Region of Russia. Procedia Engineering, 143, 530–538. https://doi.org/10.1016/j.proeng.2016.06.067.

Singh, R., Das, A., and Sathiyamoorthy, R. (2019). Efficacy of Coupled Solid–Fluid

Formulation in Regularizing an Ill-Posed Finite Element Model. Indian Geotechnical Journal, 49(4), 409–420.

Singh, I., & Sahu, A. K. (2019). A review on stone columns used for ground improvement of soft soil. Proceedings of the 4th World Congress on Civil, Structural, and Environmental Engineering, Rome. https://doi.org/10.11159/icgre19.132

Sivakumar V., Mckelvey D., Graham J. and Hughes D. (2004), Triaxial Tests on Model Sand Columns in Clay. Canadian Geotechnical Journal, Vol. 41, pp. 299-312.

Srijan, S., & Gupta, A.K. (2023). Performance of horizontally layered and vertically encased geosynthetic-reinforced stone columns in soft clay. Applied Sciences, 13(15), 8660.

Stacho, J., and Sulovska, M. (2017). Determination of the density of stone columns using in-situ testing. International Multidisciplinary Scientific GeoConference Surveying Geology and Mining Ecology Management, SGEM, 17(12), 223–230. https://doi.org/10.5593/sgem2017/12/S02.029

Verma, P., & Sahu, A. K. (2019). Effect of grouted granular column on the load carrying capacity of the expansive soil. International Journal of Recent Technology and Engineering, *8*(3), 2606–2612. https://doi.org/10.35940/ijrte.C4924.098319

Waltham, T. (2009).Foundations of engineering geology, CRC Press, London.

Wang, J., Li, H., & Zhou, Y. (2023). Field and numerical investigation of composite foundations reinforced with geosynthetic-encased stone columns. Sustainability, 15(7), 5965.

Wang, W. M., Sluys, L. J., and De Borst, R. (1997). Viscoplasticity for instabilities due to strain softening and strain-rate softening. International Journal for Numerical Methods in Engineering, 40(20), 3839–3864.

Wehr, J.(2006). The undrained cohesion of the soil as a criterion for the column

installation with a depth vibrator. Transvib 2006.Genin, Holeyman & Rocher-Lacoste. (ed) LCPC. Paris: France.

Weber, T., Laue, J., and Springman, S. (2006). Centrifuge modelling of sand compaction piles in soft clay under embankment load. Proc. of the 6th International Conference on Physical Modelling in Geotechnics, Kowloon, Hong Kong.

Wood, D. M., Hu, W., Nash, D. F. T., 2000. Group effects in stone column foundations: model tests. Geotechnique, 50(6), 689-698.

Yoo, C. and Kim, S. B. (2009). Numerical modeling of geosynthetic encased stone column-reinforced ground. Geosynthetics International, 16(3), 116–126.

CURRICULUM VITAE

ISTUTI SINGH

Tanakpur, Uttarakhand, India | +91-9634868428 | istutisingh_phd2k16@dtu.ac.in

Professional Summary

Geotechnical engineering academic with over 4 years of teaching experience and strong research expertise in ground improvement techniques, particularly stone column applications. Skilled in experimental investigations, numerical modelling (Plaxis 2D, GeoStudio, Abaqus), and integrating laboratory and field studies. Experienced in publishing in SCI/Scopus-indexed journals, presenting at national and international conferences, and guiding students.

Education

M.Tech in Soil Mechanics & Foundation Engineering, G.B. Pant University of Agriculture & Technology, Pantnagar, 2015 — 72.30%

B.Tech in Civil Engineering, G.B. Pant Engineering College, Pauri Garhwal (UTU), 2013 — 64.54%

Intermediate in Science, Beersheba Sr. Sec. School, Haldwani (CBSE), 2009 — 68.40%

High School in —, Beersheba Sr. Sec. School, Haldwani (CBSE), 2007 — 66%

Research Work & Projects

Ph.D. Research: Ground Improvement using Stone Columns

M.Tech Dissertation: Geotechnical Properties of Soil Blended with Rice Husk Ash and Lime

Publications & Presentations

- Two papers were published in "SSRG-International Journal of Civil Engineering (SSRG-IJCE)-EFES April 2015
- Paper published in proceedings of the ICGRE'19 (Scopus Indexed).
- Paper published in International Journal of Innovative Technology

and Exploring Engineering (IJITEE) ISSN: 2278-3075, Volume-8, Issue-7C2, May 2019.

- I have presented at the National Conference on "Emerging Fields in Engineering and Sciences" EFES- 2015 organized by Swami Devi Dyal Institute of Engineering and Technology, Panchkula.
- I have also presented in the All India Seminar on "Advances in Engineering and Technology for Sustainable Development" AETSD-2015 organized by The Institution of Engineers (India), Pantnagar Local Centre and College of Technology, GBPUA&T Pantnagar.
- I have participated and presented in International Conference on Geotechnical Research and Engineering (ICGRE'19) (Scopus Indexed) held in Rome, Italy.
- I have participated and presented at the Second ASCE India Conference (CRSIDE-2020) in Kolkata
- **Istuti Singh** & Anil Kumar Sahu "Multi-blended granular columns encased with geosynthetics" Z. Dt. Ges. Geowiss. (J. Appl. Reg. Geol.) Published online February 2024, DOI:10.1127/zdgg/2024/0412 Science Citation Indexed.
- **Istuti Singh** & Anil Kumar Sahu "Load Deformation of Multi-Blended Granular Columns using Geosynthetic Encasement" Z. Dt. Ges. Geowiss. (J. Appl. Reg. Geol.), Published on – October, 2024. Science Citation Indexed

Workshops & Training

- FDP on Earthquake Resistant Design of Structures, DTU, May 2019
- International Workshop GeoRiskSEA-2019, DTU
- National Training Programme on Geo-Meteorological Hazards Risk Management, NIDM & DTU, Feb 2020

Awards & Achievements

- Best Paper Award in the Engineering stream, AETSD-2015, College of Technology, GBPUA&T, Pantnagar